To the Graduate Council:

I am submitting herewith a thesis written by Cynthia M. Maples entitled "Influence of Dose Uncertainty on Dose-Response Parameter Estimation." I have examined the final copy of this thesis for form and content and recommend that it be accepted in partial fulfillment of the requirements for the degree of Master of Science, with a major in Nuclear Engineering.

Peter Groer, Major Professor

We have read this dissertation
and recommend its acceptance:

Accepted for the Council:

Associate Vice Chancellor and
Dean of The Graduate School

INFLUENCE OF DOSE UNCERTAINTY ON DOSE-RESPONSE PARAMETER ESTIMATION

A Thesis
Presented for the
Master of Science
Degree
The University of Tennessee, Knoxville

Cynthia M. Maples
May 1998

ACKNOWLEDGEMENTS

There are many people to whom I am grateful for making my time at the University of Tennessee so rewarding. I have benefited greatly from knowing the faculty and graduate students in the Department of Nuclear Engineering over the last six years, and hope that these relationships will endure. I am particularly grateful to my Dissertation Committee, Peter Groer, Lawrence Miller and Lawrence Townsend for their support and encouragement. The merit of this work is due in no small part to their suggestions. Peter Groer has been especially helpful as my major professor. It is through him that I found a part of nuclear engineering that inspired me to pursue a master of science degree.

There are a number of other people whose assistance should be recognized. I would like to thank my parents for their support throughout my college career. I have received generous financial support from the Department of Nuclear Engineering. I owe a great deal to all the faculty for believing in me and giving me the opportunity to continue my education.

Lastly, the greatest debt is owed to Steve Ledbetter. Without his patience, encouragement and support I would never have reached this moment.

ABSTRACT

Chromosome aberrations are one of the biological effects of ionizing radiation. The number of chromosome aberrations, which are represented by dicentrics in this thesis, is directly related to dose. In general, as the radiation dose increases, the number of dicentric chromosomes will also increase. By observing the number of dicentrics per cell, the human body can be used as a biological dosimeter after radiation accidents. A dose-response function can be used to model the observed data.

The two original contributions of this thesis are: (1) to estimate the dose-response function parameters with and without dose uncertainty and (2) to determine the calibrative distribution with and without an error about the calibration doses. The calibrative density can be used to find the dose corresponding to a specific number of observed dicentrics/cell. These were achieved using Bayesian estimation for two data sets.

The principal parameter of interest was the slope of the dose-response function, denoted by β for parameter estimation without dose uncertainty and θ for parameter estimation with dose uncertainty. For both data sets, β and θ agreed closely with the maximum likelihood estimate without dose uncertainty. This implied that including dose uncertainty did not change the estimation of the slope parameter significantly.

The calibrative distributions without dose uncertainty behaved as expected: as the number of dicentrics/cell increased, the estimated dose increased. Not all the calibrative distributions with dose uncertainty responded as anticipated. The mode of two calibrative

distributions decreased with an increased number of dicentrics/cell. All the calibrative dose estimates were lower than the calibrative dose estimates without dose uncertainty. The lower dose estimates can be attributed to the uncertainty in the calibrative doses. The calibrative distributions were skewed to the right. This implies that the means of the dose are greater than the modes. More examples with calibration dose uncertainty should be done in the future to see if similar patterns emerge.

TABLE OF CONTENTS

I. INTRODUCTION 1
II. PARAMETER ESTIMATION WITHOUT DOSE UNCERTAINTY 5
III. PARAMETER ESTIMATION WITH DOSE UNCERTAINTY 11
IV. CALIBRATION WITHOUT DOSE UNCERTAINTY 18
V. CALIBRATION WITH DOSE UNCERTAINTY 35
VI. CONCLUSION 52

BIBLIOGRAPHY 55

APPENDICES 57
Appendix A. Supplemental graphs for parameter estimation with dose uncertainty. 58
Appendix B. FORTRAN programs for parameter estimation and calibration with dose uncertainty 66

VITA 95

LIST OF FIGURES

Figure 1. Cell Division Cycle. 2
Figure 2. Scatter Diagram for Data Set 1 With Regression Line. 19
Figure 3. Posterior Distribution of α for Data Set 1 Without Dose Uncertainty. 20
Figure 4. Posterior Distribution of β for Data Set 1 Without Dose Uncertainty. 20
Figure 5. Posterior Distribution of σ for Data Set 1 Without Dose Uncertainty. 21
Figure 6. Calibrative Distribution with $Y_f = 0.5$ for Data Set 1 Without Dose Uncertainty. 23
Figure 7. Calibrative Distribution with $Y_f = 1.0$ for Data Set 1 Without Dose Uncertainty. 23
Figure 8. Calibrative Distribution with $Y_f = 1.5$ for Data Set 1 Without Dose Uncertainty. 24
Figure 9. Calibrative Distribution with $Y_f = 2.0$ for Data Set 1 Without Dose Uncertainty. 24
Figure 10. Calibrative Distribution with $Y_f = 2.5$ for Data Set 1 Without Dose Uncertainty. 25
Figure 11. Calibrative Distribution with $Y_f = 3.0$ for Data Set 1 Without Dose Uncertainty. 25
Figure 12. Scatter Diagram for Data Set 2 With Regression Line 27
Figure 13. Posterior Distribution of α for Data Set 2 Without Dose Uncertainty. 27
Figure 14. Posterior Distribution of β for Data Set 2 Without Dose Uncertainty. 28
Figure 15. Posterior Distribution of σ for Data Set 2 Without Dose Uncertainty. 29
Figure 16. Calibrative Distribution with $Y_f = 0.0025$ for Data Set 2 Without Dose Uncertainty. 30
Figure 17. Calibrative Distribution with $Y_f = 0.005$ for Data Set 2 Without Dose Uncertainty. 31
Figure 18. Calibrative Distribution with $Y_f = 0.0075$ for Data Set 2 Without Dose Uncertainty. 31
Figure 19. Calibrative Distribution with $Y_f = 0.01$ for Data Set 2 Without Dose Uncertainty. 32
Figure 20. Calibrative Distribution with $Y_f = 0.015$ for Data Set 2 Without Dose Uncertainty. 32
Figure 21. Calibrative Distribution with $Y_f = 0.0175$ for Data Set 2 Without Dose Uncertainty. 33
Figure 22. Calibrative Distribution with $Y_f = 0.0225$ for Data Set 2 Without Dose Uncertainty. 33
Figure 23. Calibrative Distribution with $Y_f = 0.03$ for Data Set 2 Without Dose Uncertainty. 34
Figure 24. Posterior Distribution of τ for Data Set 1 With Dose Uncertainty 36
Figure 25. Posterior Distribution of ϕ_1 for Data Set 1 With Dose Uncertainty 36
Figure 26. Posterior Distribution of ϕ_2 for Data Set 1 With Dose Uncertainty 37
Figure 27. Posterior Distribution of θ for Data Set 1 With Dose Uncertainty 38
Figure 28. Calibrative Distribution with $Y_f = 0.5$ for Data Set 1 With Dose Uncertainty 39
Figure 29. Calibrative Distribution with $Y_f = 1.0$ for Data Set 1 With Dose Uncertainty 39
Figure 30. Calibrative Distribution with $Y_f = 1.5$ for Data Set 1 With Dose Uncertainty 40
Figure 31. Calibrative Distribution with $Y_f = 2.0$ for Data Set 1 With Dose Uncertainty 40
Figure 32. Calibrative Distribution with $Y_f = 2.5$ for Data Set 1 With Dose Uncertainty 41
Figure 33. Calibrative Distribution with $Y_f = 3.0$ for Data Set 1 With Dose Uncertainty 41
Figure 34. Calibrative Distribution when $Y_f = 0.5$ for Data Set 1 With Dose Uncertainty Using the Midpoint Rule Method 42
Figure 35. Posterior Distribution of τ for Data Set 2 With Dose Uncertainty 44
Figure 36. Posterior Distribution of ϕ_1 for Data Set 2 With Dose Uncertainty 44
Figure 37. Posterior Distribution of ϕ_2 for Data Set 2 With Dose Uncertainty 45
Figure 38. Posterior Distribution of θ for Data Set 2 With Dose Uncertainty 45
Figure 39. Calibrative Distribution when $Y_f = 0.005$ for Data Set 2 With Dose Uncertainty. 47
Figure 40. Calibrative Distribution when $Y_f = 0.0075$ for Data Set 2 With Dose Uncertainty 47
Figure 41. Calibrative Distribution when $Y_f = 0.01$ for Data Set 2 With Dose Uncertainty. 48
Figure 42. Calibrative Distribution when $Y_f = 0.015$ for Data Set 2 With Dose Uncertainty. 48
Figure 43. Calibrative Distribution when $Y_f = 0.0175$ for Data Set 2 With Dose Uncertainty 49
Figure 44. Calibrative Distribution when $Y_f = 0.0225$ for Data Set 2 With Dose Uncertainty 49
Figure 45. Calibrative Distribution when $Y_f = 0.03$ for Data Set 2 With Dose Uncertainty. 50
Figure 46. Calibrative Distribution when $Y_f = 0.005$ for Data Set 2 With Dose Uncertainty Using the Midpoint Rule Method 50

CHAPTER I

INTRODUCTION

The biological effects of radiation are the effects observed when ionizing radiation interacts with living tissue by transferring energy to molecules of cellular matter. One effect of such ionizing radiation is that chromosome aberrations occur (Hall, 1994). Ionizing radiation induces specific types of chromosomal aberrations in mammalian cells and these can be identified microscopically. In 1960, the lymphocyte culture technique was developed which allowed researchers to study the human chromosome without difficulty since lymphocytes are found in blood cells (Littlefield, 1997).

A chromosome is a tiny threadlike structure in a cell nucleus that contains most or all the DNA or RNA comprising the genes. An abnormal chromosomal complement resulting from the loss, duplication, or rearrangement of genetic material characterizes a chromosome aberration (Dept. of Plant Biology, 1998). The severity of the injury depends on the type of radiation, the absorbed dose, the rate at which the dose was absorbed, and the radiosensitivity of the tissues involved.

The damage to the body from radiation occurs in the DNA but can be seen in chromosomes. Chromosomes can only be seen in cells that are undergoing mitosis. The type of damage done to chromosomes depends on which phase of mitosis the cell is in (Littlefield, 1997). The cell cycle is the sequence of events between mitotic

divisions. Figure 1 shows the cell cycle. Mitosis (M phase) is followed by a growth (G_1) phase, then by the synthesis phase during which the DNA is replicated (S phase), then by another growth (G_2) phase, and finally by another mitosis. The four phases in mitosis are anaphase, metaphase, prophase and telophase. Interphase is the period between succeeding mitoses. Chromosome aberrations occur if a cell is irradiated before the chromosome material has been duplicated (Hall, 1994).

There are three basic types of radiation-induced aberrations that adversely affect the cell: the dicentric, the ring and deletion. These can be viewed when a human cell is in metaphase. The dicentric forms when two separate chromosomes in the prereplication stage (G_1) are in the same proximity and are "broken." The "broken" pieces rejoin to form an exchange between the two chromosomes. The incorrectly formed chromosome replicates in the DNA synthetic period resulting in one

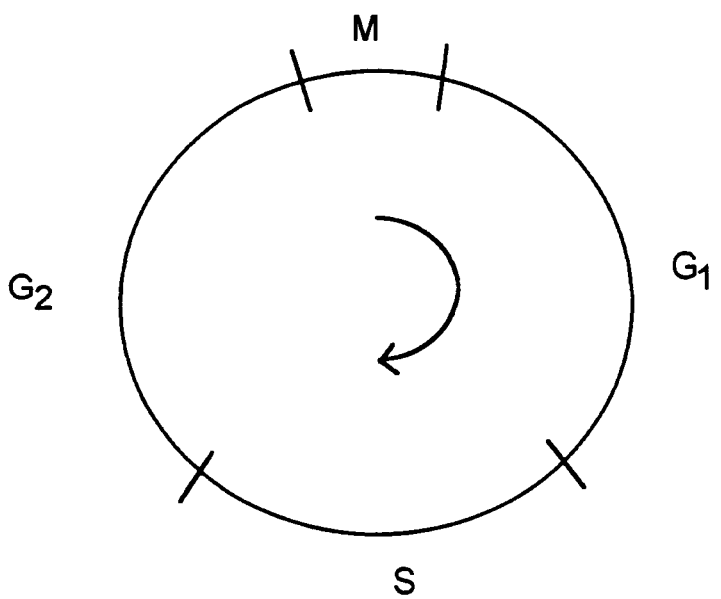


Figure 1. Cell Division Cycle.

chromosome with two centromeres, a dicentric. The ring forms when two breaks occur in the same chromosome in the prereplication stage (G_1). The ends rejoin to form a ring. The chromosome then replicates and forms overlapping rings. A deletion occurs when a single chromosome is "broken". In each of these types of aberrations, there is also a fragment formed that has no centromere (acentric fragment). Since deletions frequently occur spontaneously, dicentrics are considered to be the most reliable indicator of exposure in human lymphocytes (spontaneous frequency of dicentrics estimated to be 1 in 4000 lymphocytes metaphases) (NCRP Report No. 64, 1980).

The number of chromosome aberrations are related directly to dose. In general, as the radiation dose increases, the number of dicentric chromosomes will also increase. The dose-response relationship for dicentrics is curvilinear in mammalian cells exposed to moderate to high doses of low LET (Linear Energy Transfer) radiation, delivered at high dose rates. For various high LET radiations, the dose-response function is linear in mammalian cells (NCRP Report No. 104, 1990).

By observing the number of dicentric chromosomes per cell, the human body can be used as a dosimeter. Naturally, the number of dicentrics is random. Hence, the dose-response function has a range of dicentric values for each dose. Nevertheless, calibration can be performed. The unknown dose corresponding to an observed number of dicentrics can be characterized by a probability density, the so-called calibrative density. The following chapters will describe the methodology of estimating

the dose-response function parameters with and without dose uncertainty. The goal is to determine the calibrative distribution with and without an error about the dose that can be used to find the dose at which a specific number of dicentrics per cell is observed.

CHAPTER II

PARAMETER ESTIMATION WITHOUT DOSE UNCERTAINTY

The objective is to estimate the parameters of the mathematical model and determine the calibrative distribution. First, it can be achieved without dose uncertainty. This is accomplished by performing simple linear regression on the model below

$$Y_i = \mu_{Y|Xi} + \varepsilon_i = \alpha + \beta X_i + \varepsilon_i \qquad (1)$$

where α and β are unknown, $\mu_{Y|Xi}$ is the mean of Y given X_i, and Y_i and X_i are the observed data. The errors ε_i about Y_i are assumed to be normally distributed with mean 0 and variance σ^2 or

$$\varepsilon_i = N(0, \sigma^2) \propto \frac{1}{\sigma} e^{-\frac{\varepsilon^2}{2\sigma^2}}. \qquad (2)$$

We assume that σ^2 does not vary with X_i so that the errors ε_i are given by (2) for simplicity.

Construction of the Likelihood

The likelihood is defined to be the joint probability of all observations. If there are n observations, the likelihood for model (2) is:

$$\mathcal{L}(\varepsilon_i|\ \alpha, \beta, \sigma, X_i) \ \propto \ \frac{1}{\sigma^n} e^{-\frac{1}{2\sigma^2}\sum_{i=1}^{n}\varepsilon_i^2} \tag{3}$$

or

$$\mathcal{L}(\alpha, \beta, \sigma|D) \ \propto \ \frac{1}{\sigma^n} e^{-\frac{1}{2\sigma^2}\sum_{i=1}^{n}(Y_i-\alpha-\beta x_i)^2} . \tag{4}$$

where D is the observed data pairs (X_i, Y_i) i = 1, ..., n and n is the number of data points.

Posterior Distributions

The joint posterior density of α, β, and σ given the data D ($D = (X_i, Y_i)$ for i = 1, ..., n) is proportional to:

$$p(\alpha, \beta, \sigma|D) \ \propto \ \mathcal{L}(\alpha, \beta, \sigma|D)\ f(\alpha, \beta, \sigma) \tag{5}$$

where $f(\alpha, \beta, \sigma)$ is the prior distribution. The prior distribution can be written as

$$f(\alpha, \beta, \sigma) = f(\alpha)\ f(\beta)\ f(\sigma) \tag{6}$$

if the parameters are independent of each other. We assume that the prior distributions are uniform for α and β and proportional to σ^{-1} for the standard deviation, as shown below:

$$f(\alpha) \ \propto \ \text{constant},\ f(\beta) \ \propto \ \text{constant, and } f(\sigma) \propto \sigma^{-1} \quad \Rightarrow \quad f(\alpha, \beta, \sigma) \propto \sigma^{-1} \tag{7}$$

Then, the posterior density of α, β and σ given the data is proportional to:

$$p(\alpha, \beta, \sigma|D) \propto \frac{1}{\sigma^{n+1}} e^{-\frac{1}{2\sigma^2}\sum_{i=1}^{n}(Y_i-\alpha-\beta X_i)^2} \quad (8)$$

Integrating over one of the parameters will give the joint posterior density of the other parameters. Consequently, integration over two parameters will give the marginal posterior density over the third parameter. After the integration over σ, the posterior density of α and β is:

$$p(\alpha, \beta|D) \propto \int_0^{\infty} \frac{1}{\sigma^{n+1}} e^{-\frac{1}{2\sigma^2}\sum_{i=1}^{n}(Y_i-\alpha-\beta X_i)^2} d\sigma = \quad (9)$$

$$p(\alpha, \beta|D) \propto \left\{ (n-2)s^2 + n(\alpha-\hat{\alpha})^2 + (\beta-\hat{\beta})^2\sum_{i=1}^{n} X_i^2 + 2(\alpha-\hat{\alpha})(\beta-\hat{\beta})\sum_{i=1}^{n} X_i \right\}^{-\frac{n}{2}} \quad (10)$$

where $\hat{\alpha}$ and $\hat{\beta}$ are the maximum likelihood estimators of α and β and s^2 is an unbiased estimator of σ^2 (Press, 1989). The maximum likelihood estimators are given by the following formulas:

$$\hat{\alpha} = \overline{Y} - \hat{\beta}\overline{X} \quad (11)$$

and

$$\hat{\beta} = \frac{\sum_{i=1}^{n}(X_i - \overline{X})(Y_i - \overline{Y})}{\sum_{i=1}^{n}(X_i - \overline{X})^2} \quad (12)$$

where $\overline{X} = \frac{1}{n}\sum_{i=1}^{n} X_i$ and $\overline{Y} = \frac{1}{n}\sum_{i=1}^{n} Y_i$. (13)

The unbiased estimator of the variance is given by:

$$s^2 = \frac{1}{n-2}\sum_{i=1}^{n}(Y_i - \hat{\alpha} - \hat{\beta}X_i)^2. \tag{14}$$

A t-distribution describes the marginal densities of α and β if X_i is exactly known and σ^2 does not vary with X_i. A t-distribution with $\nu = n-2$ degrees of freedom is defined as

$$h(t) = \frac{\Gamma[(\nu+1)/2]}{\Gamma[(\nu/2)]\sqrt{\pi\nu}}\left(1+\frac{t^2}{\nu}\right)^{-(\nu+1)/2}, \qquad -\infty < t < \infty. \tag{15}$$

If Eqn (10) is integrated with respect to β, the marginal density of α is

$$p(\alpha|D) \propto \left\{(n-2)s^2\sum_{i=1}^{n}X_i^2 + (\alpha-\hat{\alpha})^2(n\sum_{i=1}^{n}X_i^2 - (\sum_{i=1}^{n}X_i)^2)\right\}^{-\frac{(n-1)}{2}} \tag{16}$$

which has the form of a t-distribution with t defined as:

$$t = (\alpha-\hat{\alpha})\sqrt{\frac{\sum_{i=1}^{n}(X_i-\bar{X})^2}{\frac{s^2}{n}\sum_{i=1}^{n}X_i^2}}. \tag{17}$$

If Eqn (10) is integrated with respect to α, the marginal density of β is

$$p(\beta|D) \propto \left\{(n-2)ns^2 + (\beta-\hat{\beta})^2(n\sum_{i=1}^{n}X_i^2 - (\sum_{i=1}^{n}X_i)^2)\right\}^{-\frac{(n-1)}{2}} \tag{18}$$

which also has the form of a t-distribution with

$$t = (\beta-\hat{\beta})\sqrt{\frac{\sum_{i=1}^{n}(X_i-\bar{X})^2}{s^2}}. \tag{19}$$

Integrating (8) over α and β gives the marginal density for σ:

$$p(\sigma|D) \propto \frac{1}{\sigma^{n-1}} e^{-\frac{(n-2)s^2}{2\sigma^2}}. \tag{20}$$

Calibrative Distributions

A controlled calibration experiment is one in which the independent variable is fixed by the experimenter and the variance does not change with each value of the independent variable. The calibrative density for a controlled experiment is proportional to the prior density times the predictive density (Groer, 1996).

$$\text{Calibrative} \propto (\text{Prior})(\text{Predictive}) \tag{21}$$

The posterior predictive density is the posterior density multiplied by the likelihood of a new observation which is integrated over all parameters excepting the new observation parameters (X_f, Y_f), see Eqn (25). The likelihood of a new observation using the model from Eqn (1) is

$$\mathcal{L}(X_f, Y_f|D) \propto \frac{1}{\sigma} e^{-\frac{(Y_f-\alpha-\beta X_f)^2}{2\sigma^2}} \tag{22}$$

where X_f and Y_f are the new observations which makes the posterior predictive density $p(Y_f|X_f,D)$ (Press, 129):

$$p(Y_f|X_f,D) \propto \int_{-\infty}^{\infty}\int_{-\infty}^{\infty}\int_{0}^{\infty} p(\alpha,\beta,\sigma|D)\frac{1}{\sigma} e^{-\frac{(Y_f-\alpha-\beta X_f)^2}{2\sigma^2}} d\sigma\, d\beta\, d\alpha. \tag{23}$$

The predictive density has again the form of a t-distribution with

$$t = \frac{Y_f - \hat{\alpha} - \hat{\beta}X_f}{s\sqrt{1 + \frac{1}{n}\frac{(X_f - \bar{X})^2}{\sum_{i=1}^{n}(X_i - \bar{X})^2}}}. \tag{24}$$

To determine the calibrative distribution, fix Y_f and let X_f be variable. This is not a t-distribution but an entirely different distribution. Thus, according to Eqn (21) the calibrative density is given by the following formula:

$$p(X_f | Y_f, D) \propto p(Y_f | X_f, D) f(X_f) \tag{25}$$

where $f(X_f)$ is the prior distribution of X_f which will be uniform in some cases. However, note that Eqn (25) is only true for a controlled experiment (Groer, 1996).

CHAPTER III

PARAMETER ESTIMATION WITH DOSE UNCERTAINTY

To estimate the parameters with dose uncertainty, a method described in a paper by Lindley and El-Sayyad (1968) utilized a simple model so that computations are reduced to a minimum and to better present the general method:

$$\eta_i = \theta\xi_i \tag{26}$$

where η_i is the true value of the dependent variable, ξ_i is the true value of the independent variable and θ, the slope, is unknown. The observations X_i and Y_i are assumed to be normally distributed as described by the following:

$$X_i = N(\xi_i, \phi_1)$$

$$Y_i = N(\eta_i = \theta\xi_i, \phi_2) \tag{27}$$

The structural parameters are θ, ϕ_1, and ϕ_2 because they occur in the joint distribution of every observation pair. The incidental parameters are ξ_i which are incidental to the pair (X_i, Y_i) alone.

Likelihood Approach

The likelihood method may be used to find the maximum-likelihood estimate of the slope with dose uncertainty. Using this methodology, the likelihood is

$$\mathcal{L}(\theta,\phi_1,\phi_2|D) \propto \frac{1}{(\phi_1\phi_2)^{-\frac{1}{2}n}} e^{-\frac{1}{2}\left\{\frac{\sum_{i=1}^{n}(X_i-\xi_i)^2}{\phi_1}+\frac{\sum_{i=1}^{n}(Y_i-\theta\xi_i)^2}{\phi_2}\right\}}. \tag{28}$$

When ordinary maximum-likelihood estimation is applied, "it says that the maximum-likelihood estimate of the slope is equal to the estimate of the ratio of the standard deviations of the two errors of observation in Y and X" as shown in Eqn (29) (Lindley, 1968):

$$\hat{\theta} = \sqrt{\frac{\hat{\phi}_2}{\hat{\phi}_1}} \tag{29}$$

"$\hat{\theta}$ does converge in probability to a value as $n \to \infty$ ...which only equals θ if $\theta = \{\phi_2/\phi_1\}^{1/2}$" (compare Eqn(29)) (Lindley, 1968). Apart from the exceptional case, the maximum likelihood of θ converges to the wrong value (Lindley, 1968). The problem is now reconsidered using Bayesian techniques.

Bayesian Approach

In a Bayesian approach, all variables are random and consequently have a probability distribution. This can be done for the general case by using incidental and structural parameters. The incidental parameter ξ_i is incidental to the observation pair (X_i, Y_i) alone whereas the structural parameters occur in the joint distribution of every

observation pair. The incidental parameters will be represented by $\xi = (\xi_1, \xi_2, ..., \xi_n)$ and the structural parameters by θ. All other parameters are denoted by τ. The observation pairs are described by $\mathbf{z} = (z_1, z_2, ..., z_n)$ where $z_i = (X_i, Y_i)$ (Lindley, 1968). For the problem demonstrated in this paper, X_i will represent the observed dose and Y_i will represent the observed number of chromosome dicentrics per cell. Lindley and El-Sayyad (1968) make the following assumptions:

(1) θ and τ have a joint prior distribution $p(\theta, \tau)$,

(2) the ξ_i, given θ and τ are independent:

$$p(\xi | \theta, \tau) = \prod_{i=1}^{n} p\xi | \theta, \tau), \tag{30}$$

(3) the z_i, given ξ, θ and τ are independent:

$$p(\mathbf{z} | \xi, \theta, \tau) = \prod_{i=1}^{n} p(z_i | \xi, \theta, \tau), \tag{31}$$

(4) for any given ξ_i, θ and τ; z_i is independent of all ξ_j with j not equal to i:

$$p(z_i | \xi, \theta, \tau) = p(z_i | \xi_i, \theta, \tau). \tag{32}$$

The incidental parameters can now be eliminated to give:

$$p(\mathbf{z} | \theta, \tau) = \int p(\mathbf{z}, \xi | \theta, \tau) d\xi = \prod_{i=1}^{n} p(z_i | \theta, \tau). \tag{33}$$

Functional Relationship

The Bayesian method will now be applied to the linear model described in Eqn (26). The structural parameters θ can be written as (θ, ϕ_1, ϕ_2). Eqn (30) is specialized to

read that given θ, ϕ_1, ϕ_2 and τ, the ξ_i are independent N(0, τ). The joint prior distribution of θ and τ is written as $\pi(\theta, \phi_1, \phi_2, \tau)$. The independent and dependent variables respectively are also written as:

$$\left.\begin{aligned} X_i &= \xi_i + \varepsilon_{i1} \text{ and} \\ Y_i &= \theta\xi_i + \varepsilon_{i2} \end{aligned}\right\} \tag{34}$$

where ε_{ij} are independent N(0, ϕ_j) for j = 1,2.

Thus, the observation pair (X_i, Y_i) have a bivariate normal distribution with zero means and

$$\left.\begin{aligned} &\mathrm{var}(X_i|\theta,\phi_1,\phi_2,\tau) = \tau + \phi_1, \\ &\mathrm{cov}(X_i, Y_i|\theta,\phi_1,\phi_2,\tau) = \theta\tau \text{ and} \\ &\mathrm{var}(Y_i|\theta,\phi_1,\phi_2,\tau) = \theta^2\tau + \phi_2. \end{aligned}\right\} \tag{35}$$

Define the sum of the squares to be

$$\left.\begin{aligned} s_{11} &= \frac{1}{n}\sum_{i=1}^{n} X_i^2, \\ s_{12} &= \frac{1}{n}\sum_{i=1}^{n} X_i Y_i, \text{ and} \\ s_{22} &= \frac{1}{n}\sum_{i=1}^{n} Y_i^2. \end{aligned}\right\} \tag{36}$$

Then, by Bayes formula, the posterior density is

$$p(\theta,\phi_1,\phi_2,\tau|D) \propto \frac{\pi(\theta,\phi_1,\phi_2,\tau)}{(\phi_1\phi_2 + \tau\phi_2 + \tau\phi_1\theta^2)^{\frac{1}{2}n}} e^{\left\{-\frac{1}{2}n\frac{s_{11}(\theta^2\tau+\phi_2) - 2s_{12}\theta\tau + s_{22}(\tau+\phi_1)}{\phi_1\phi_2 + \tau\phi_2 + \tau\phi_1\theta^2}\right\}} \tag{37}$$

Eqn (37) can be used to find the posterior densities of θ, ϕ_1, ϕ_2 and τ respectively by integrating over the three parameters that are not of interest. For example,

$$p(\tau|D) \propto \int_0^{\infty}\int_0^{\infty}\int_{-\infty}^{\infty} \frac{\pi(\theta,\phi_1,\phi_2,\tau)}{(\phi_1\phi_2+\tau\phi_2+\tau\phi_1\theta^2)^{\frac{1}{2}n}} e^{\left\{-\frac{1}{2}n\frac{s_{11}(\theta^2\tau+\phi_2)-2s_{12}\theta\tau+s_{22}(\tau+\phi_1)}{\phi_1\phi_2+\tau\phi_2+\tau\phi_1\theta^2}\right\}} d\theta\, d\phi_1\, d\phi_2. \quad (38)$$

Since θ is the most important parameter of interest, Eqn (37) can be rearranged to make the posterior distribution of θ easier to find by making the following substitutions:

$$\lambda = \frac{\phi_2}{\phi_1}, \rho = \frac{\tau}{\phi_1} \text{ and } \phi = \phi_1. \quad (39)$$

The posterior density of θ, ϕ_1, ϕ_2 and τ is transformed into the posterior density of θ, ϕ, λ and ρ

$$p(\theta,\phi,\lambda,\rho|D) \propto \frac{\pi(\theta,\phi,\lambda,\rho)}{\phi^n(\lambda+\lambda\rho+\rho\theta^2)^{\frac{1}{2}n}} e^{\left\{-\frac{1}{2}n\frac{s_{11}(\theta^2\rho+\lambda)-2s_{12}\theta\rho+s_{22}(\rho+1)}{\phi(\lambda+\lambda\rho+\rho\theta^2)}\right\}}. \quad (40)$$

Approximating the Posterior Distribution of θ

If the prior distribution is assumed to be ϕ^{-1}, the integration with respect to ϕ can be performed exactly, with the result:

$$p(\theta,\lambda,\rho|D) \propto \pi(\theta,\lambda,\rho)\left[\frac{\rho(\lambda+\theta^2)+\lambda}{\{\rho(s_{11}\theta^2-2s_{12}\theta+s_{22})+\lambda s_{11}+s_{22}\}^2}\right]^{\frac{1}{2}n}. \quad (41)$$

The integration over ρ cannot be done analytically and thus an approximation has to be

used. For the approximation we used (42) to find θ_λ where θ_λ is the root of the equation

$$\theta^2 + t\theta - \lambda = 0 \tag{42}$$

and $t = (\lambda s_{11} - s_{22})/s_{12}$. In large samples, the approximate marginal posterior distribution of θ for fixed λ is normal with mean θ_λ and variance $\theta_\lambda^2 u^2/n$ where $u^2 = s_{11}s_{22}/s_{12}^2 - 1$. This method is satisfactory for the distribution of θ for fixed λ provided the sample is large.

Another method used to obtain the marginal posterior density of θ described by Lindley and El-Sayyad (1968) yields the result:

$$p(\theta|D) \propto \int_0^\infty \frac{\lambda+\theta_\lambda^2}{\lambda^2 s_{11}^2 + 2\lambda(s_{12}^2 - s_{11}s_{22}) + s_{22}^2} u^{-1} \sqrt{\frac{n}{2\pi\theta_\lambda^{-1}}}\, e^{-\frac{1}{2}n(\theta-\theta_\lambda)^2/\theta_\lambda^2 u^2}\, d\lambda. \tag{43}$$

The important feature of this result is that as the number of observations, n, tends to infinity the joint distribution does not concentrate around any value.

Construction of the Calibrative Distribution

Recall from Eqn (25) that the calibrative density for a controlled experiment is proportional to the prior density of X_f times the predictive density of X_f where X_f is the future dose associated with the observed number of dicentrics per cell Y_f. The likelihood of a new observation pair using the model from Eqn (26), which includes dose uncertainty, is:

$$\mathcal{L}(X_f, Y_f | D) \propto \frac{1}{\sqrt{2\pi\phi_1\phi_2\tau}} e^{-\left\{\frac{(X_f-\xi_f)^2}{2\phi_1} + \frac{(Y_f-\theta\xi_f)^2}{2\phi_2} + \frac{\xi_f^2}{2\tau}\right\}}. \quad (44)$$

This is very similar to the likelihood using the Likelihood Approach (Eqn (28)). It is the normal distribution of X_f is independent $N(\xi_f, \phi_1)$ and Y_f is independent $N(\theta\xi_f, \phi_2)$ with the uncertainty about ξ included where ξ_f is independent $N(0, \tau)$.

The predictive density is the posterior density times the likelihood of the new observation:

$$p(Y_f | X_f, D) \propto \int_0^\infty\int_0^\infty\int_0^\infty\int_{-\infty}^{\infty}\int_{-\infty}^{\infty} p(\theta, \phi_1, \phi_2, \tau | D) \frac{1}{\sqrt{2\pi\phi_1\phi_2\tau}} e^{-\left\{\frac{(X_f-\xi_f)^2}{2\phi_1} + \frac{(Y_f-\theta\xi_f)^2}{2\phi_2} + \frac{\xi_f^2}{2\tau}\right\}} d\tau d\phi_1 d\phi_2 d\theta d\xi_f. \quad (45)$$

Since $p(\theta, \phi_1, \phi_2, \tau|D)$ does not depend on ξ_f, integration over ξ_f can be performed analytically to give the full expression of the predictive density as:

$$p(Y_f | X_f, D) \propto \int_0^\infty\int_0^\infty\int_0^\infty\int_{-\infty}^{\infty} \frac{\tau}{2(\phi_1\phi_2 + \tau\phi_2 + \tau\phi_1\theta^2)^{\frac{n+3}{2}}} \otimes$$
$$e^{\left\{-\frac{1}{2}\left\{\frac{(\theta^2\tau + \phi_2)(n s_{11} + X_f^2) - 2\theta\tau(n s_{12} + X_f Y_f) + (\tau + \phi_1)(n s_{22} + Y_f^2)}{\phi_1\phi_2 + \tau\phi_2 + \tau\phi_1\theta^2}\right\}\right\}} \otimes \quad (46)$$
$$\left(2 - Erf\left[\frac{\sqrt{\tau}(-X_f\phi_2 - \theta Y_f\phi_1)}{\sqrt{2\phi_1\phi_2(\phi_1\phi_2 + \tau\phi_2 + \tau\phi_1\theta^2)}}\right] - Erf\left[\frac{\sqrt{\tau}(X_f\phi_2 + \theta Y_f\phi_1)}{\sqrt{2\phi_1\phi_2(\phi_1\phi_2 + \tau\phi_2 + \tau\phi_1\theta^2)}}\right]\right) d\theta d\phi_1 d\phi_2 d\tau.$$

To find the calibrative distribution, integrate numerically over θ, ϕ_1, ϕ_2 and τ while assigning a value to Y_f and letting X_f be variable. Remember, as before, this is true only for a controlled calibration experiment.

CHAPTER IV

CALIBRATION WITHOUT DOSE UNCERTAINTY

An important application of this theory is dose estimation by observing the number of dicentrics/cell of a person who has been exposed to ionizing radiation. By using the methodology described in Chapter 2, a probability distribution of the dose can be calculated to give the best estimate of the dose the exposed person received. To illustrate this application, two sample data sets will be used. Table 1 is the first sample data set of a controlled experiment. The data is based on the analysis of dicentric chromosome aberrations in a sample of lymphocytes exposed to a ^{210}Po-Be neutron source (Groer, 1987).

Table 1. Data Set 1: Observed Dose and Chromosome Dicentrics in Human Blood Lymphocytes.

	Dose (Rad)	*# of Cells*	*# of Dicentrics*	*Dicentrics/Cell*
i	X_i	N_i	y_i	Y_i
1	50	269	109	0.405204461
2	75	78	47	0.602564103
3	100	115	94	0.817391304
4	150	90	114	1.266666667
5	200	84	138	1.642857143
6	250	59	125	2.118644068
7	300	37	97	2.621621622

The data of Table 1 have been plotted in Figure 2 to give a scatter diagram. From an inspection of this scatter diagram, it is seen that the points follow closely a straight line, indicating that the assumption of linearity between the two variables appears to be reasonable.

Figure 2 depicts the fitted regression line, namely

$$\mu_{Y|X_i} = \hat{\alpha} + \hat{\beta} X_i . \tag{47}$$

We also want to know the posterior distributions of the parameters to draw inferences about the precision of the parameter's estimates. Using Eqns (15) through (17), the posterior distribution of α can be derived and is shown in Figure 3. The maximum value occurs when α is zero and the expectation of α is positive and can be used as a point estimate for α. Figure 4 shows the probability distribution of β given

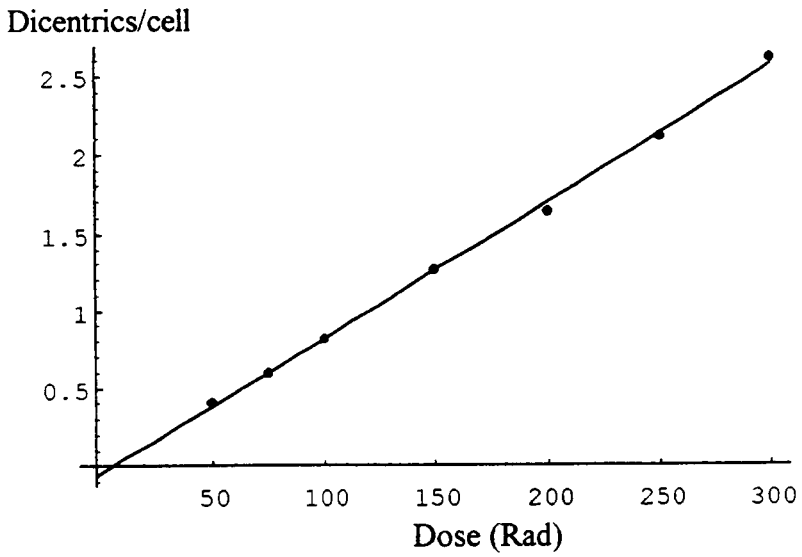


Figure 2. Scatter Diagram for Data Set 1 With Regression Line.

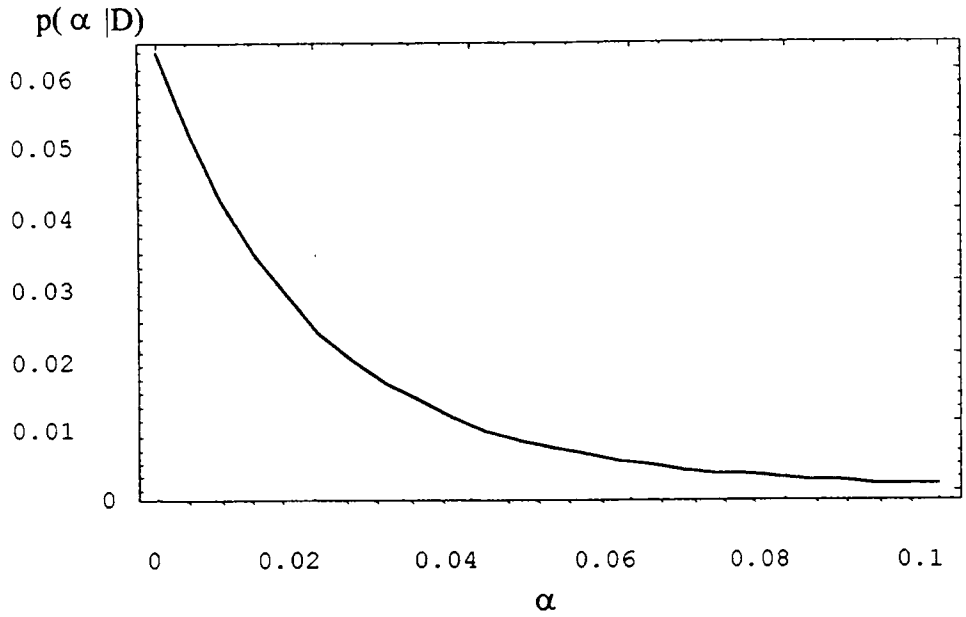


Figure 3. Posterior Distribution of α for Data Set 1 Without Dose Uncertainty.

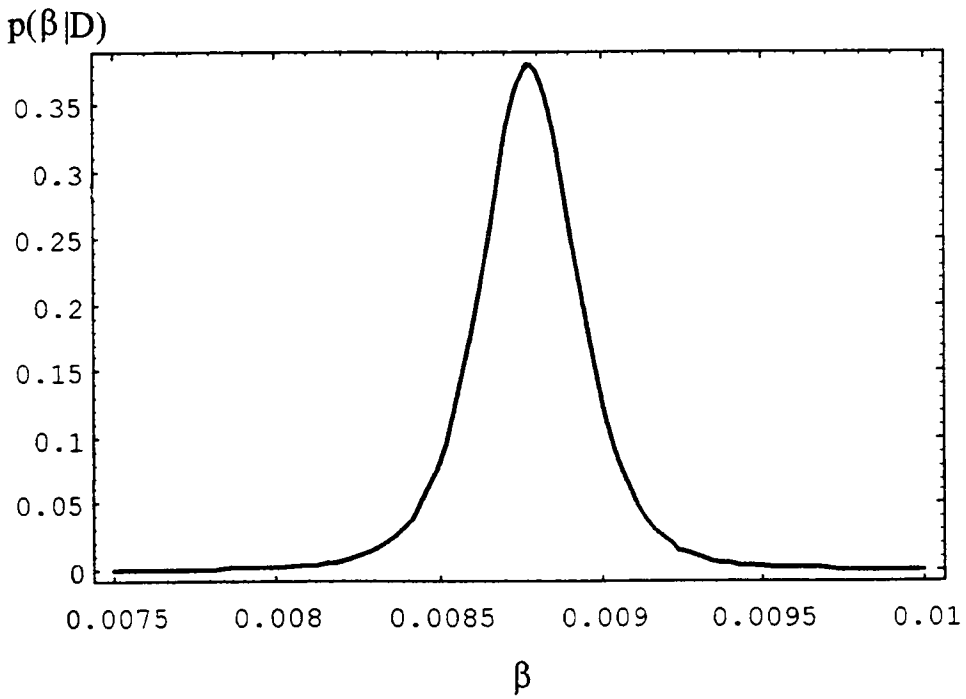


Figure 4. Posterior Distribution of β for Data Set 1 Without Dose Uncertainty.

by Eqn (19). The mode appears to be at 0.00877 which agrees very closely with the maximum likelihood of 0.00878. As more data is collected, the distributions for α and β will become narrower and will be a better approximation of the true value.

Figure 5 shows the probability distribution of the standard deviation. As the plot exhibits, the standard deviation is skewed to the right. The mode appears to be at approximately 0.0245 which would give a variance to be approximately 6.00×10^{-4}. If the standard deviation is assumed to be 0.0245, then the relative error about the data is less than 10% for each value of Y_i.

Calibrative Distributions

The calibrative distributions in this controlled calibration experiment can be calculated for various values of Y_f where Y_f is defined as the future number of

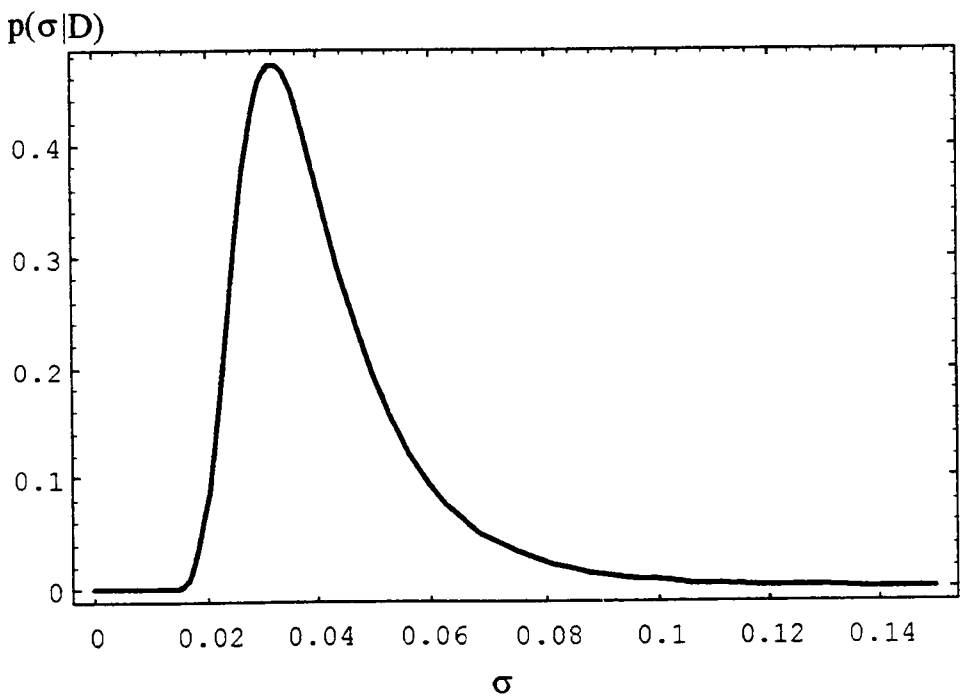


Figure 5. Posterior Distribution of σ for Data Set 1 Without Dose Uncertainty.

dicentrics per cell. The dose can be calibrated given that the radiation is of similar quality and type. As the dose increased, Y_f, the number of dicentrics/cell, is also increased. This is consistent with the sample data set in Table 1. These results show that an increase in radiation dose leads to an increased number of aberrations per cell. Chromosome aberrations considered here are dicentrics. The calibrative distributions behave as expected (as Y_f was increased, the estimated dose increased). This is demonstrated in the figures on the following pages.

Figure 6 shows the calibrative distribution when $Y_f = 0.5$. The plot shows that the dose is estimated to be about 60 Rad. When $Y_f = 1.0$, the calibrative distribution shown in Figure 7 shows the dose to be approximately 120 Rad. In Figure 8, the calibrative distribution with $Y_f = 1.5$ indicates that 175 Rad would be a good estimate for the dose. The dose is estimated to be 230 Rad when $Y_f = 2.0$ as shown by the calibrative distribution in Figure 9. Figure 10 indicates that the dose is approximately 290 Rad as the calibrative distribution shows when $Y_f = 2.5$. Last, Figure 11 shows the calibrative distribution when $Y_f = 3.0$ with a dose estimate of 350 Rad.

Table 2 is the second sample data set of a controlled calibration experiment. The data is based on the analysis of dicentric chromosome aberrations in a sample of rabbit blood lymphocytes exposed to low doses of a ^{252}Cf neutron source (Inoue, 1995).

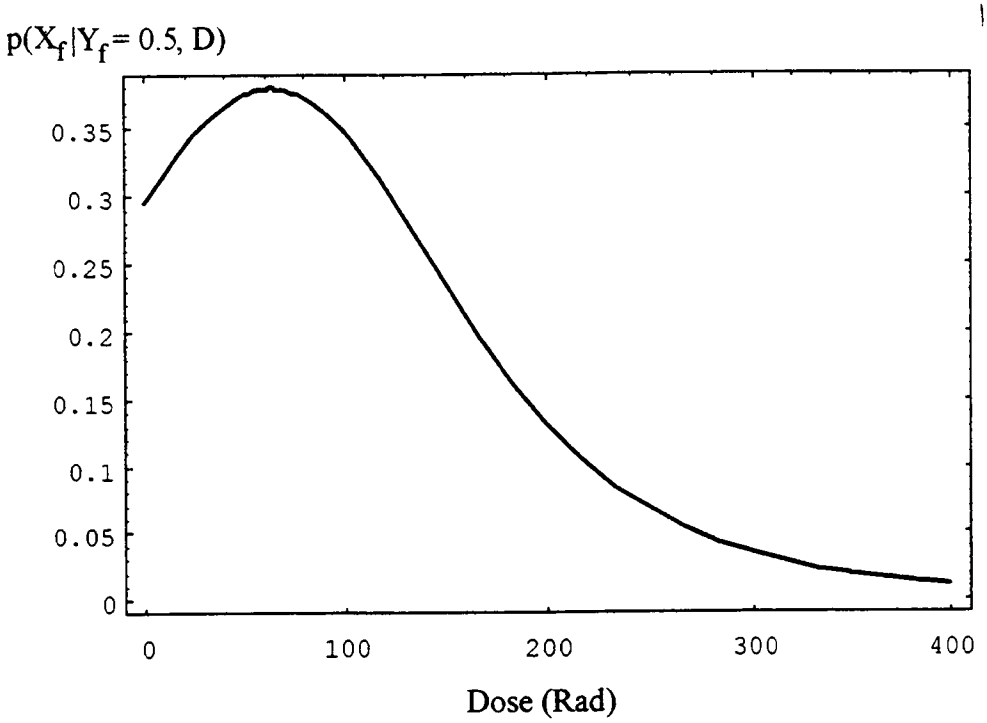


Figure 6. Calibrative Distribution with $Y_f = 0.5$ for Data Set 1 Without Dose Uncertainty.

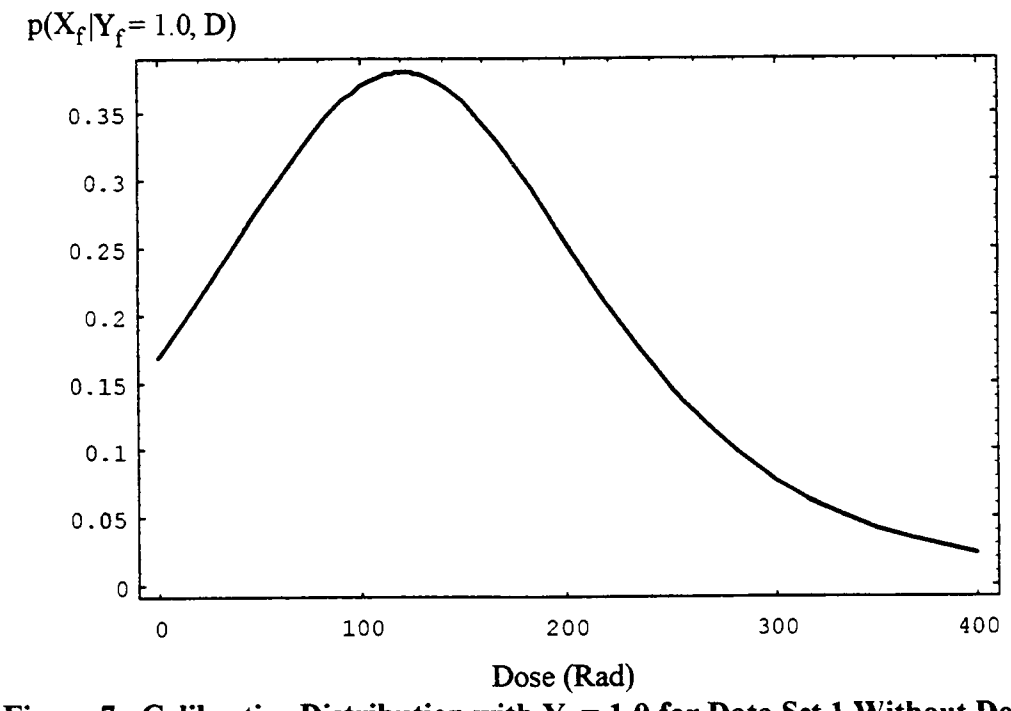


Figure 7. Calibrative Distribution with $Y_f = 1.0$ for Data Set 1 Without Dose Uncertainty.

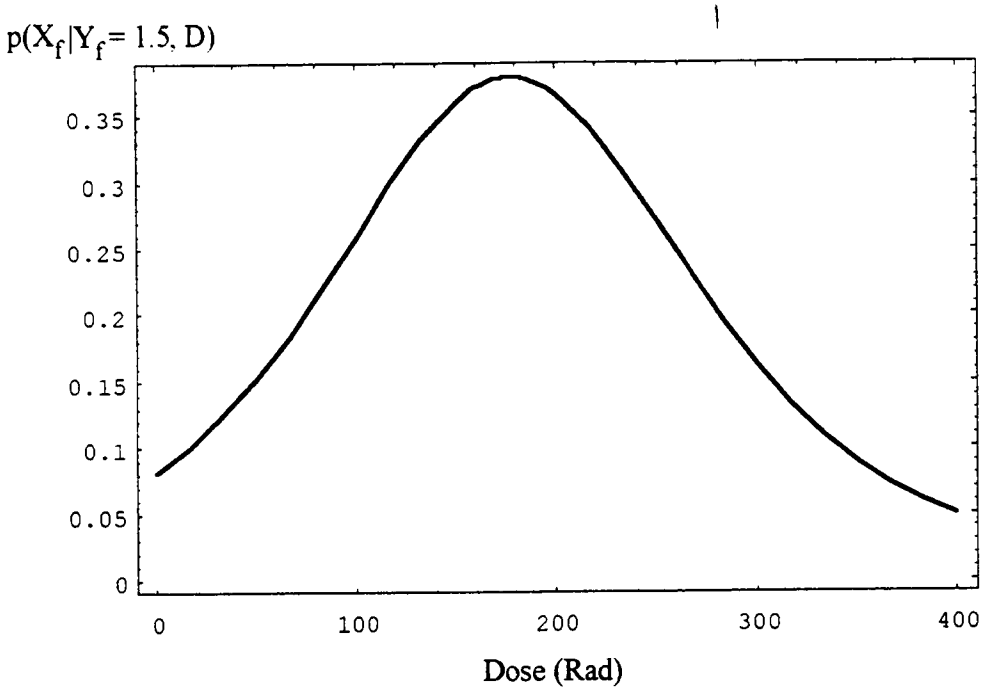


Figure 8. Calibrative Distribution with $Y_f = 1.5$ for Data Set 1 Without Dose Uncertainty.

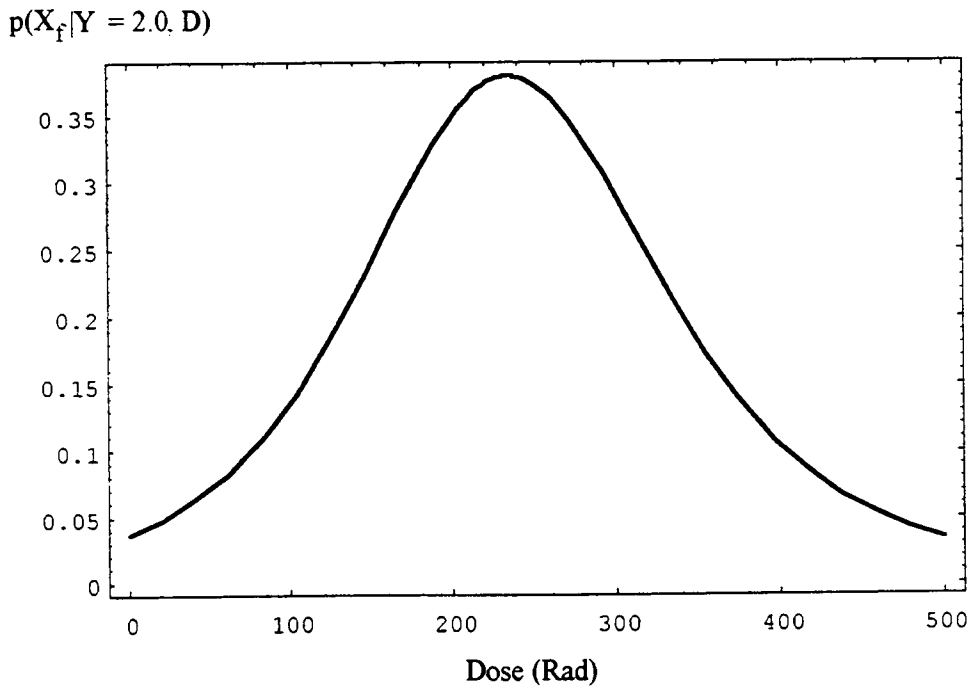


Figure 9. Calibrative Distribution with $Y_f = 2.0$ for Data Set 1 Without Dose Uncertainty.

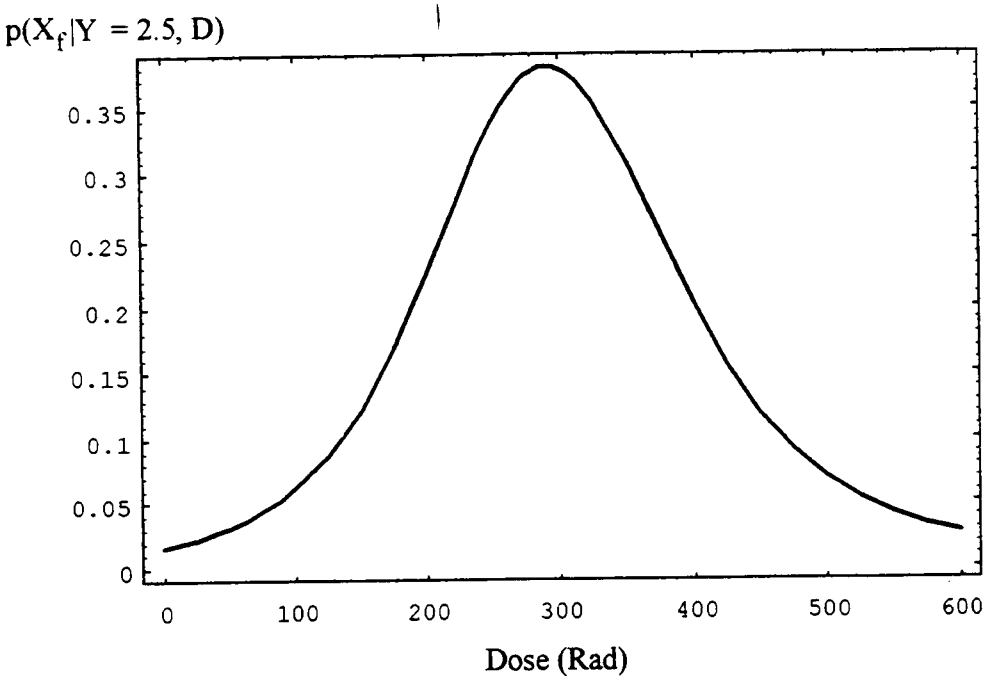


Figure 10. Calibrative Distribution with $Y_f = 2.5$ for Data Set 1 Without Dose Uncertainty.

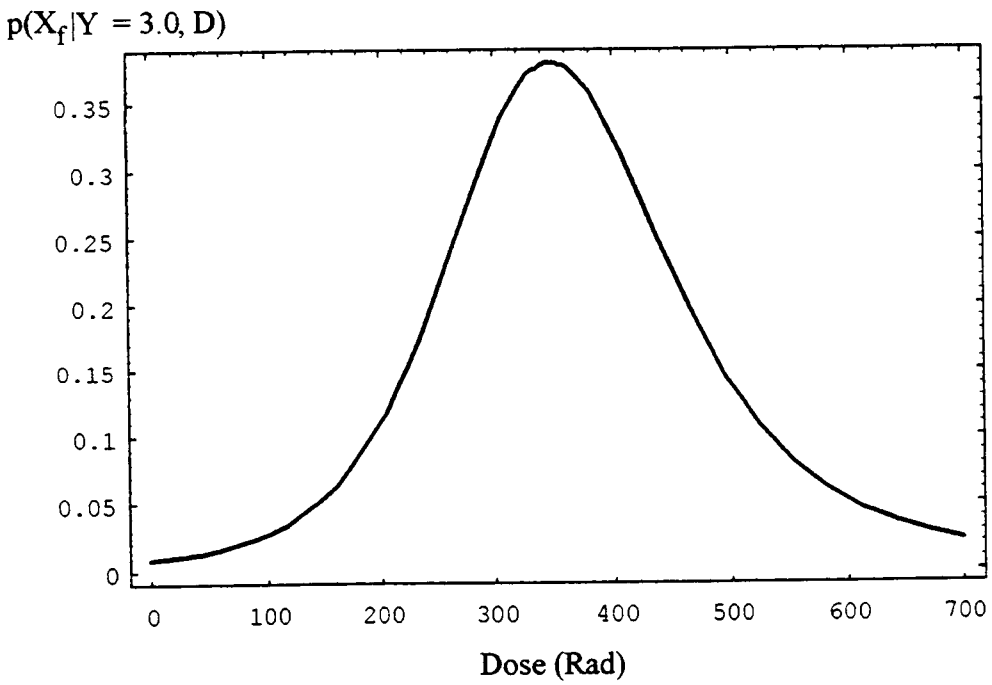


Figure 11. Calibrative Distribution with $Y_f = 3.0$ for Data Set 1 Without Dose Uncertainty.

Table 2. Data Set 2: Observed Dose and Chromosome Dicentrics in Rabbit Blood Lymphocytes.

	Dose (Rad)	*# of Cells*	*# of Dicentrics*	*Dicentrics/Cell*
i	X_i	N_i	y_i	Y_i
0	0	16000	10	0.000625
1	0.2	10000	35	0.0035
2	0.5	9300	70	.0075268817
3	0.75	4660	47	0.0100858369
4	1.0	2477	39	0.0157448526
5	2.0	708	24	0.0338983051

We will assume that the background rate for dicentric aberrations is negligible and will not include it in the analysis of the data. The data of Table 2 have been plotted in Figure 12 to give a scatter diagram. From an inspection of this scatter diagram, it is seen that the points closely follow a straight line, indicating that the assumption of linearity between the two variables appears to be reasonable. Figure 12 depicts the fitted regression line, namely

$$\mu_{Y_i|X_i} = \hat{\alpha} + \hat{\beta} X_i . \tag{48}$$

We also want to know the probability distributions of the parameters to draw inferences about the precision of the parameter estimates. Using Eqns (15) through (17), the probability distribution of α is shown in Figure 13. The maximum value occurs at zero and the expectation of α is positive and can be used as a point estimate for α. Figure 14 shows the probability distribution of β. The mode appears to be at 0.0172 which agrees with the maximum likelihood of 0.0172. As more data is

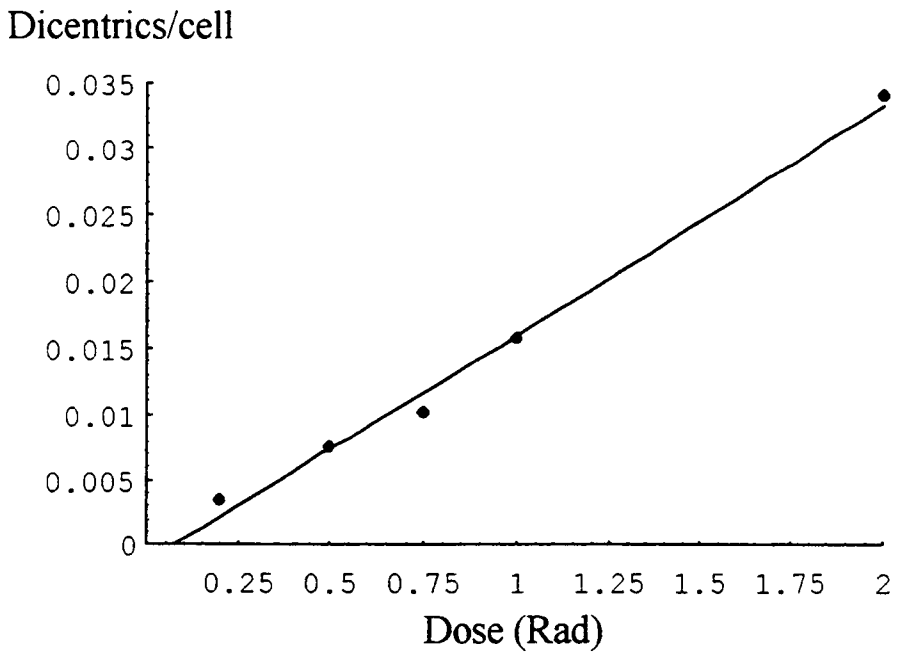


Figure 12. Scatter Diagram Data Set 2 With Regression Line.

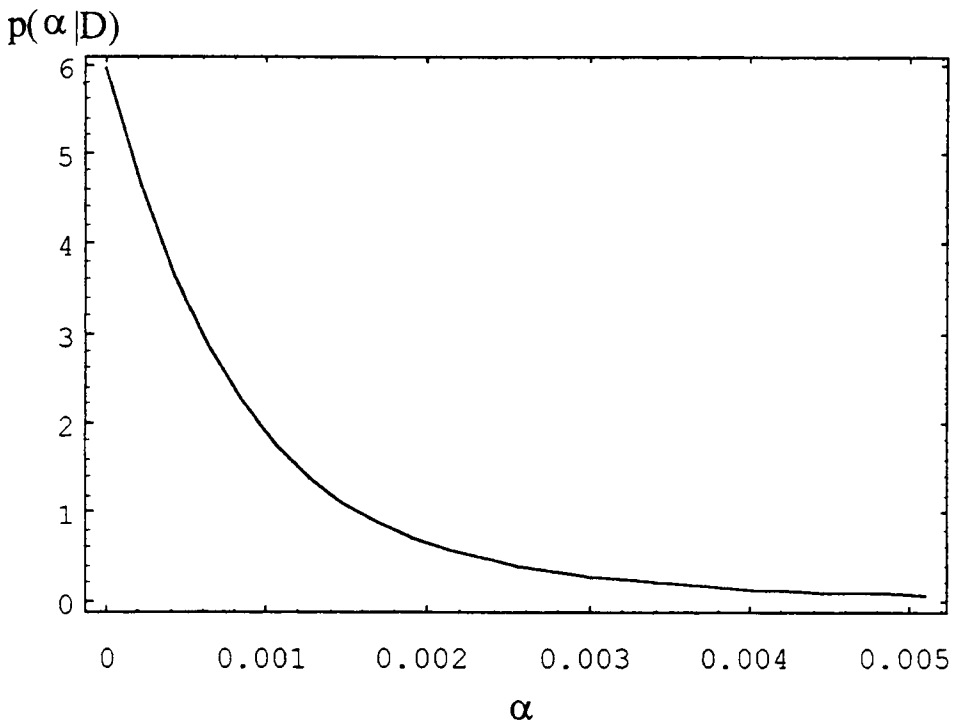


Figure 13. Posterior Distribution of α for Data Set 2 Without Dose Uncertainty.

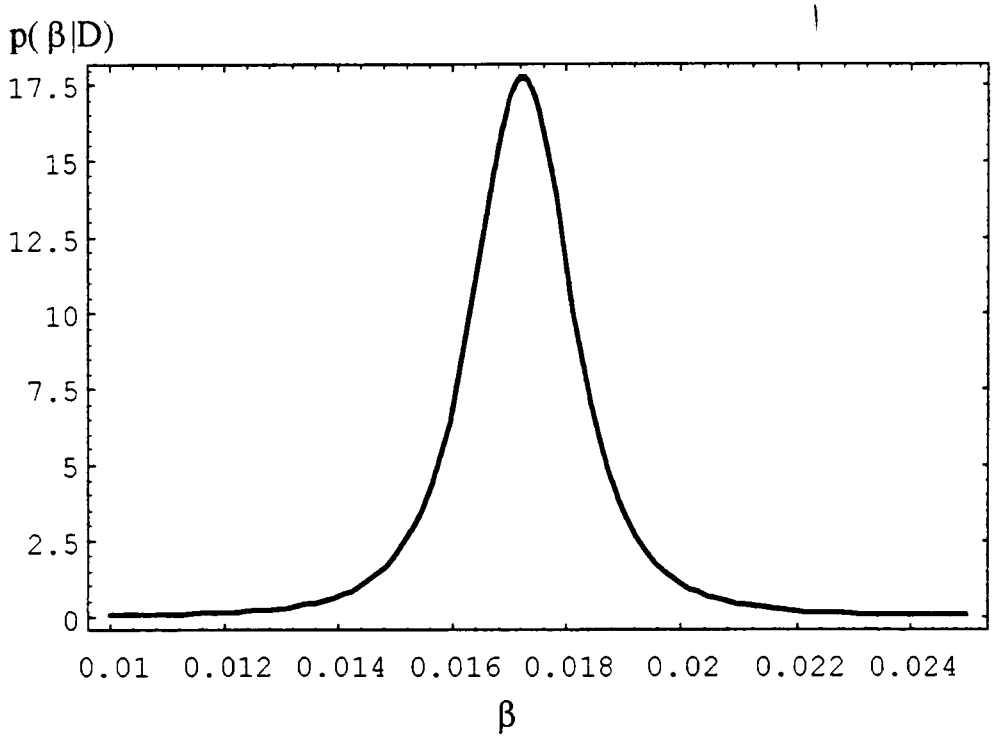


Figure 14. Posterior Distribution for β for Data Set 2 Without Dose Uncertainty.

collected, the distributions for α and β will show increased precision and will represent better approximations of the true value.

Figure 15 shows the probability distribution of the standard deviation. As the plot exhibits, the standard deviation is skewed to the right. The mode appears to be at approximately 0.0011 which would give the variance to be approximately 1.21×10^{-6}. If the standard deviation is assumed to be 0.0011, then the relative error about the data is approximately 31% for Y_1 and less than 15% for the remaining values of Y_i.

Calibrative Distributions

The calibrative distributions in this controlled experiment can also be calculated and graphed for various values of Y_f where Y_f is the future number of

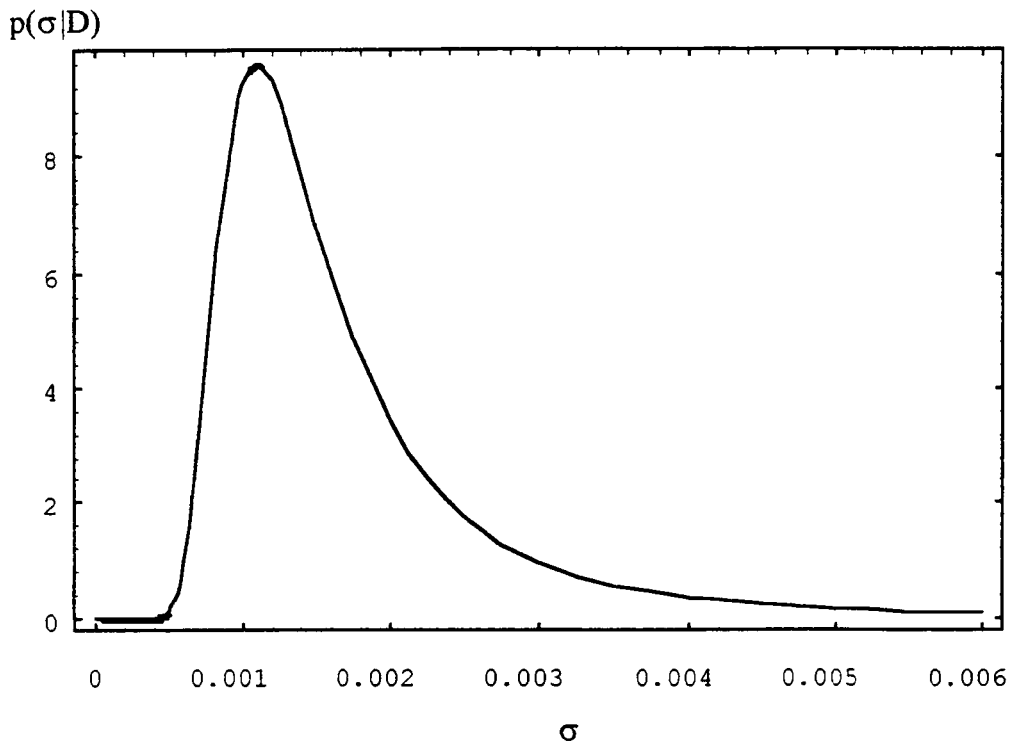


Figure 15. Posterior Distribution of σ for Data Set 2 Without Dose Uncertainty.

dicentrics/cell. As the dose increased, Y_f, the number of dicentrics/cell, also increased. This is consistent with the sample data set in Table 2. These results show that an increase in radiation dose also leads to an increased number of aberrations per cell. Chromosome aberrations in rabbit lymphocytes considered here are dicentrics. The calibrative distribution behaves as expected (as Y_f was increased, the estimated dose increased). This is demonstrated in the figures on the following pages.

Figure 16 shows the calibrative distribution when $Y_f = 0.0025$. The plot shows that the dose is estimated to be about 0.0215 Rad. When $Y_f = 0.005$, the calibrative distribution shown in Figure 17 shows the dose to be approximately 0.36 Rad. In Figure 18, the calibrative distribution with $Y_f = 0.0075$ indicates that 0.5 Rad would be

a good estimate for the dose. The dose is estimated to be 0.64 Rad when $Y_f = 0.01$ as shown by the calibrative distribution in Figure 19. Figure 20 indicates that the dose is approximately 0.94 Rad as the calibrative distribution shows when $Y_f = 0.015$. If $Y_f = 0.0175$, Figure 21 shows the calibrative distribution with a dose estimate of 1.08 Rad. Figure 22 shows the calibrative distribution when $Y_f = 0.0225$. The plot shows that a good estimate for the dose is 1.37 Rad. Last, Figure 23 shows the dose is estimated to be 1.9 Rad when $Y_f = 0.03$.

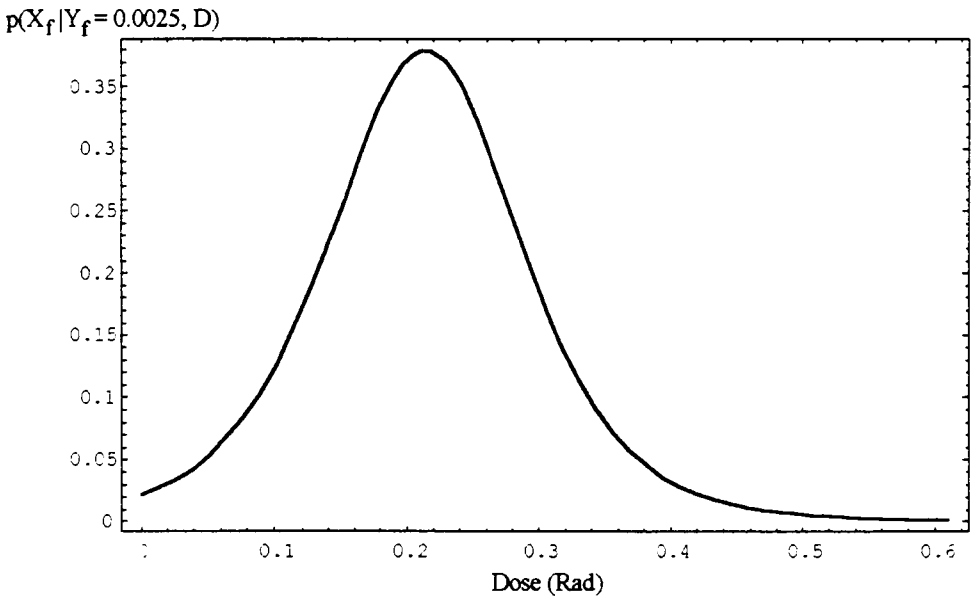


Figure 16. Calibrative Distribution with $Y_f = 0.0025$ for Data Set 2 Without Dose Uncertainty.

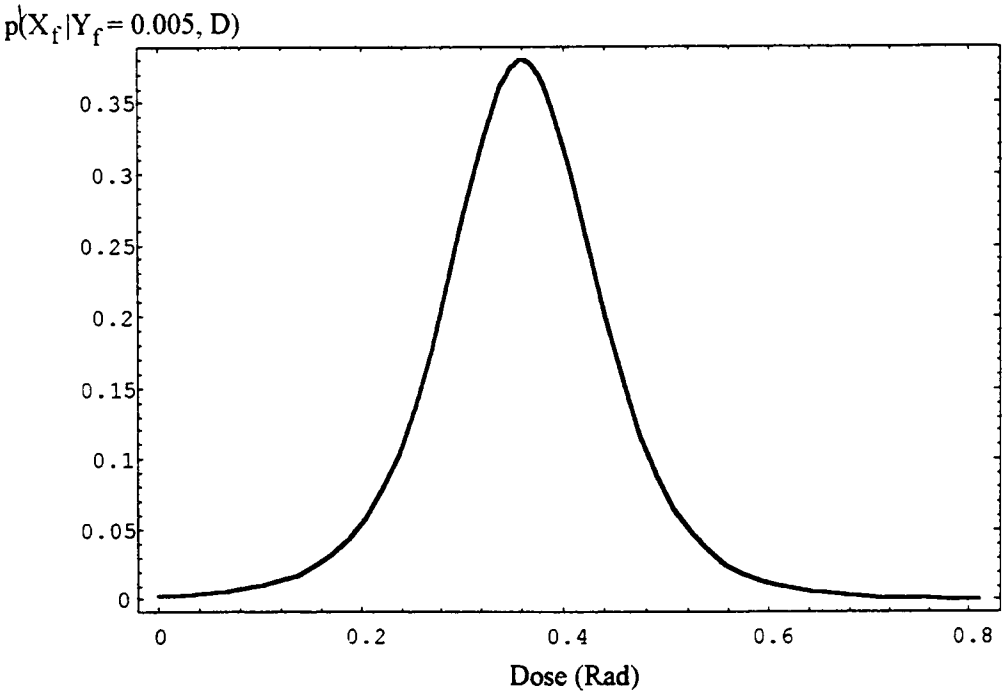


Figure 17. Calibrative Distribution with $Y_f = 0.005$ for Data Set2 Without Dose Uncertainty.

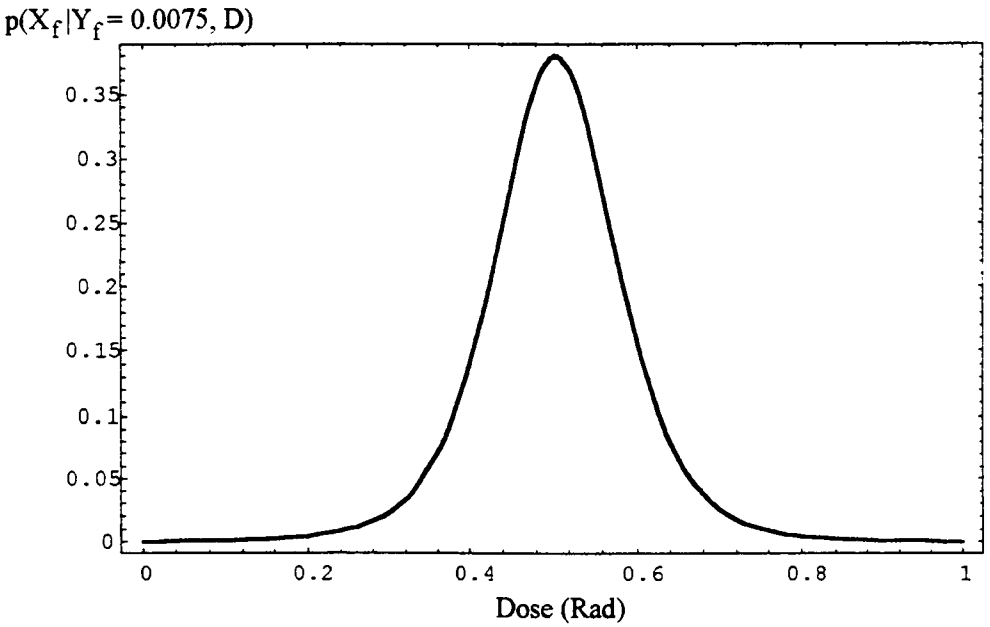


Figure 18. Calibrative Distribution with $Y_f = 0.0075$ for Data Set 2 Without dose Uncertainty.

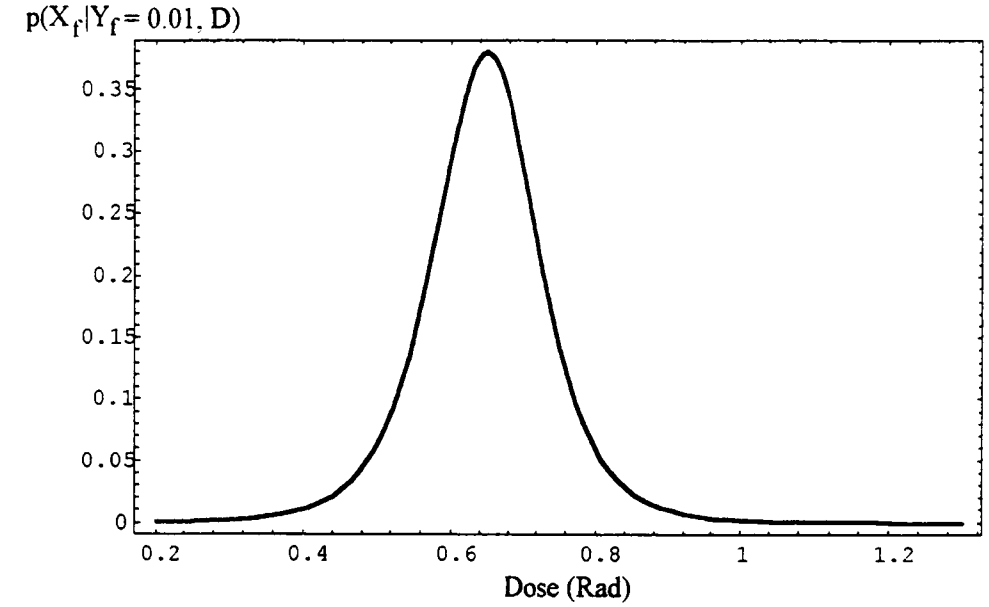


Figure 19. Calibrative distribution with $Y_f = 0.01$ for Data Set 2 Without Dose Uncertainty.

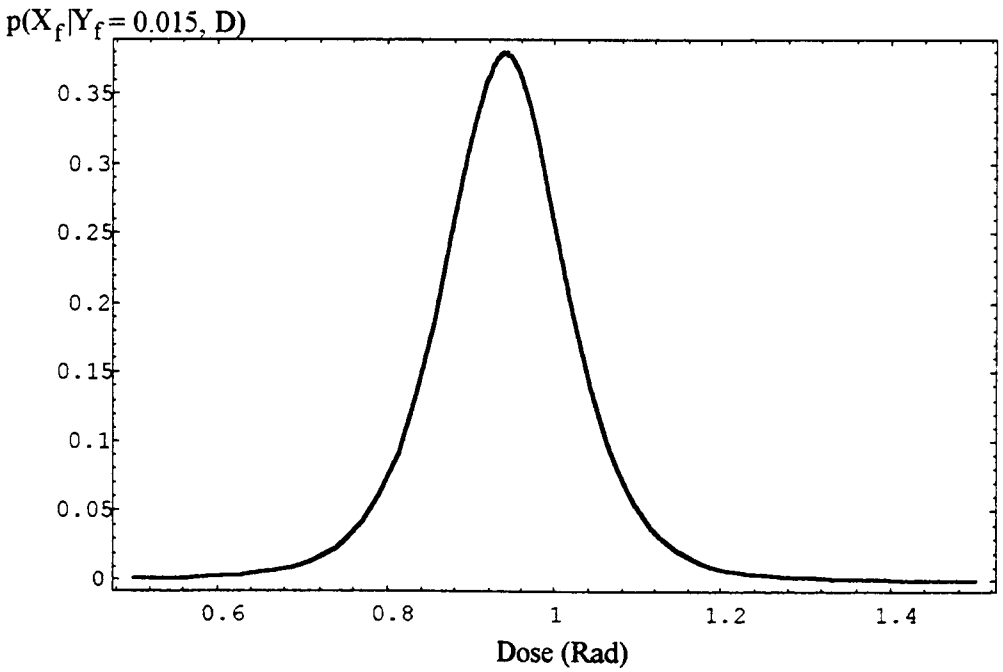


Figure 20. Calibrative Distribution with $Y_f = 0.015$ for Data Set 2 Without Dose Uncertainty.

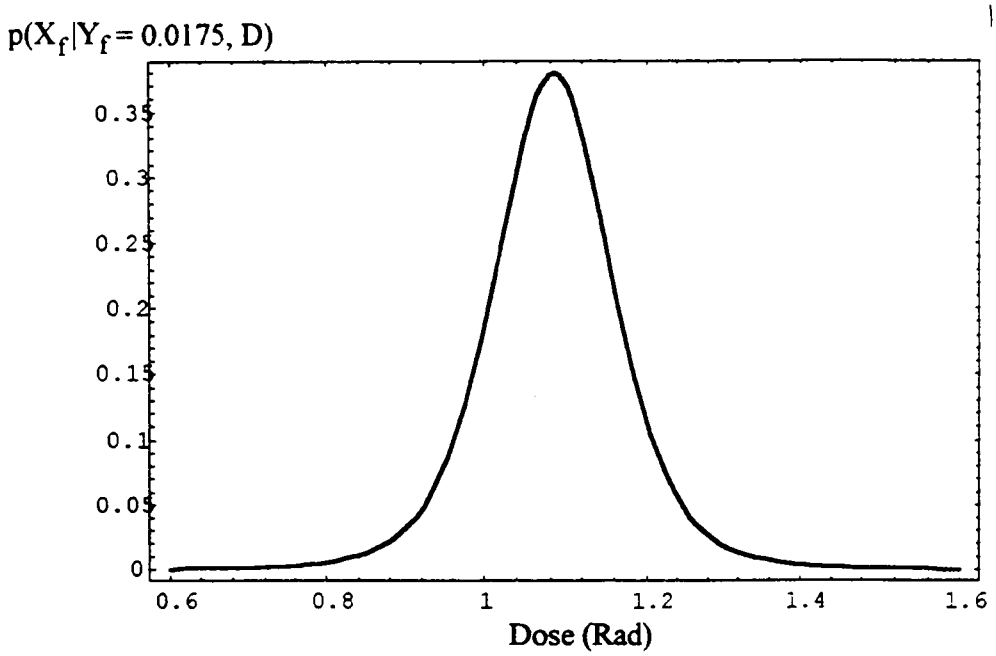


Figure 21. Calibrative Distribution with $Y_f = 0.0175$ for Data Set 2 Without Dose Uncertainty.

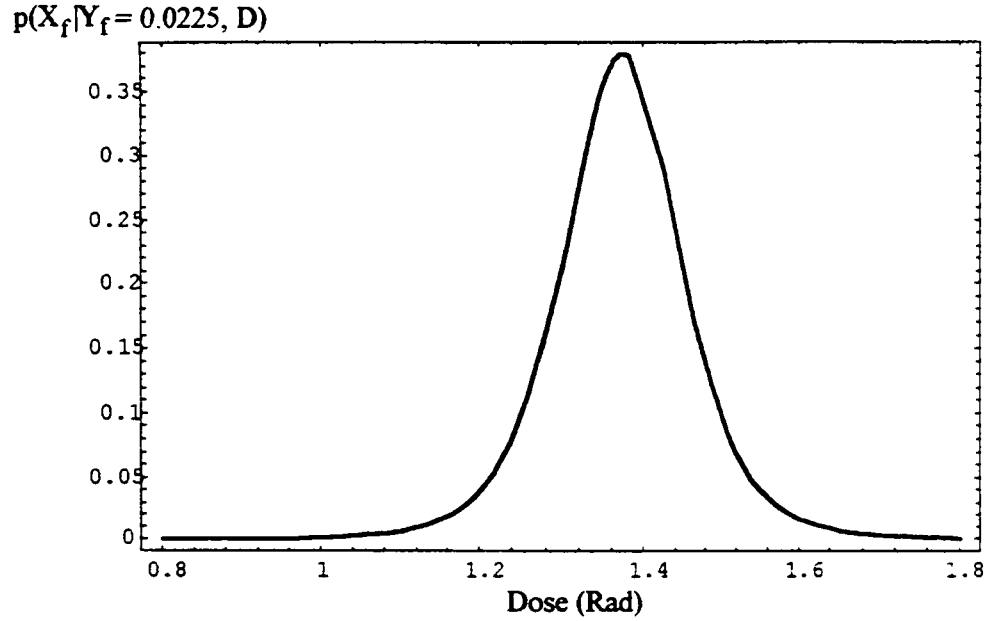


Figure 22. Calibrative Distribution with $Y_f = 0.0225$ for Data Set 2 Without Dose Uncertainty.

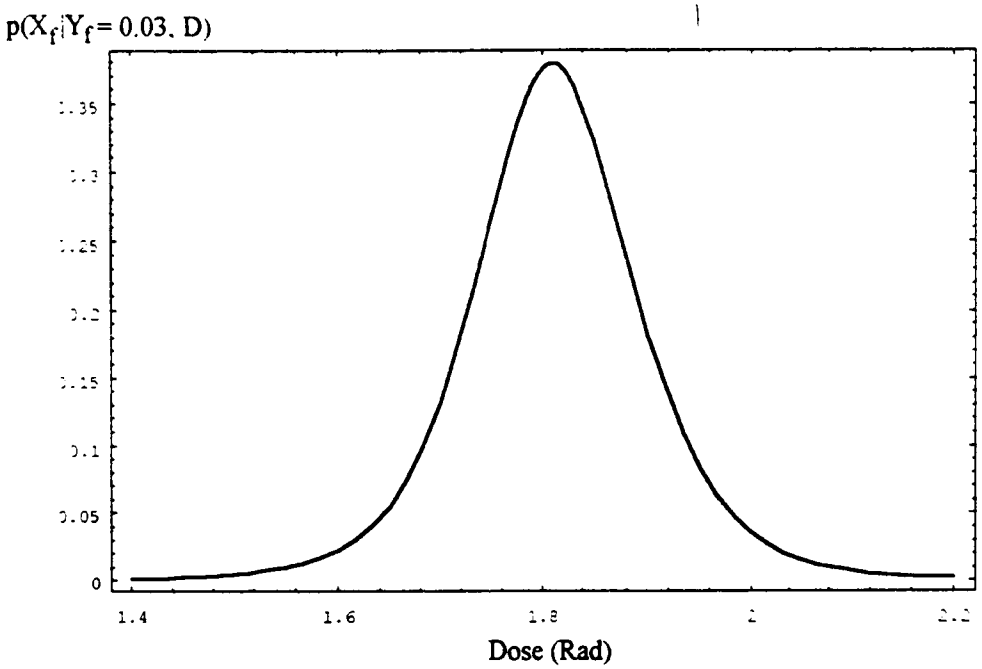


Figure 23. Calibrative Distribution with $Y_f = 0.03$ for Data Set 2 Without Dose Uncertainty.

CHAPTER V

APPLICATION OF CALIBRATION WITH DOSE UNCERTAINTY

It has been demonstrated that the estimation of the parameters can be performed without dose uncertainty. It is important to include dose uncertainty as well as uncertainty about the number of chromosome dicentrics in the calibration problem. Using the methods described in Chapter III, the posterior distributions of the parameters can be determined. Using the data set from Table 1, the following plots describe the behavior of the parameters τ, ϕ_1, ϕ_2 and θ. Figures 24, 25 and 26 show the posterior densities of τ, ϕ_1 and ϕ_2 to asymptotically approach the ordinate as the variable of interest decreases. As the variable of interest approaches zero, the posterior density increases, where the variable of interest is τ, ϕ_1 or ϕ_2. All posterior densities were obtained using Mathematica on a personal computer (PC). The posterior density of τ using 30-point Gaussian Quadrature (Appendix A1) and the Midpoint Rule method (Appendix A2) agreed with Mathematica. The three approximations yielded the same result, a curve which resembles 1/x. The posterior densities of ϕ_1 and ϕ_2 using the Midpoint Rule method (Appendix A3 and A5) and Mathematica on a UNIX workstation (Appendix A4 and A6) agreed with Mathematica. The approximations also show a curve which resembles 1/x.

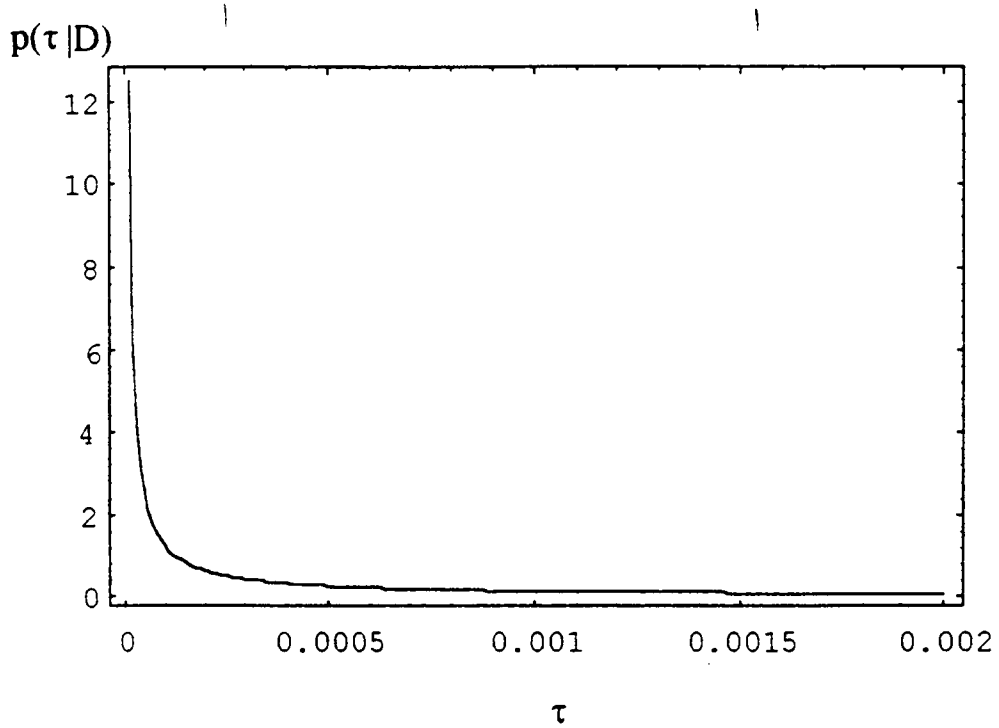


Figure 24. Posterior Distribution of τ for Data Set 1 With Dose Uncertainty.

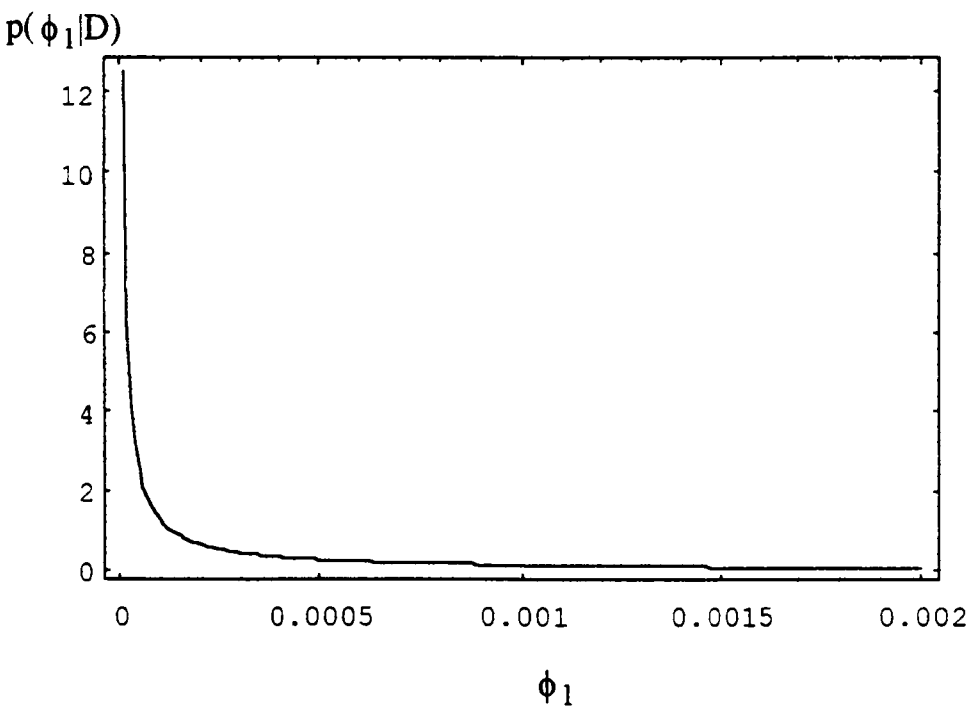


Figure 25. Posterior Distribution of ϕ_1 for Data Set 1 With Dose Uncertainty.

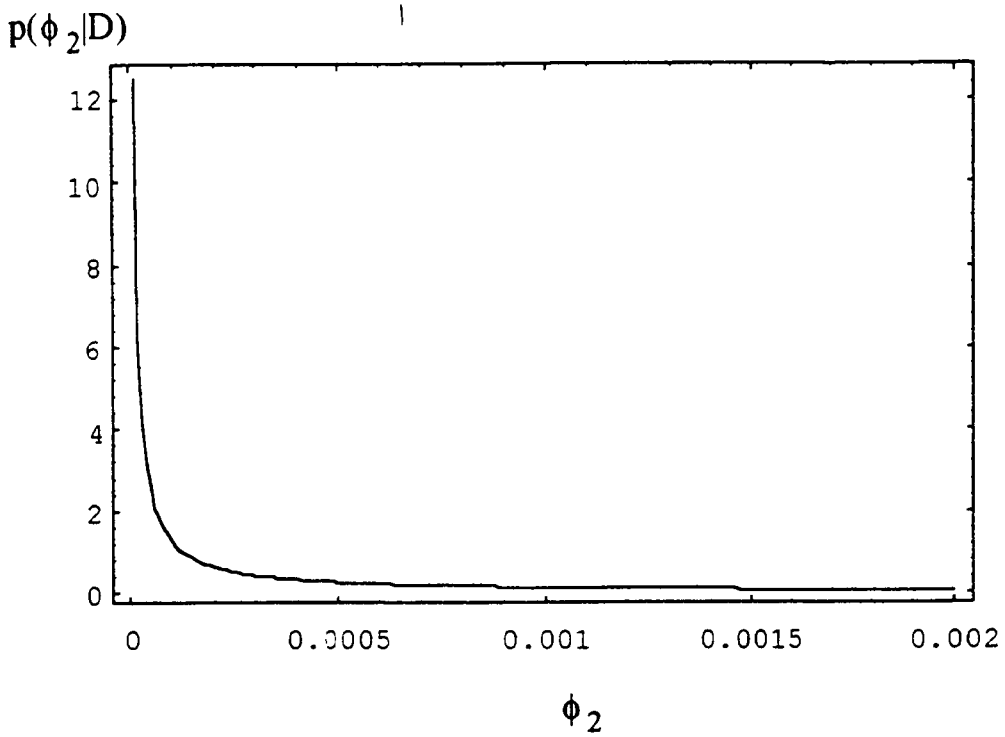


Figure 26. Posterior Distribution of ϕ_2 for Data Set 1 With Dose Uncertainty.

Figure 27 shows the posterior distribution of θ. The posterior density of the slope, θ, is found using the root of Eqn (43), θ_λ, and an estimate of Eqn (44) by numerically integrating over λ. The posterior distribution for θ peaks at 0.00849 which agrees closely with the maximum likelihood estimator of β (0.00878) where β is the slope of the linear regression line without dose uncertainty.

It has been shown that the calibrative density can be calculated with uncertainty only about the number of dicentrics per cell. It is more difficult to obtain the calibrative density with uncertainty about the number of dicentrics per cell and about the doses to which the cells were exposed. This is the more realistic problem for seldom are doses exactly known.

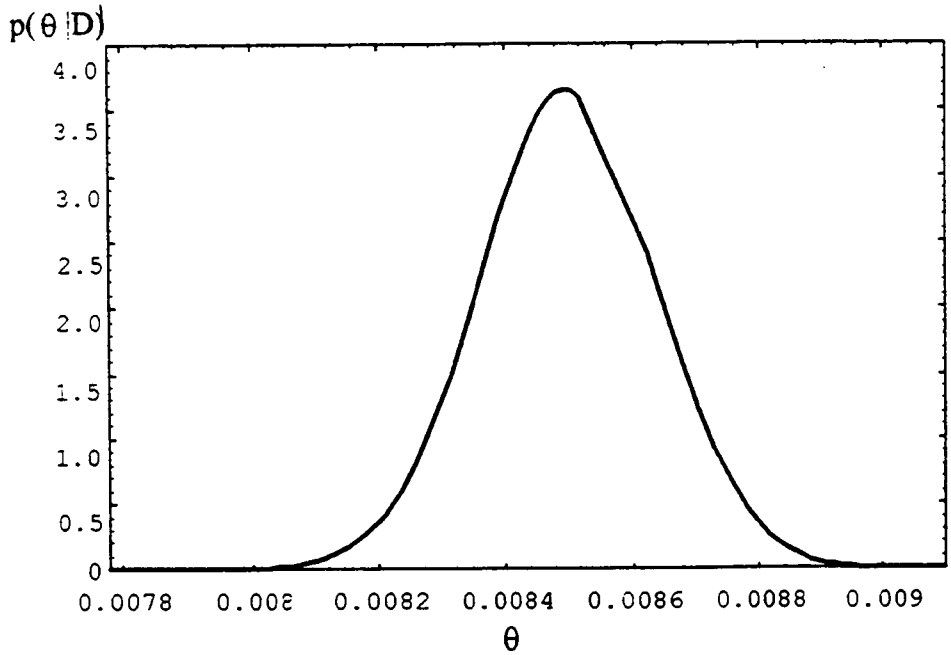


Figure 27. Posterior Distribution of θ for Data Set 1 With Dose Uncertainty.

The following figures show the calibrative density for various values of Y_f that represent the number of dicentrics per cell. The calibrative densities are approximations of Eqn (47) using 30-point Gaussian Quadrature (Appendix B4). The results agree with the calculations using the Midpoint Rule (Appendix B8). As Figure 28 illustrates, when $Y_f = 0.5$, the calibrative density peaks at 21 Rad. In Figure 29, the calibrative density peaks at 39 Rad when $Y_f = 1.0$. Figure 30 shows the calibrative distribution when $Y_f = 1.5$. The plot shows that the dose is estimated to be about 61 Rad. When $Y_f = 2.0$, the calibrative distribution shown in Figure 31 shows the dose to be approximately 73 Rad. In Figure 32, the calibrative distribution with $Y_f = 2.5$ indicates that 70 Rad would be a good estimate for the dose. The dose is estimated to be 55 Rad when $Y_f = 3.0$ as shown by the calibrative distribution in Figure 33. Figure 34 shows the calibrative distribution when $Y_f = 0.5$ using the Midpoint Rule with 40

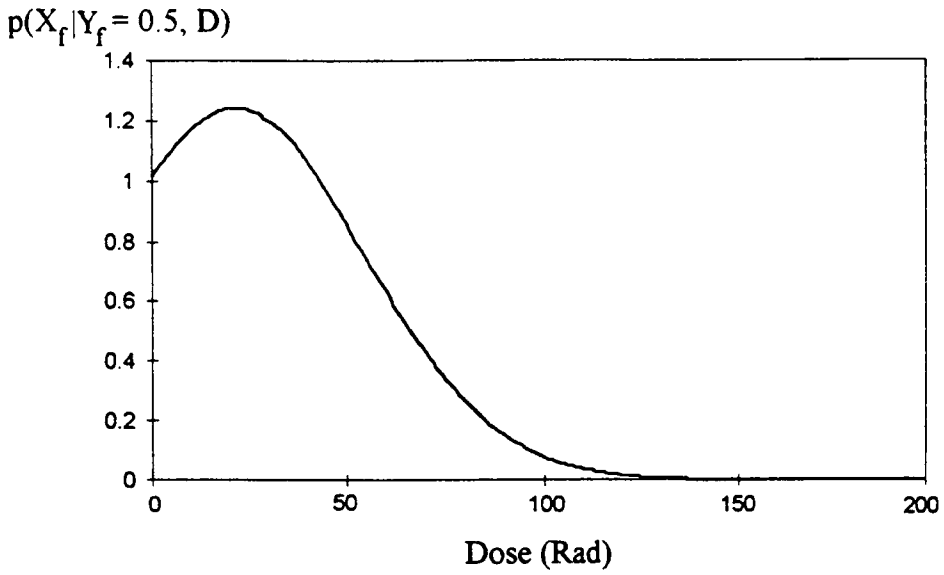


Figure 28. Calibrative Distribution with $Y_f = 0.5$ for Data Set 1 With Dose Uncertainty.

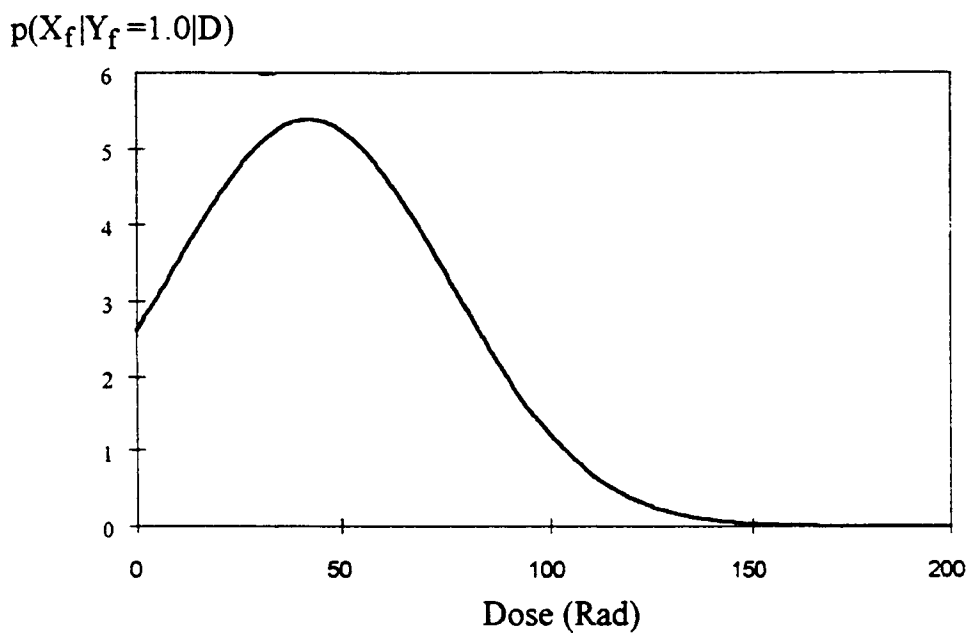


Figure 29. Calibrative Distribution with $Y_f = 1.0$ for Data Set 1 With Dose Uncertainty.

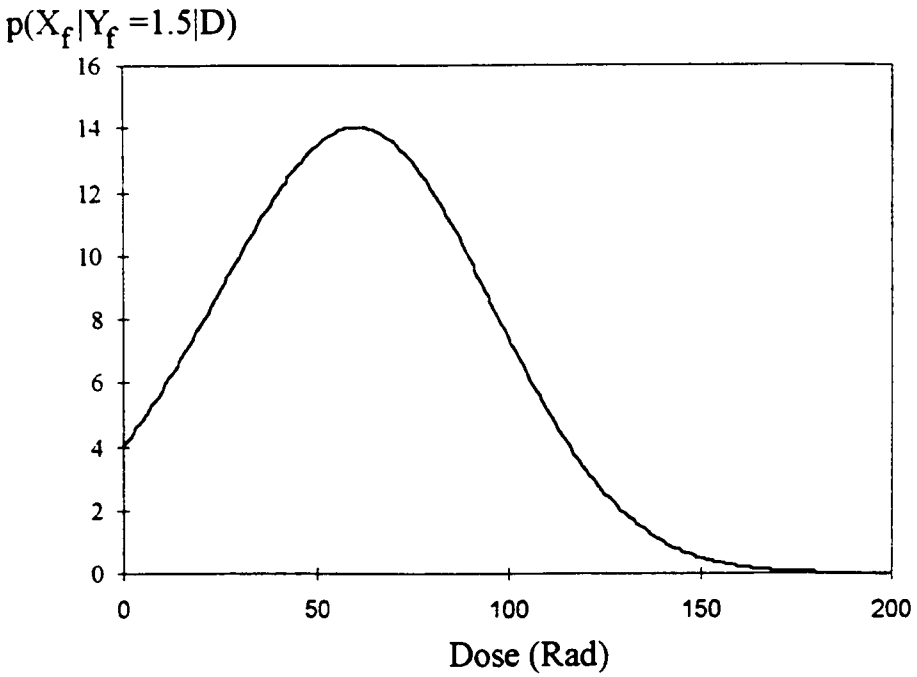


Figure 30. Calibrative Distribution with Y_f = 1.5 for Data Set 1 With Dose Uncertainty.

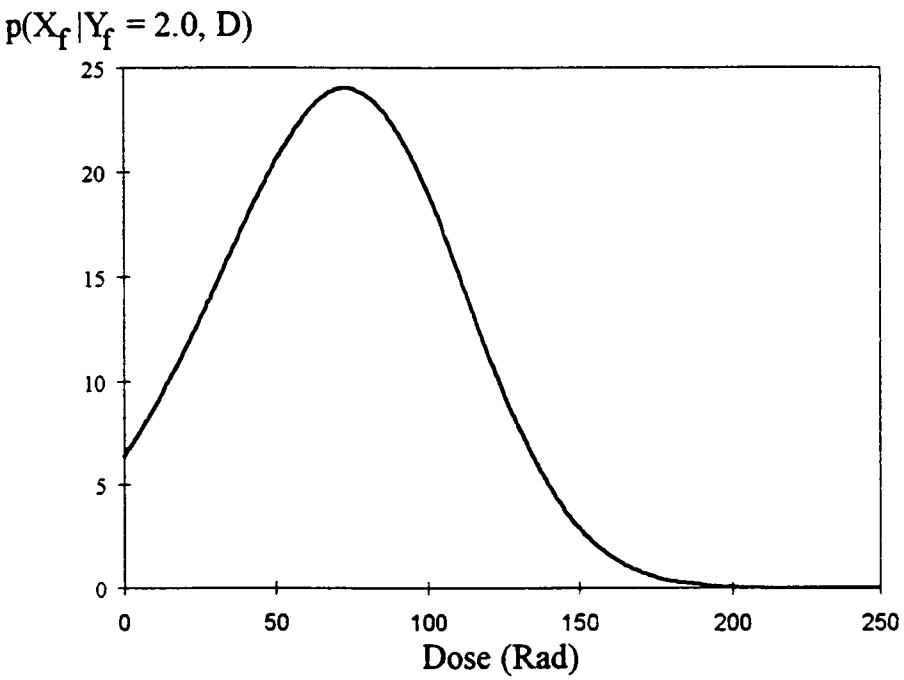


Figure 31. Calibrative Distribution with Y_f = 2.0 for Data Set 1 With Dose Uncertainty.

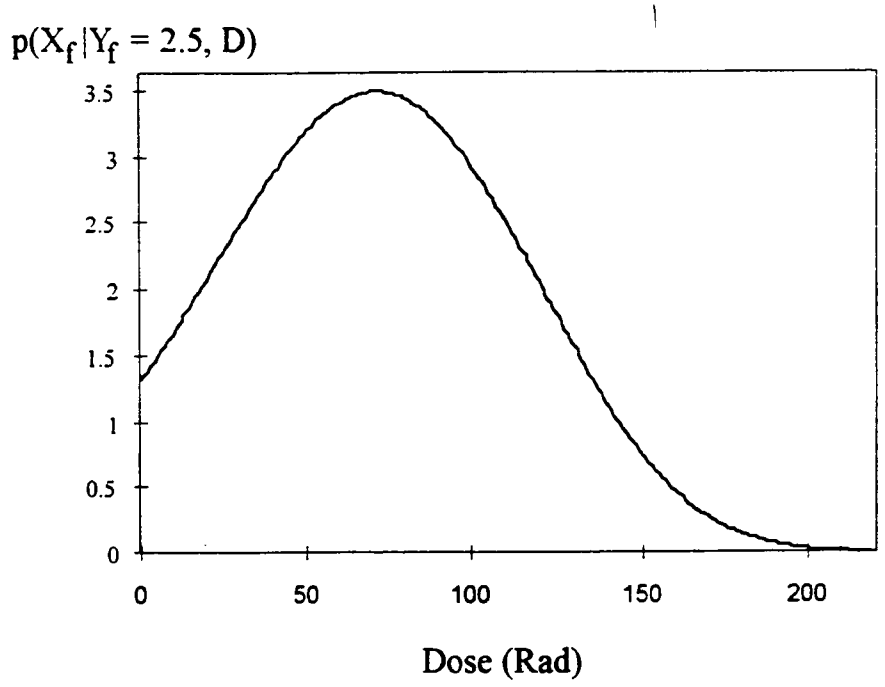


Figure 32. Calibrative Distribution with $Y_f = 2.5$ for Data Set 1 With Dose Uncertainty.

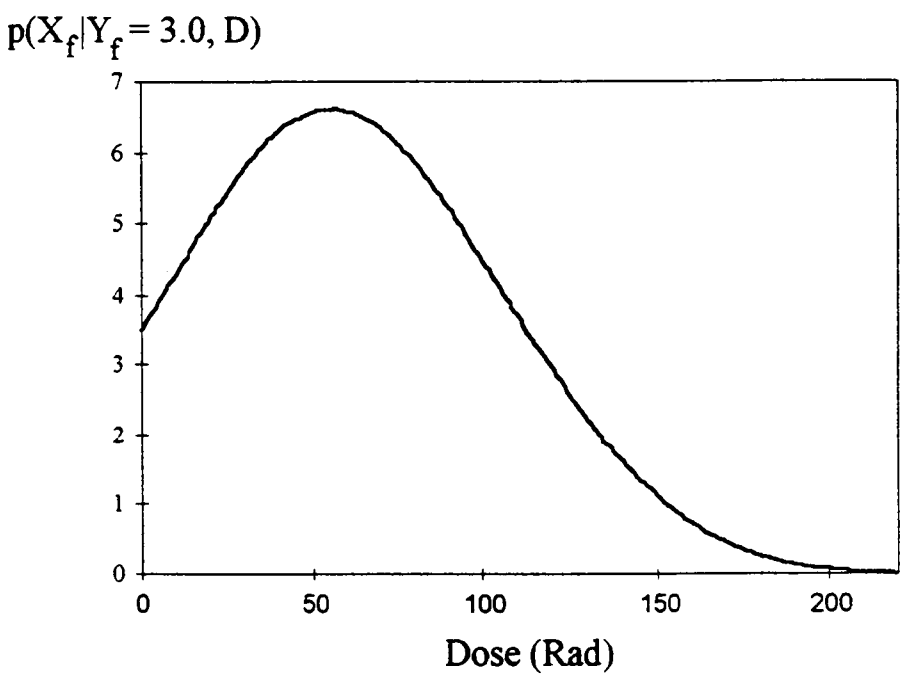


Figure 33. Calibrative Distribution with $Y_f = 3.0$ for Data Set 1 With Dose Uncertainty.

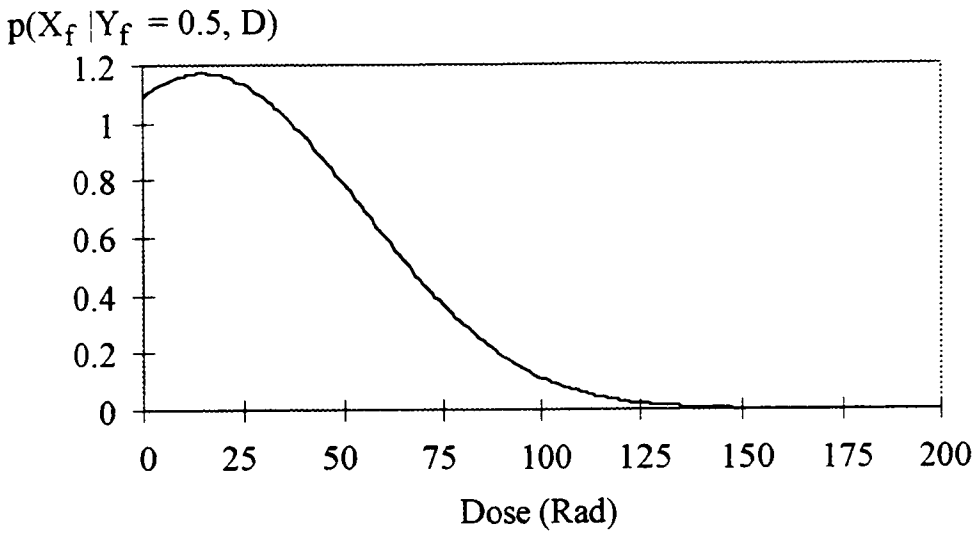


Figure 34. Calibrative Distribution When $Y_f = 0.5$ for Data Set 1 With Dose Uncertainty Using the Midpoint Rule Method.

nodes. The peak occurs at 15 Rad which is consistent with the results from 30-point Gaussian Quadrature.

While these results are conceivable, they do not agree with the calibration data set. Intuitively, one would expect the calibrative density to peak at approximately the same point as the calibrative density without dose uncertainty and one would expect a wider distribution of the dose. The wider distribution would indicate increased uncertainty about the dose which would be expected. However, these results appear to be accurate. The peaks at low values of the dose can be attributed to the uncertainty in the dose. The densities for X_f are also skewed to the right, especially for the higher values of Y_f. This implies that the means of X_f are greater than the modes. One expects the peak values to increase as Y_f increases. The peak values do increase as the number of dicentrics per cell

increases while Y_f is less than 2.5. In contrast, at $Y_f = 2.5$ and $Y_f = 3.0$ the peak values decrease. Notice that the density is more skewed to the right than the other plots show which would suggest the ratio of mean/mode (around 5) is much greater when compared to the ratio of mean/mode of the lower values of Y_f (approximately 3).

Using the data set from Table 2, the following plots describe the behavior of the parameters τ, ϕ_1, ϕ_2 and θ. Figures 35 shows the posterior density of τ to peak at approximately 0.8 using Mathematica on a personal computer. This agrees with the result using Mathematica on a UNIX workstation in which the posterior density of τ also peaks at approximately 0.8 (Appendix A7). Figure 36 shows the posterior density of ϕ_1 to asymptotically reach zero as ϕ_1 decreases. The shape using 30-point Gaussian Quadrature and the Midpoint Rule method also resembles the shape 1/x (Appendix A8 and A9). Figure 37 shows the posterior density of ϕ_2 to asymptotically reach zero as ϕ_2 decreases. This agrees with the result using 30-point Gaussian Quadrature, the Midpoint Rule method and Mathematica on a UNIX workstation (Appendix A10, A11 and A12).

The posterior density of θ, the slope, is found using Eqn (43) for θ_λ and an approximation of Eqn (44) by numerically integrating over λ. As shown in Figure 38, the posterior distribution for θ peaks at 0.0163 which agrees closely with the maximum likelihood estimator of β (0.0172) where β is the slope of the linear regression line without dose uncertainty.

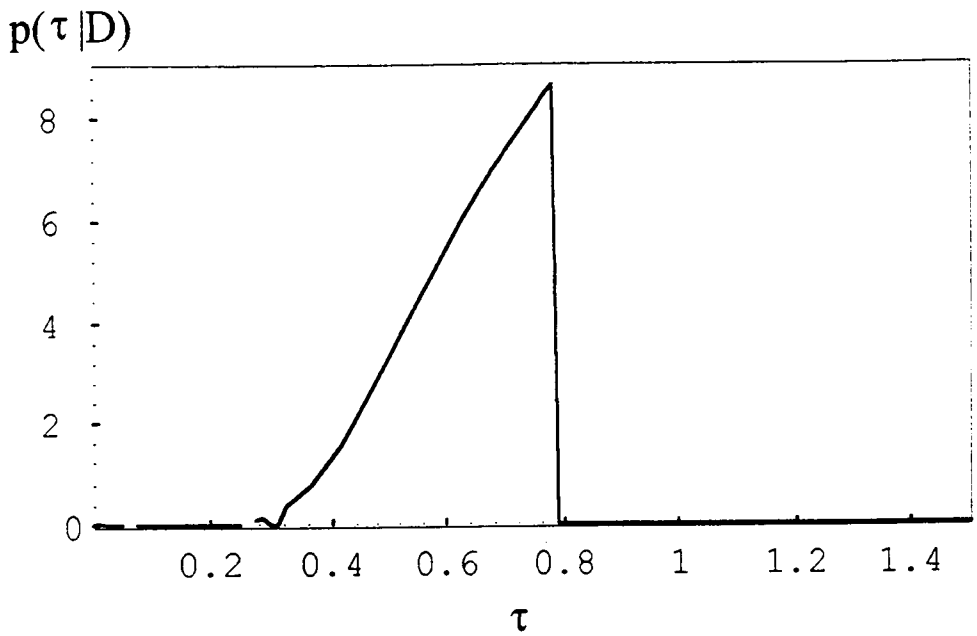


Figure 35. Posterior Distribution of τ for Data Set 2 With Dose Uncertainty.

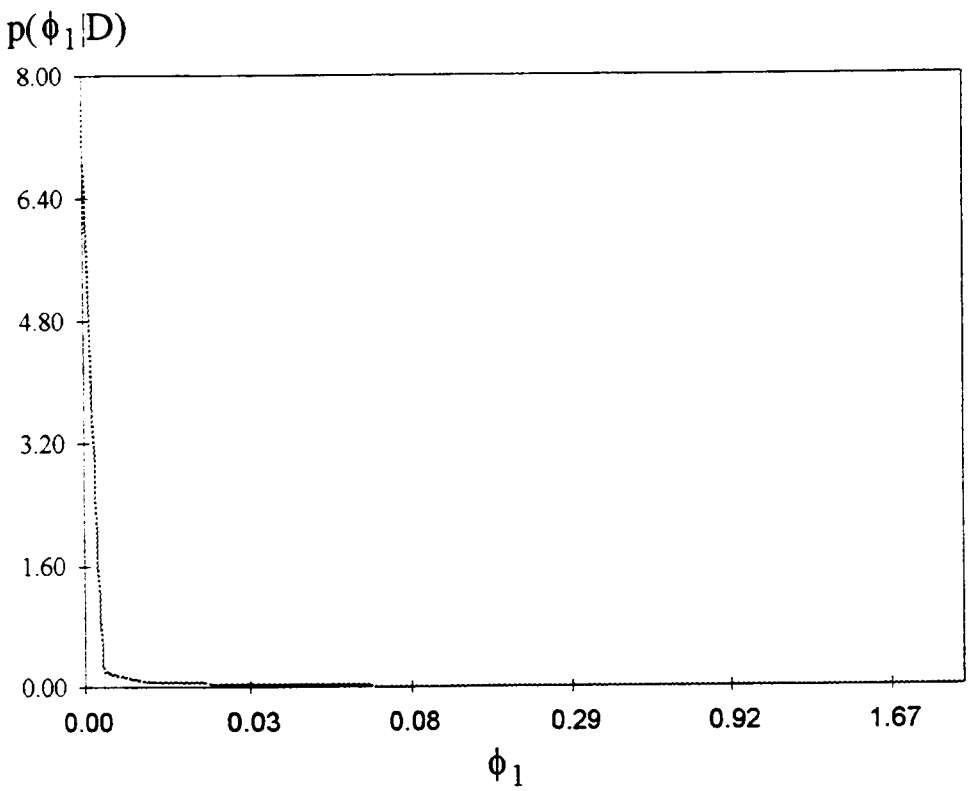


Figure 36. Posterior Distribution of ϕ_1 for Data Set 2 with Dose Uncertainty.

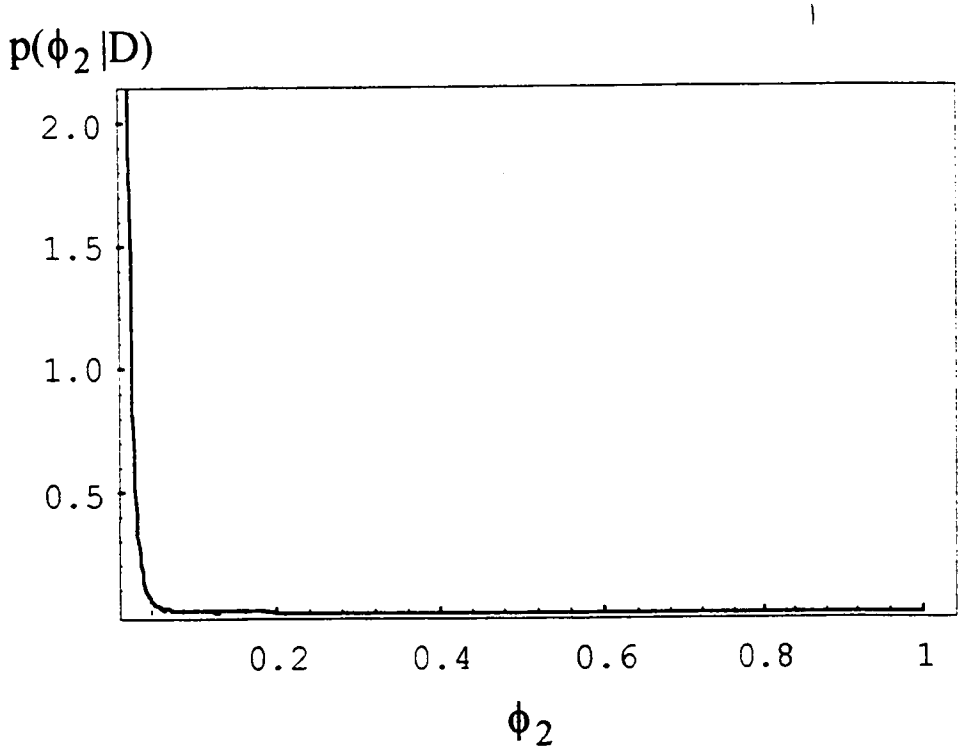


Figure 37. Posterior Distribution of ϕ_2 for Data Set 2 With dose Uncertainty.

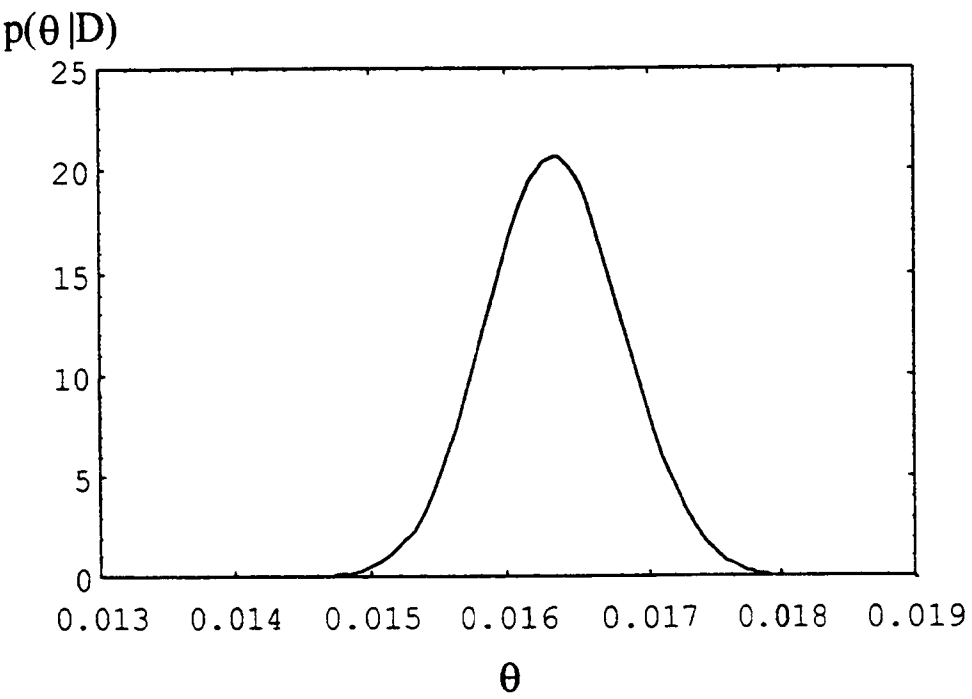


Figure 38. Posterior Distribution of θ for Data Set 2 With Dose Uncertainty.

The following figures show the calibrative density for various values of Y_f that represent the number of dicentrics per cell. The calibrative densities are approximations of Eqn (47) using 30-point Gaussian Quadrature (Appendix B4). The results agree with the calculations using the Midpoint Rule Method (Appendix B8). As Figure 39 illustrates, when $Y_f = 0.005$, the calibrative density peaks at 0.015 Rad. In Figure 40, the calibrative density peaks at 0.020 Rad when $Y_f = 0.0075$. Figure 41 shows the calibrative distribution when Yf = 0.01. The plot shows that the dose is estimated to be about 0.025 Rad. When $Y_f = .015$, the calibrative distribution shown in Figure 42 shows the dose to be approximately 0.040 Rad. In Figure 43, the calibrative distribution with $Y_f = 0.0175$ indicates that 0.045 Rad would be a good estimate for the dose. The dose is estimated to be 0.06 Rad when $Y_f = 0.0225$ as shown by the calibrative distribution in Figure 44. Figure 45 shows the calibrative distribution peak at approximately 0.09 when $Y_f = 0.03$. Figure 46 shows the calibrative distribution when $Y_f = 0.005$ using the Midpoint Rule method with 40 points. The peak occurs at 0.01 Rad which is consistent with the results from 30-point Gaussian Quadrature.

These results are conceivable but do not agree with the calibration data set. Instinctively, one would expect the calibrative density to peak at approximately the same point as the calibrative density without dose uncertainty. However, the calibrative distributions are wide which indicates an increased uncertainty about the dose which is to be expected. The results appear to be accurate because the peak

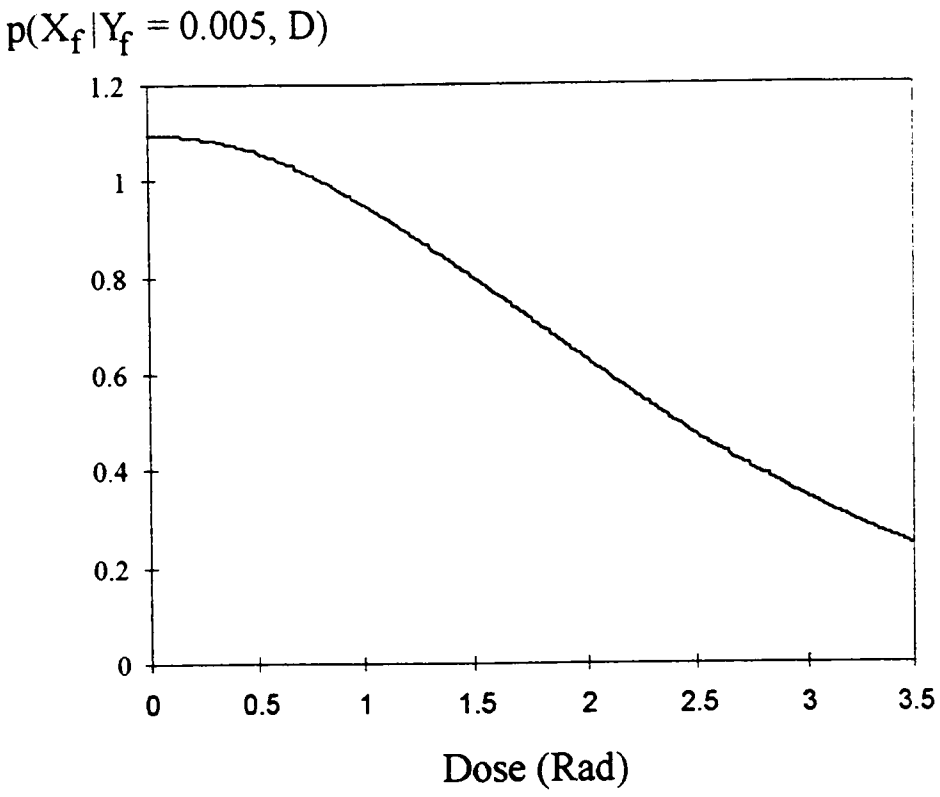


Figure 39. Calibrative Distribution When $Y_f = 0.005$ for Data Set 2 With Dose Uncertainty.

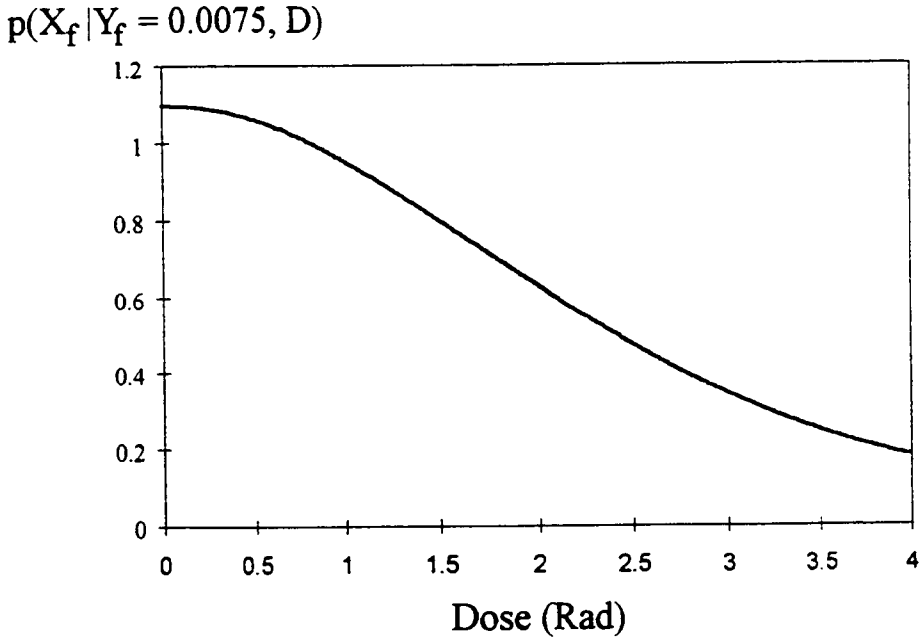


Figure 40. Calibrative Distribution When $Y_f = 0.0075$ for Data Set 2 With Dose Uncertainty.

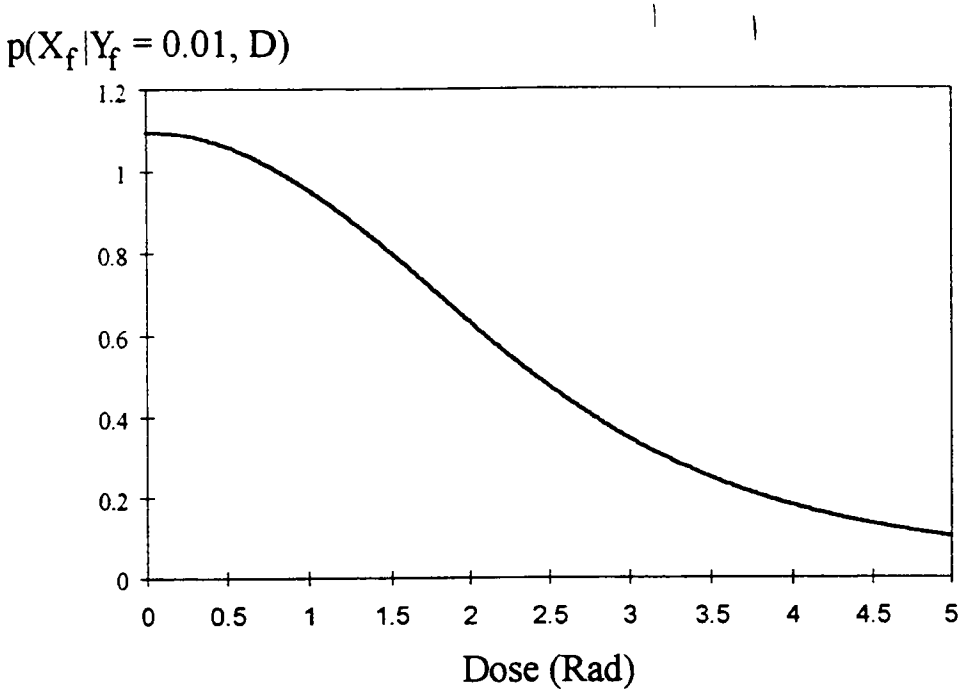


Figure 41. Calibrative Distribution When $Y_f = 0.01$ for Data Set 2 With Dose Uncertainty.

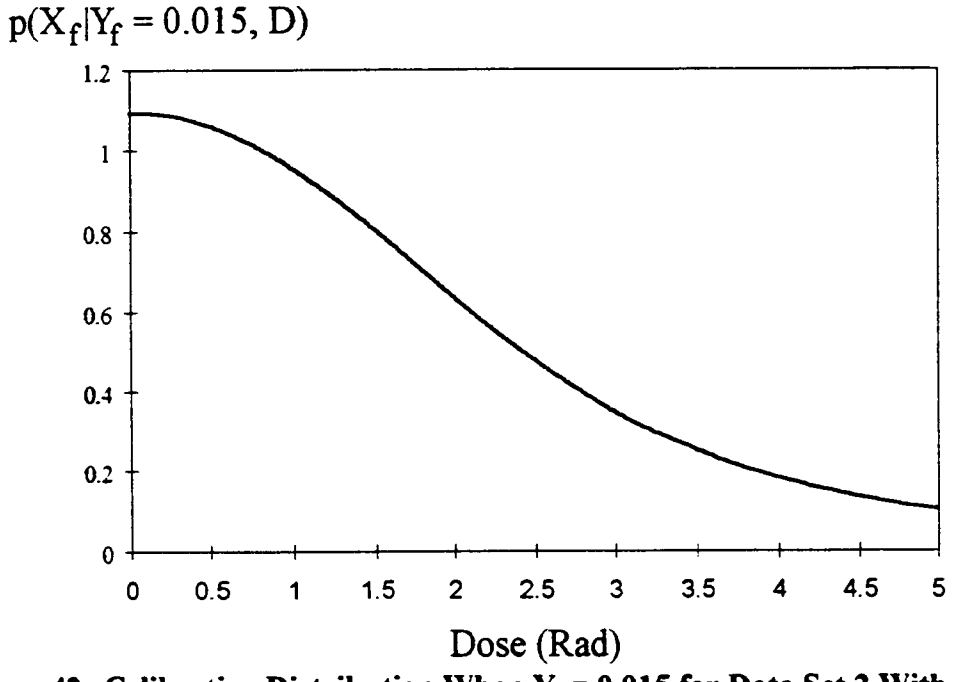


Figure 42. Calibrative Distribution When $Y_f = 0.015$ for Data Set 2 With Dose Uncertainty.

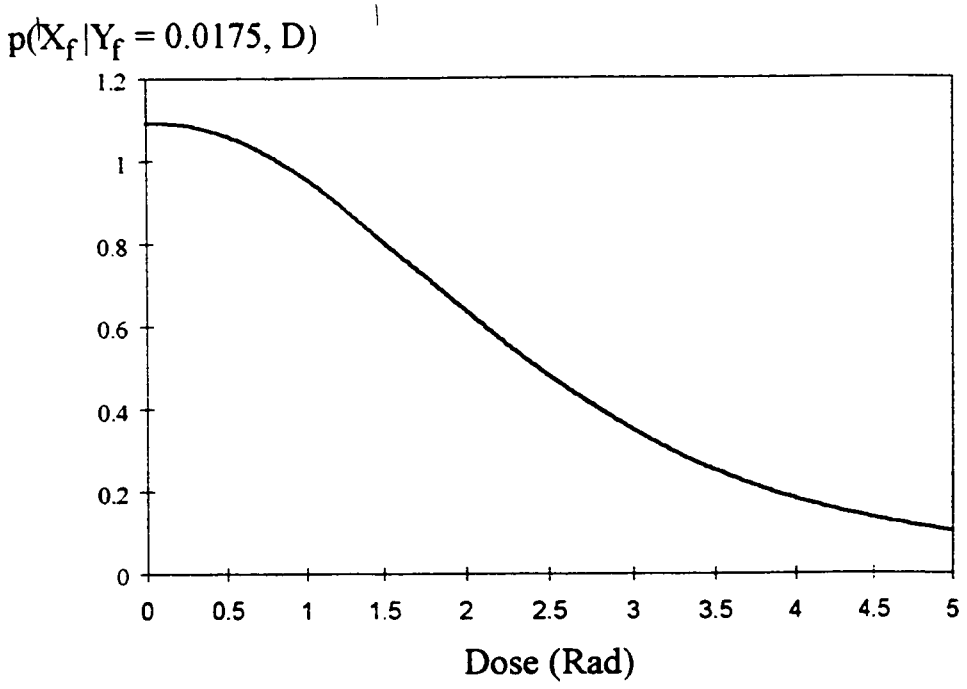


Figure 43. Calibrative Distribution When $Y_f = 0.0175$ for Data Set 2 With Dose Uncertainty.

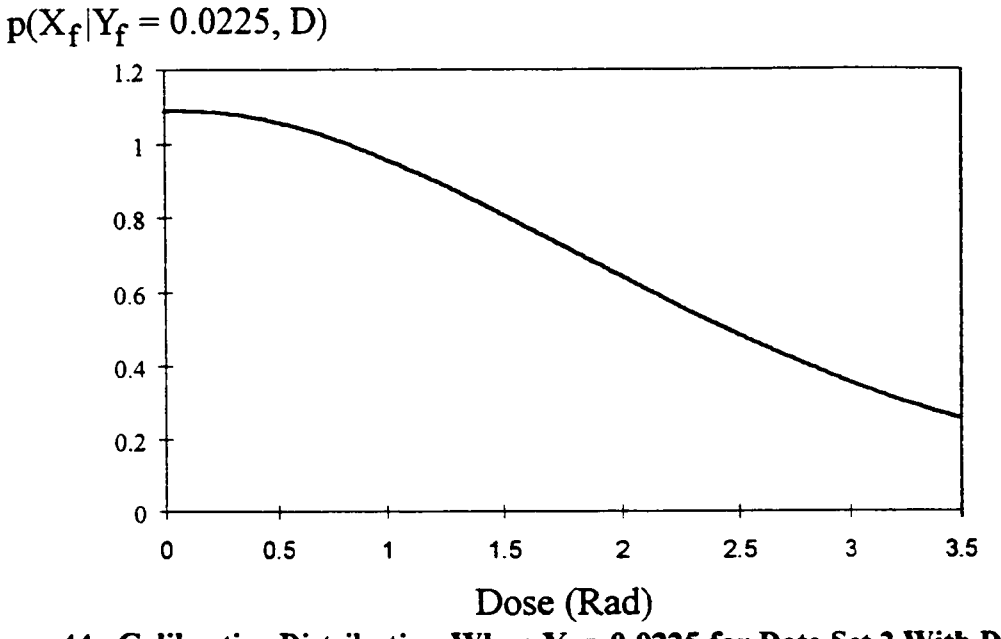


Figure 44. Calibrative Distribution When $Y_f = 0.0225$ for Data Set 2 With Dose Uncertainty.

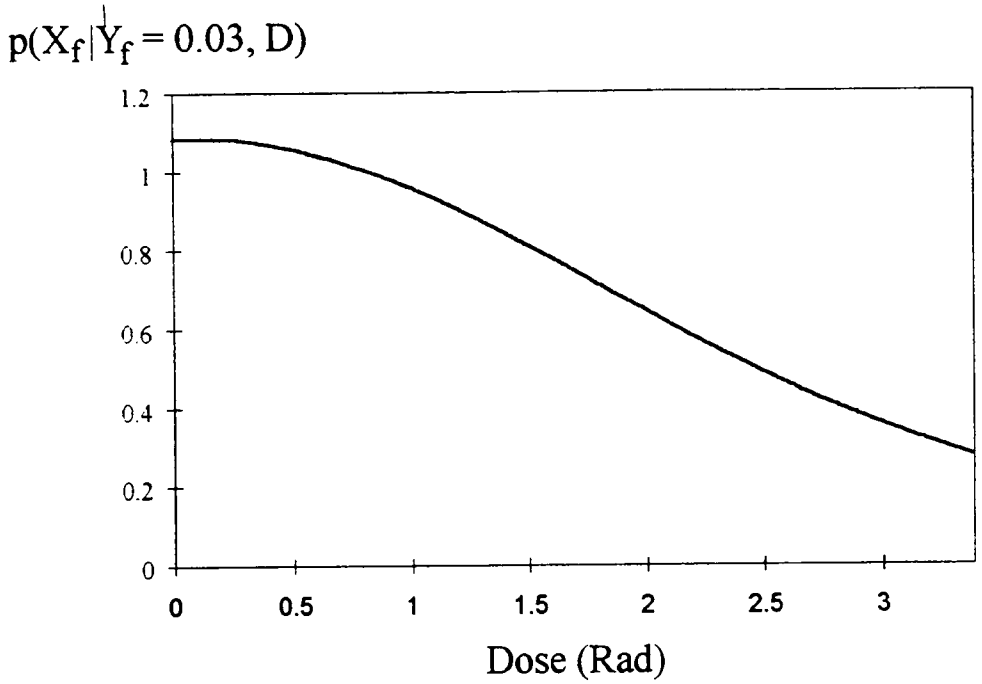


Figure 45. Calibrative Distribution When $Y_f = 0.03$ for Data Set 2 With Dose Uncertainty.

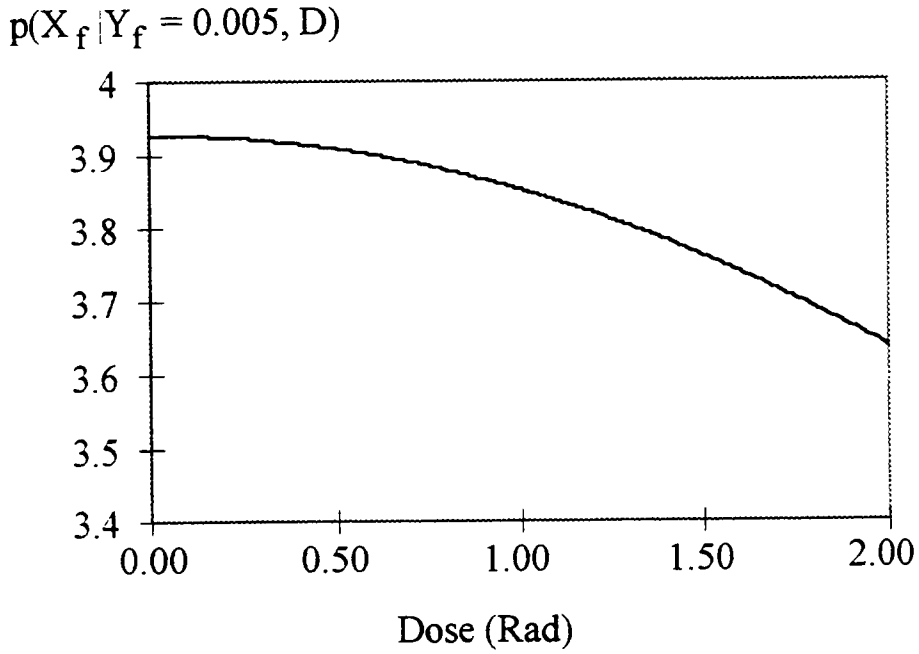


Figure 46. Calibrative Distribution When $Y_f = 0.005$ for Data Set 2 With Dose Uncertainty Using the Midpoint Rule Method.

values increase as the number of dicentrics/cell increase and the calibrative densities are very skewed to the right, implying the means of X_f are greater than the modes. Dose uncertainty may also contribute to low values of the modes.

CHAPTER VI

CONCLUSION

In this thesis, we use chromosome aberrations as a biological dosimeter and develop statistical procedures to estimate radiation dose for accident dosimetry. Chromosome aberrations are one of the biological effects of ionizing radiation. Dicentric chromosome aberrations are the most reliable indicator of radiation exposure in lymphocytes. The number of chromosome aberrations is directly related to dose. The dose-response function for high LET radiation, such as neutrons, is linear in mammalian cells and can be used to model the observed data.

The two original contributions of this thesis are: (1) to estimate the dose-response function parameters with and without dose uncertainty and (2) to determine the calibrative distribution with and without an error about the calibration doses. The calibrative density can be used to find the dose corresponding to a specific number of observed dicentrics per cell. Parameter estimation and determination of the calibrative distribution were demonstrated for two data sets.

For the first data set, the dose-response function parameters without dose uncertainty were α, β and σ, where α represents the y-intercept, β denotes the slope and σ stands for the standard deviation. The posterior distribution for α was highest at 0 with a positive expectation. The posterior distribution for β peaked at approximately 0.00877 which agreed closely with the maximum likelihood of 0.00878. The posterior distribution

for σ peaked around 0.0245 which would give a variance of about 6.00×10^{-4}. The calibrative distributions without dose uncertainty behaved as expected: as Y_f was increased, the estimated dose increased. The dose estimations were consistent with the observed values from Data Set 1. The dose-response function parameters with dose uncertainty were τ, ϕ_1, ϕ_2 and θ where τ represents the variance of the true value of dose, ϕ_1 denotes the variance about the observed value of dose, ϕ_2 stands for the variance about the observed number of dicentrics/cell and θ represents the slope. The posterior distributions of τ, ϕ_1 and ϕ_2 asymptotically approached the ordinate as the variable of interest decreased. The posterior distribution of θ peaked at 0.00849 which agreed with the maximum likelihood estimator of β, 0.00878. Not all the calibrative distributions with dose uncertainty behaved as expected. In two of the calibrative distributions, the estimated dose decreased with an increased number of dicentrics/cell. All the modes of the estimated dose were considerably lower than the corresponding estimates without dose uncertainty. However, the lower dose estimates can be attributed to the uncertainty in the calibration doses. The densities for X_f are skewed to the right. This implies that the means of X_f are greater than the modes.

For the second data set, the dose-response function parameters without dose uncertainty were also α, β and σ. The posterior distribution for α was highest at 0 with a positive expectation consistent with a positive background rate for dicentrics. The posterior distribution for β peaked at approximately 0.0172 which agreed with the maximum likelihood of 0.0172. The posterior distribution for σ peaked around 0.0011 which would give a variance of about 1.21×10^{-6}. The calibrative distributions without

dose uncertainty behaved as expected: as Y_f was increased, the estimated dose increased. The dose estimations were consistent with the values from Data Set 2. The dose-response function parameters with dose uncertainty were τ, ϕ_1, ϕ_2 and θ. The posterior distribution of τ peaked at approximately 0.8. The posterior distributions of ϕ_1 and ϕ_2 asymptotically approached the ordinate as the variable of interest decreased. The posterior distribution of θ peaked at 0.0163 which is close to the maximum likelihood estimator of β, 0.0172. The calibrative distributions with dose uncertainty roughly behaved as expected: as Y_f was increased, the estimated dose increased. The modes of the dose estimates were considerably lower than the modes of the calibrative distributions without dose uncertainty. However, the low dose estimates can be attributed to the uncertainty in the dose. The densities for X_f are skewed to the right. This implies that the means of X_f are greater than the modes.

In conclusion, dose uncertainty increased the uncertainty of the dose-response parameter estimates to a degree greater than expected. When dose uncertainty was included, the parameter representing the slope, θ, behaved as expected. Not all the calibrative distributions behaved as expected. The mode of two distributions decreased with an increased number of dicentrics/cell. For example, when $Y_f = 2.0$, the mode was 73 Rad while the mode was 70 Rad for $Y_f = 2.5$. When $Y_f = 3.0$, the dose is estimated to be 55 Rad. These two examples were not consistent with the rest of the calibrative distributions. More examples with calibration dose uncertainty should be done in the future to see if similar patterns emerge.

BIBLIOGRAPHY

BIBLIOGRAPHY

Department of Plant Biology, University of Maryland, College Park and U.S. Department of Agriculture, National Agriculture Library Genome Informatics Group. *Agricultural Genome Information System: Cytogenetic Terms Index . . . Chromosome Aberrations.* March 1998. Online. Available: http://probe.nalusda.gov:8000/otherdocs/thesauri/cytogenetics/aaaaaaaw.html.

Groer, Peter G. and Carlos A. De B. Pereira. "Calibration of a Radiation Detector: Chromosome Dosimetry for Neutrons." *Probability and Bayesian Statistics.* Plenum Publishing Corporation, 1987. p. 225-232.

Groer, Peter G. Lecture from University of Tennessee, Knoxville. Class: Radiation Protection, October, 28, 1996.

Hall, Eric J. *Radiobiology for the Radiologist.* 4th ed. Philadelphia, PA: J. B. Lippincott Company, 1994. p. 16-27.

Inoue, Y. *Dicentric yields in Rabbit Blood Lymphocyes by Low Doses of ^{252}Cf Neutrons.* JAERI-Research Report 95-073. Japan Atomic Research Institute, Tokai-mura, 319-11. Japan, 1995.

Lindley, D. V. and G. M. El-Sayyad (1968). *The Bayesian Estimation of a Linear Functional Relationship.* Journals of the Royal Statistical Society B, Vol. 30. p. 190-202.

Littlefield, Gayle. Lecture from University of Tennessee, Knoxville Evening School, Oak Ridge, TN. Class: Radiation Biology, September 24, 1997.

NCRP Report No. 64. *Influence of Dose and Its Distribution in Time on Dose-Response Relationships for Low-LET Radiations.* Issued April 1, 1980. Washington, D.C. p. 23-37

NCRP Report No. 104. *The Relative Biological Effectiveness of Radiations of Different Quality.* Issued December 15, 1990. Bethesda, MD. p. 29-40.

Press, S. James. *Bayesian Statistics: Principles, Models, And Applications.* New York, NY: John Wiley & Sons, Inc., 1989. p. 125-131.

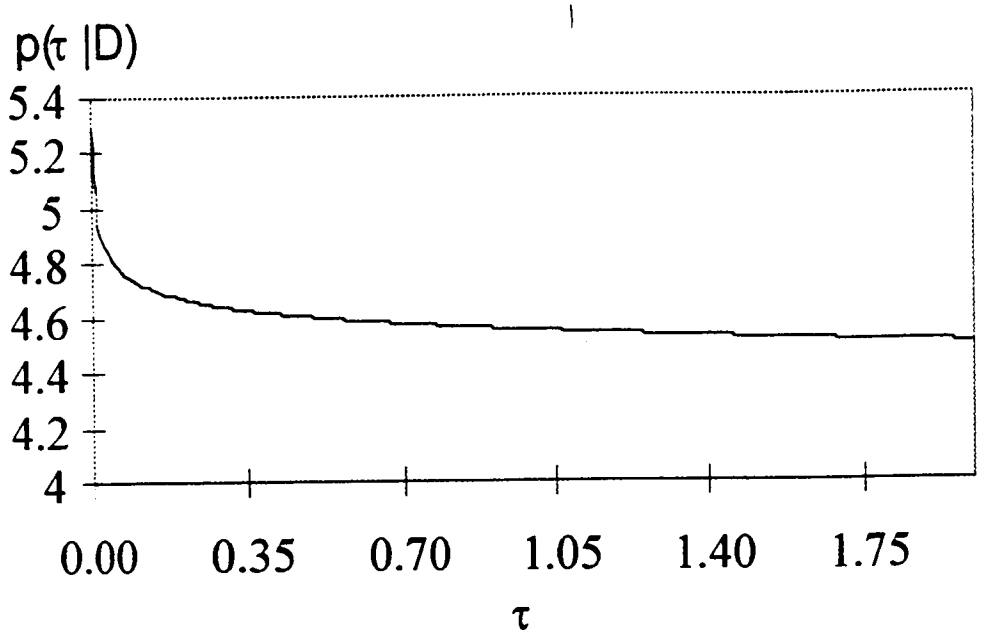
APPENDICES

APPENDIX A

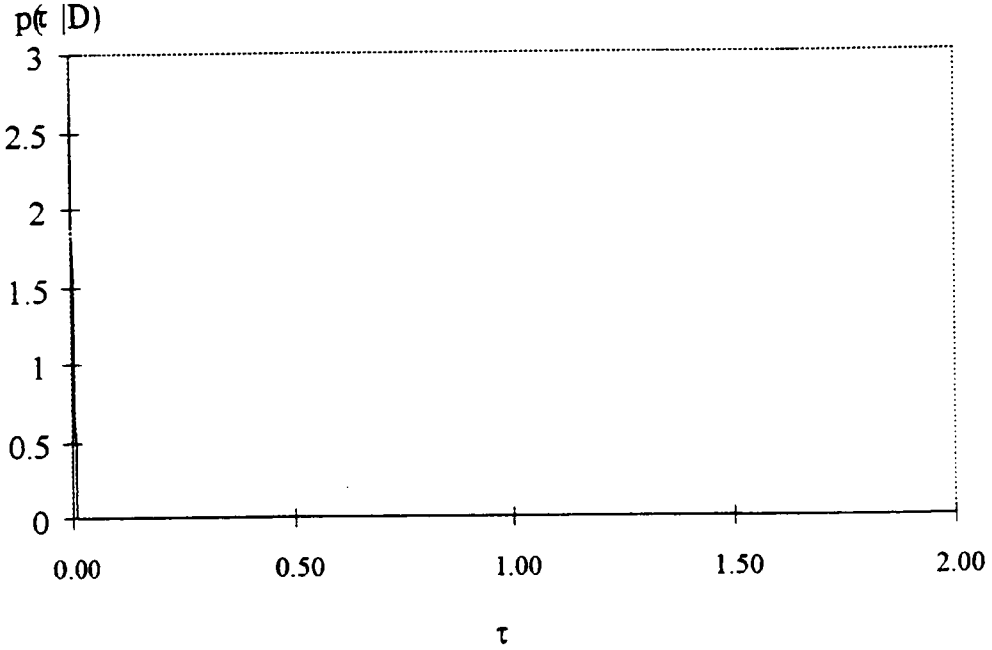
SUPPLEMENTAL GRAPHS FOR PARAMETER ESTIMATION WITH DOSE UNCERTAINTY

CONTENTS—APPENDIX A

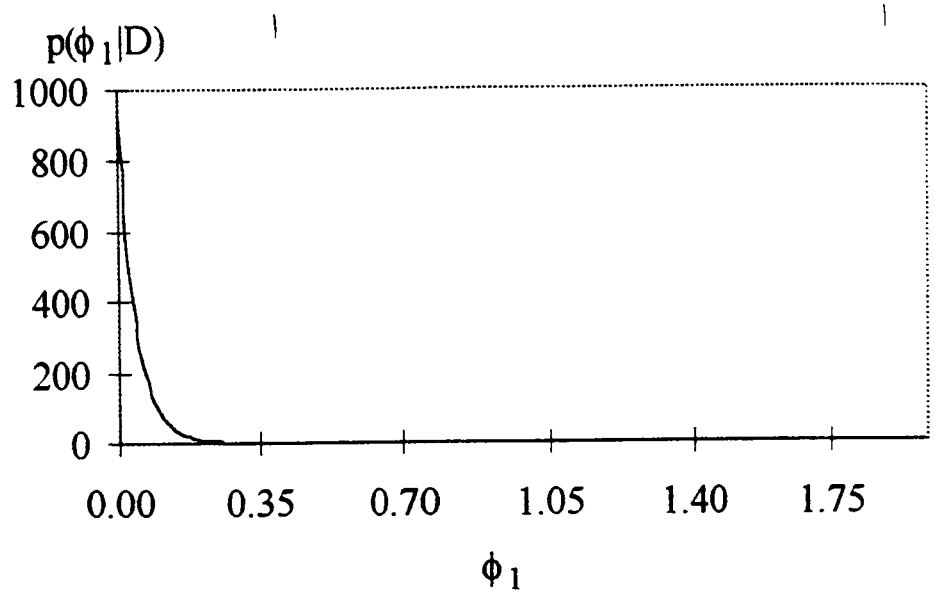
A1. Posterior Distribution of τ for Data Set 1 Using 30-point Gaussian Quadrature 60
A2. Posterior Distribution of τ for Data Set 1 Using 50-point Midpoint Rule 60
A3. Posterior Distribution of ϕ_1 for Data Set 1 Using 100-point Midpoint Rule 61
A4. Posterior Distribution of ϕ_1 for Data Set 1 Using Mathematica on a UNIX Workstation 61
A5. Posterior Distribution of ϕ_2 for Data Set 1 Using 30-point Gaussian Quadrature 62
A6. Posterior Distribution of ϕ_2 for Data Set 1 Using Mathematica on a UNIX Workstation 62
A7. Posterior Distribution of τ for Data Set 2 Using Mathematica on a UNIX Workstation 63
A8. Posterior Distribution of ϕ_1 for Data Set 2 Using 30-point Gaussian Quadrature 63
A9. Posterior Distribution of ϕ_1 for Data Set 2 Using 50-point Midpoint Rule 64
A10. Posterior Distribution of ϕ_2 for Data Set 2 Using 30-point Gaussian Quadrature 64
A11. Posterior Distribution of ϕ_2 for Data Set 2 Using 50-point Midpoint Rule 65
A12. Posterior Distribution of ϕ_2 for Data Set 2 Using Mathematica on a UNIX Workstation 65



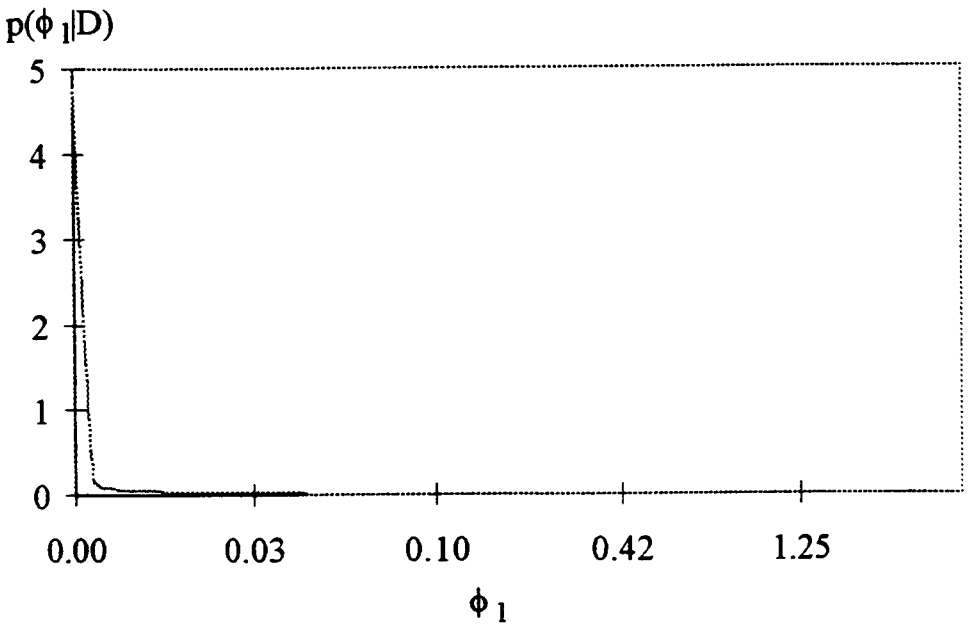
A1. Posterior Distribution of τ for Data Set 1 Using 30-point Gaussian Quadrature.



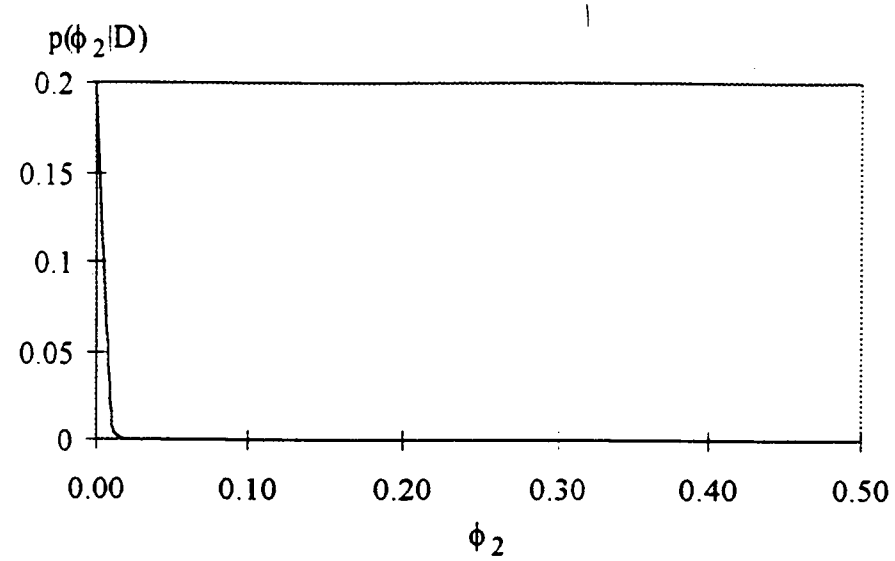
A2. Posterior Distribution of τ for Data Set 1 Using 50-point Midpoint Rule.



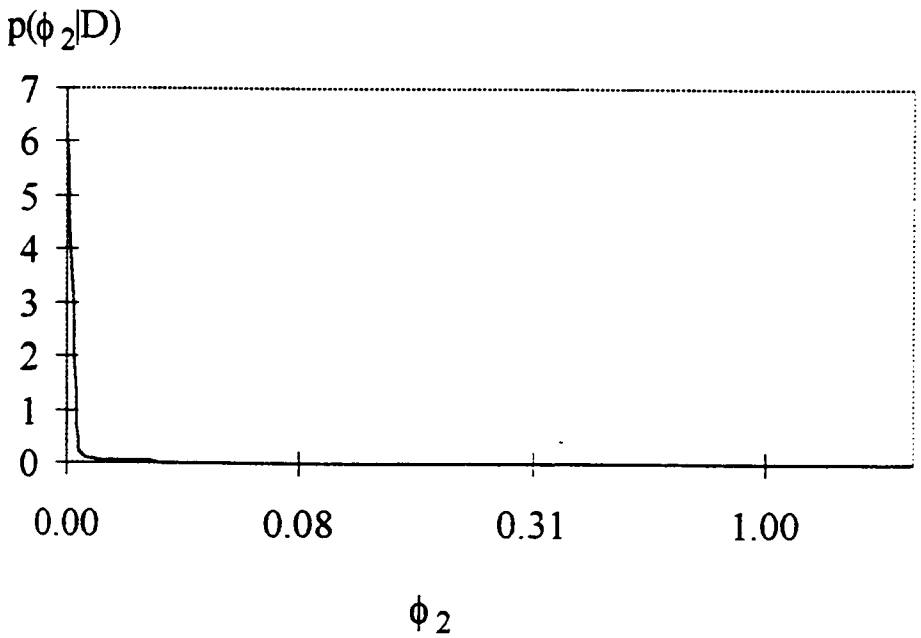
A3. Posterior Distribution of ϕ_1 for Data Set 1 Using 100-point Midpoint Rule.



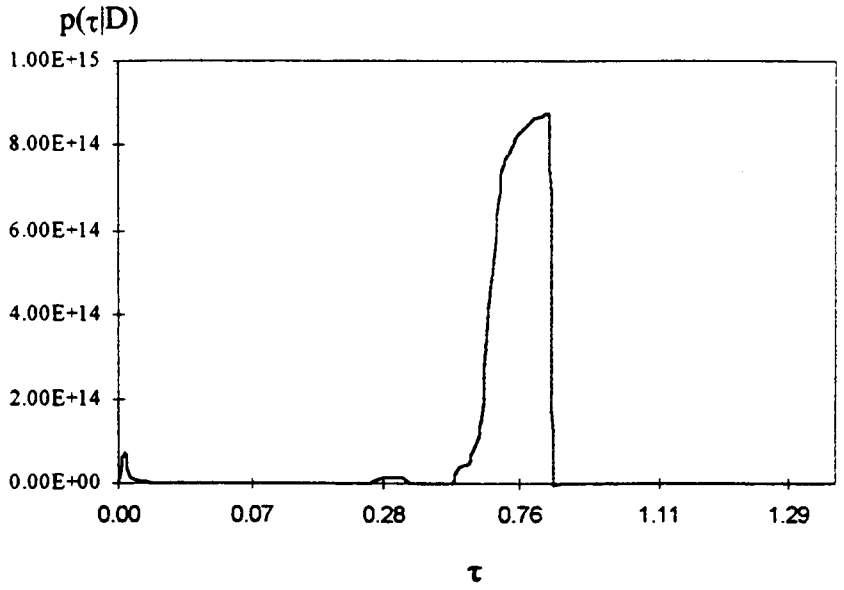
A4. Posterior Distribution of ϕ_1 for Data Set 1 Using Mathematica on a UNIX Workstation.



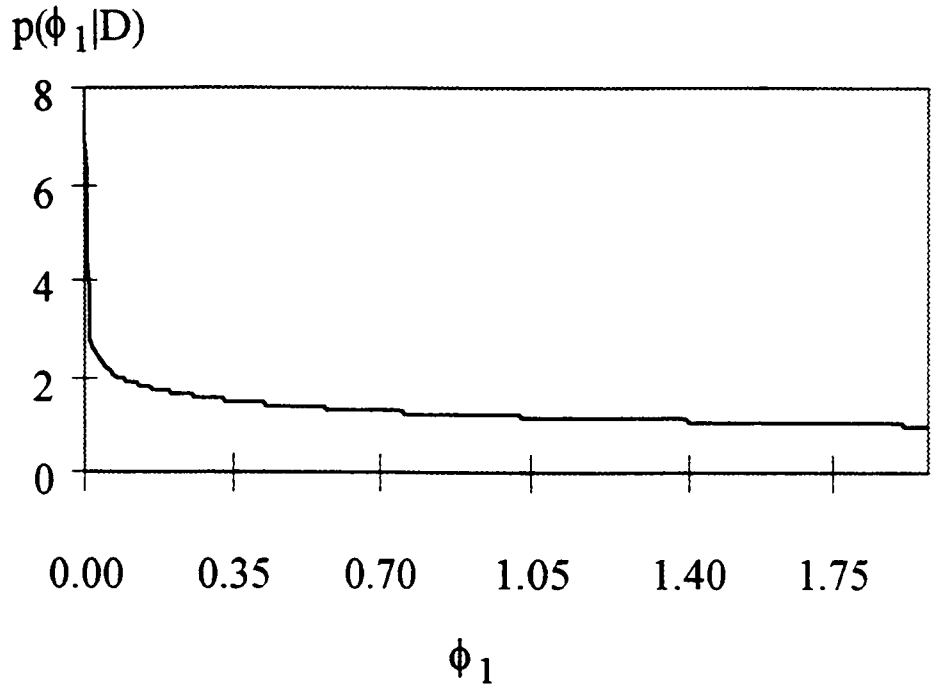
A5. Posterior Distribution of ϕ_2 for Data Set 1 Using 50-point Midpoint Rule.



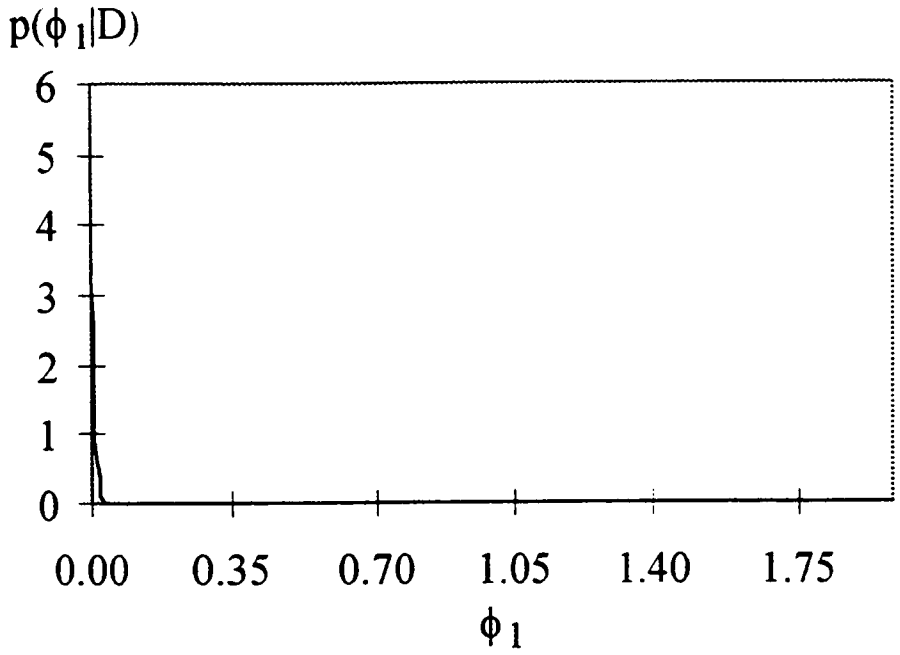
A6. Posterior Distribution of ϕ_2 for Data Set 1 Using Mathematica on a UNIX Workstation.



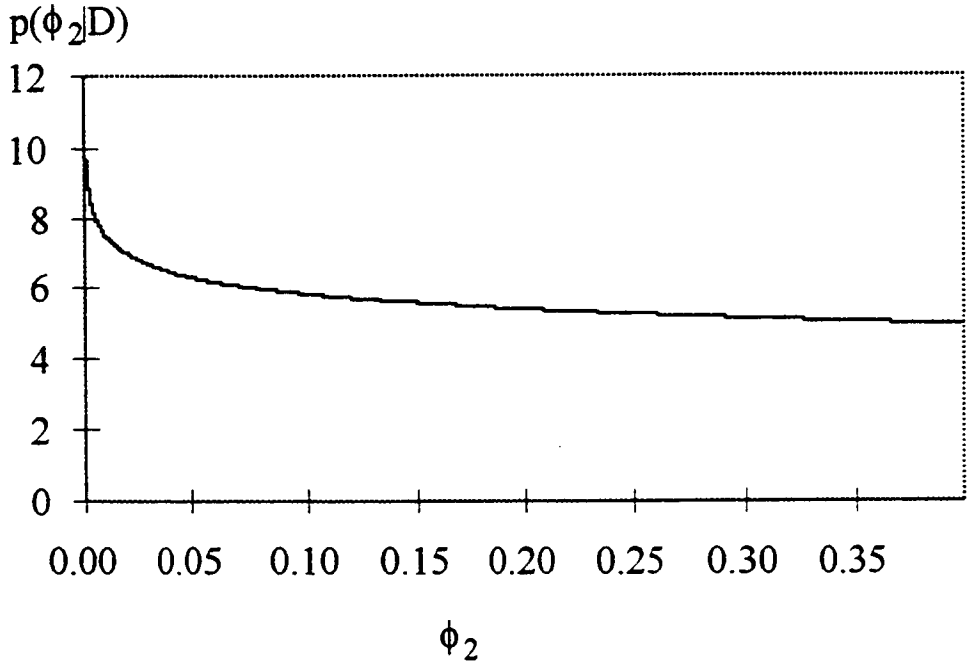
A7. Posterior Distribution of τ for Data Set 2 Using Mathematica on a UNIX Workstation.



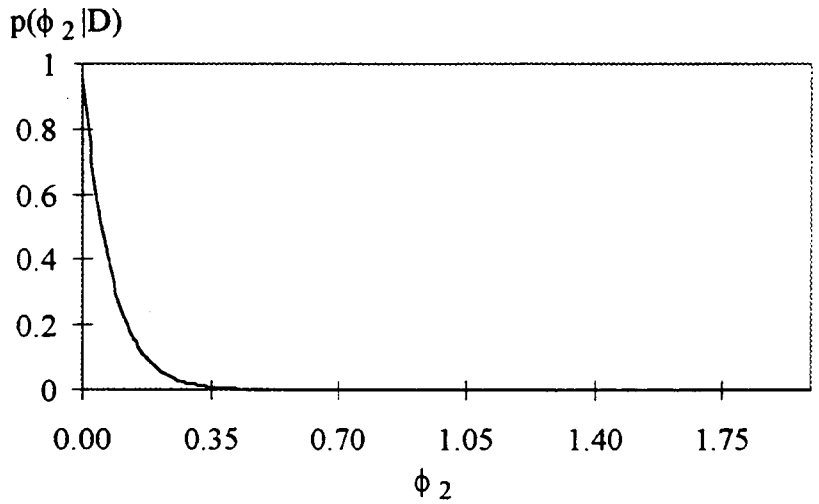
A8. Posterior Distribution of ϕ_1 for Data Set 2 Using 30-point Gaussian Quadrature.



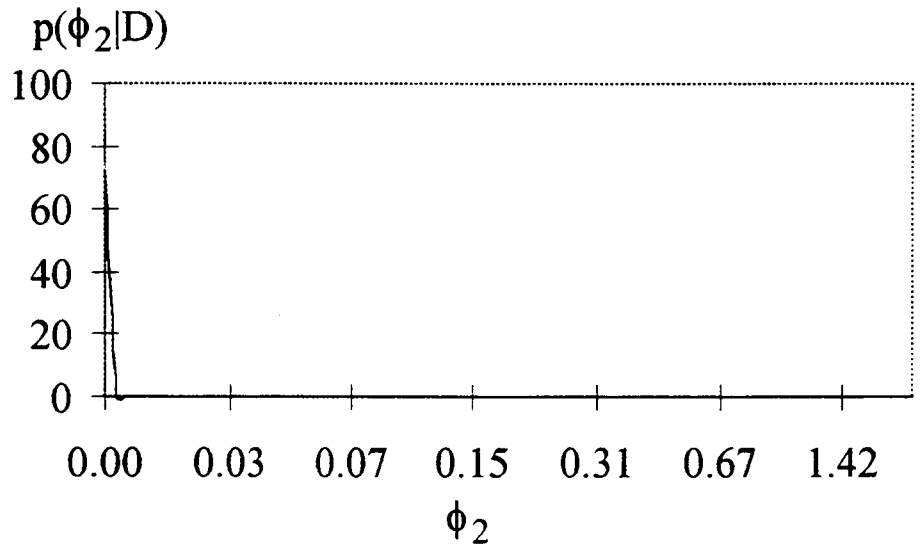
A9. Posterior Distribution of ϕ_1 for Data Set 2 Using 50-point Midpoint Rule.



A10. Posterior Distribution of ϕ_2 for Data Set 2 Using 30-point Gaussian Quadrature.



A11. Posterior Distribution of ϕ_2 for Data Set 2 Using 50-point Midpoint Rule.



A12. Posterior Distribution of ϕ_2 for Data Set 2 Using Mathematica on a UNIX Workstation.

APPENDIX B

FORTRAN PROGRAMS FOR PARAMETER ESTIMATION AND CALIBRATION WITH DOSE UNCERTAINTY

CONTENTS—APPENDIX B

B1. Posterior Density of τ Using 30-point Gaussian Quadrature 68
B2. Posterior Density of ϕ_1 Using 30-point Gaussian Quadrature 72
B3. Posterior Density of ϕ_2 Using 30-point Gaussian Quadrature 76
B4. Calibrative Density Using 30-point Gaussian Quadrature 80
B5. Posterior Density of τ Using Midpoint Rule Method 84
B6. Posterior Density of ϕ_1 Using Midpoint Rule Method 87
B7. Posterior Density of ϕ_2 Using Midpoint Rule Method 90
B8. Calibrative Density Using Midpoint Rule Method 92

B1. POSTERIOR DENSITY OF τ USING 30-POINT GAUSSIAN QUADRATURE

```
C CALCULATES THE POSTERIOR DENSITY FOR τ

    REAL A, B, ALPHA, BETA, C1, D, SXX, SXY, SYY, JJ

c defines the limits of integration for θ
    A = 0.0
    B = 1000.0
c defines the limits of integration for φ1
    ALPHA = 0.00001
    BETA = 1000.0
c defines the limits of integration for φ2
    C1 = 0.00001
    D = 1000.0

c calls a subroutine to perform numerical integration over θ, φ1 and φ2 and plot τ vs. the approximation JJ
    CALL QUAD(A,B,ALPHA,BETA,C1,D,SXX,SXY,SYY,JJ)
    END

c subroutine performs numerical integration θ, φ1 and φ2 and plot τ vs. the approximation JJ using
c 30- point Gaussian Quadrature
    SUBROUTINE QUAD(A,B,ALPHA,BETA,C1,D,SXX,SXY,SYY,JJ)
    REAL A, B, ALPHA, BETA, C1, D, THETA, PHI1, PHI2, TAU
    REAL JJ, JJX, JJY, Q1
    REAL SXX, SXY, SYY,AA1,BB1,ALPHA1, BETA1, INC
    REAL H1, H2, KK1, KK2, LL1, LL2, R(30), C(30)
    INTEGER i, j1, k1

c opens the file to write the output data to
    OPEN (2, FILE = 'TAUgauss1.DAT', STATUS = 'new')

C ASSIGNS THE GAUSSIAN QUADRATURE TO CONSIST OF 30 POINTS
C ROOTS ARE R(i), COEFFICIENTS ARE C(i)

    R(1) = -.996893483227463
    R(2) = -.98366812605347
    R(3) = -.960021860372149
    R(4) = -.926200052585185
    R(5) = -.882560531772885
    R(6) = -.829565764524011
    R(7) = -.7677774313483522
    R(8) = -.6978504949608971
    R(9) = -.6205261829691513
    R(10) = -.536624148142427
    R(11) = -.4470337695383449
    R(12) = -.352704725530834
    R(13) = -.2546369261678911
```

```
R(14) = -.1538699136085835
R(15) = -.05147184255531768
R(16) = -R(15)
R(17) = -R(14)
R(18) = -R(13)
R(19) = -R(12)
R(20) = -R(11)
R(21) = -R(10)
R(22) = -R(9)
R(23) = -R(8)
R(24) = -R(7)
R(25) = -R(6)
R(26) = -R(5)
R(27) = -R(4)
R(28) = -R(3)
R(29) = -R(2)
R(30) = -R(1)
C(1) = .007968190983633772
C(2) = .01846646958397418
C(3) = .02878471292532192
C(4) = .03879917826810256
C(5) = .04840269416474252
C(6) = .05749313279911294
C(7) = .06597425155169129
C(8) = .07375595616647974
C(9) = .0807559108368005
C(10) = .0868997741656539
C(11) = .0921225328883375
C(12) = .0963687288905029
C(13) = .0995934264835904
C(14) = .1017623862319278
C(15) = .1028526540601282
C(16) = C(15)
C(17) = C(14)
C(18) = C(13)
C(19) = C(12)
C(20) = C(11)
C(21) = C(10)
C(22) = C(9)
C(23) = C(8)
C(24) = C(7)
C(25) = C(6)
C(26) = C(5)
C(27) = C(4)
C(28) = C(3)
C(29) = C(2)
C(30) = C(1)

C FOR THE FOLLOWING VALUES
C       DOSE            DICENTRICS/CELL
C       50                      .4052
C       75                      .6026
```

```
C       100                 .8174
C       150                 1.26667
C       200                 1.6429
C       250                 2.1186
C       300                 2.6216
c defines N as the number of data points
        N = 7
c defines SXX as the sum of the squares  SUM_{i=1}^{N} X_i^2 / N
        SXX = 33304.0
c defines SXY as the sum of the squares  (SUM_{i=1}^{N} X_i Y_i) / N
        SXY = 283.0
c defines SYY as the sum of the square  ( SUM_{i=1}^{N} Y_i^2 ) / N
        SYY = 2.408

c allows user to input the limits to plot τ
    WRITE (*,*) 'ENTER THE LOWER LIMIT OF THE RANGE OF THE PLOT TAU'
    READ (*,*) ALPHA1
    WRITE (*,*) 'ENTER THE UPPER LIMIT OF THE RANGE OF THE PLOT TAU'
    READ (*,*) BETA1
    WRITE (*,*) 'ENTER THE INCREMENT'
    READ (*,*) INC

    DO TAU = ALPHA1, BETA1, INC

    H1 = (B-A)/2
    H2 = (B+A)/2
    JJ = 0

      DO i = 1, 30
      JJX = 0
      THETA = H1*R(i) + H2
      KK1 = (BETA-ALPHA)/2
      KK2 = (BETA+ALPHA)/2

        DO j1 = 1, 30
        JJY = 0
        PHI1 = KK1*R(j1) + KK2
        LL1 = (D-C1)/2
        LL2 = (D+C1)/2

          DO k1 = 1, 30
          PHI2 = LL1*R(k1) + LL2
          AA1 = SXX*(THETA**2*TAU+PHI2)-2*SXY*THETA*TAU+SYY*(TAU+PHI1)
          BB1 = PHI1*PHI2 + TAU*PHI2+TAU*PHI1*THETA**2
c Q1 is the natural logarithm of the equation due to underflow
```

```
            Q1 = (-0.5*N*AA1/BB1)-log(PHI1*PHI2*BB1**(0.5*N))
            JJY = JJY + C(k1)*Q1
            END DO
          JJX = JJX + C(j1)*LL1*JJY
          END DO
        JJ = JJ + C(i)*KK1*JJX
        END DO
      JJ = H1*JJ
c writes the data to the output file
      WRITE (2, *) TAU, JJ
      END DO
 END
```

B2. POSTERIOR DENSITY OF ϕ_1 USING 30-POINT GAUSSIAN QUADRATURE

```
C CALCULATES THE POSTERIOR DENSITY FOR φ1

      REAL A, B, C1, D,T1, T2, SXX, SXY, SYY, JJ

c defines the limits of integration for θ
      A = 0.0
      B = 1.0
c defines the limits of integration for τ
      T1 = 0.0
      T2 = 1000.0
c defines the limits of integration for φ2
      C1 = 0.00001
      D = 20.0

c calls a subroutine to perform numerical integration over θ, τ and φ2 and plot φ1 vs. the approximation JJ
      CALL QUAD(A,B,C1,D,T1, T2.SXX.SXY,SYY.JJ)
      END

c subroutine performs numerical integration θ, τ and φ2 and plot φ1 vs. the approximation JJ using
c 30- point Gaussian Quadrature
      SUBROUTINE QUAD(A,B,C1.D,T1,T2,SXX,SXY,SYY,JJ)
      REAL A, B, ALPHA, BETA, C1, D, THETA, PHI1, PHI2, TAU
      REAL JJ, JJX, JJY, Q1
      REAL SXX, SXY, SYY,AA1,BB1,ALPHA1, BETA1, INC
      REAL H1, H2, KK1, KK2, LL1, LL2, R(30), C(30)
      INTEGER i, j1, k1

c opens the file to write the output data to
 OPEN (2, FILE = 'phi1dataset1.DAT', STATUS = 'new')
C ASSIGNS THE GAUSSIAN QUADRATURE TO CONSIST OF 30 POINTS
C ROOTS ARE R(I, J), COEFFICIENTS ARE C(LJ)

      R(1) = -.996893483227463
      R(2) = -.98366812605347
      R(3) = -.960021860372149
      R(4) = -.926200052585185
      R(5) = -.882560531772885
      R(6) = -.829565764524011
      R(7) = -.7677774313483522
      R(8) = -.697850494960897 1
      R(9) = -.6205261829691513
      R(10) = -.536624148142427
      R(11) = -.4470337695383449
      R(12) = -.3527047255308344
```

R(13) = -.2546369261678911
R(14) = -.1538699136085835
R(15) = -.05147184255531768
R(16) = -R(15)
R(17) = -R(14)
R(18) = -R(13)
R(19) = -R(12)
R(20) = -R(11)
R(21) = -R(10)
R(22) = -R(9)
R(23) = -R(8)
R(24) = -R(7)
R(25) = -R(6)
R(26) = -R(5)
R(27) = -R(4)
R(28) = -R(3)
R(29) = -R(2)
R(30) = -R(1)
C(1) = .007968190983633772
C(2) = .01846646958397418
C(3) = .02878471292532192
C(4) = .03879917826810256
C(5) = .04840269416474252
C(6) = .05749313279911294
C(7) = .06597425155169129
C(8) = .07375595616647974
C(9) = .0807559108368005
C(10) = .0868997741656539
C(11) = .0921225328883375
C(12) = .0963687288905029
C(13) = .0995934264835904
C(14) = .1017623862319278
C(15) = .1028526540601282
C(16) = C(15)
C(17) = C(14)
C(18) = C(13)
C(19) = C(12)
C(20) = C(11)
C(21) = C(10)
C(22) = C(9)
C(23) = C(8)
C(24) = C(7)
C(25) = C(6)
C(26) = C(5)
C(27) = C(4)
C(28) = C(3)
C(29) = C(2)
C(30) = C(1)

```
C FOR THE FOLLOWING VALUES
C       DOSE            DICENTRICS/CELL
C       50                      .4052
C       75                      .6026
C       100                     .8174
C       150                     1.26667
C       200                     1.6429
C       250                     2.1186
C       300                     2.6216
c defines N as the number of data points
        N = 7
```

c defines SXX as the sum of the squares $\sum_{i=1}^{N} X_i^2 / N$

```
        SXX = 33304.0
```

c defines SXY as the sum of the squares $(\sum_{i=1}^{N} X_i Y_i) / N$

```
        SXY = 283.0
```

c defines SYY as the sum of the square $\left(\sum_{i=1}^{N} Y_i^2\right) / N$

```
        SYY = 2.408


c allows user to input the limits to plot ϕ1
    WRITE (*,*) 'ENTER THE LOWER LIMIT OF THE RANGE TO PLOT(NOT = 0)'
    READ (*,*) ALPHA1
    WRITE (*,*) 'ENTER THE UPPER LIMIT OF THE RANGE TO PLOT'
    READ (*,*) BETA1
    WRITE (*,*) 'ENTER THE INCREMENT'
    READ (*,*) INC

    DO PHI1 = ALPHA1, BETA1, INC

    H1 = (T2-T1)/2
    H2 = (T1+T2)/2
    JJ = 0

      DO i = 1, 30
      JJX = 0
      TAU = H1*R(i) + H2
      HK1 = (B-A)/2
      HK2 = (B+A)/2

        DO j1 = 1, 30
        JJY = 0
        THETA = HK1*R(j1) + HK2
        L1 = (D-C1)/2
```

```
          L2 = (D+C1)/2

             DO k1 = 1, 30
             PHI2 = L1*R(k1) + L2
             A1 = SXX*(THETA**2*TAU+PHI2)-2*SXY*THETA*TAU+SYY*(TAU+PHI1)
             B1 = PHI1*PHI2 + TAU*PHI2+TAU*PHI1*THETA**2
c defines Q as the natural logarithm of the equation due to underflow
             Q = (-0.5*N*A1/B1)-log(PHI1*PHI2*B1**(0.5*N))
             JJY = JJY + C(k1)*Q
             END DO
           JJX = JJX + C(j1)*L1*JJY
           END DO
         JJ = JJ + C(i)*HK1*JJX
         END DO
      JJ = H1*JJ
c writes the data to the output file
 WRITE (2, *) PHI1, JJ
     END DO
   END
```

B3. POSTERIOR DENSITY OF ϕ_2 USING 30-POINT GAUSSIAN QUADRATURE

```
C CALCULATES THE POSTERIOR DENSITY FOR φ2

    REAL A, B, ALPHA, BETA,T1, T2,  SXX, SXY, SYY, JJ

c defines the limits of integration for θ
    A = 0.0
    B = 1000.0
c defines the limits of integration for τ
    T1 = 0.0
    T2 = 1000.0
c defines the limits of integration for φ1
    ALPHA = 0.00001
    BETA = 1000.0

c calls a subroutine to perform numerical integration over θ, τ and φ1 and plot φ2 vs. the approximation JJ
CALL QUAD(A,B,ALPHA,BETA,T1,T2,JJ)
    END

C THIS SUBROUTINE WILL READ A LIST OF VALUES FOR THETA AND THE
C APPROXIMATION INTO A FILE WHILE PERFORMING A TRIPLE INTEGRATION
C USING 30 POINT GAUSSIAN QUADRATURE
    SUBROUTINE QUAD(A,B,ALPHA,BETA,T1,T2,JJ)
    REAL A, B, ALPHA, BETA, T1, T2,THETA, PHI1, PHI2, TAU
    REAL JJ, JJX, JJY, Q
    REAL SXX, SXY, SYY,A1,B1, ALPHA1, BETA1, INC
    REAL H1,H2,K1, K2,L1, L2
        DIMENSION R(30), C(30)
    INTEGER i, j1, kk1, N

c opens the output file to write φ2 and JJ
    OPEN (2, FILE = 'PHI2dataset1.DAT', STATUS = 'new')
C ASSIGNS THE GAUSSIAN QUADRATURE TO CONSIST OF 30 POINTS
C ROOTS ARE R(I, J), COEFFICIENTS ARE C(I,J)

    R(1) = -.996893483227463
    R(2) = -.98366812605347
    R(3) = -.960021860372149
    R(4) = -.926200052585185
    R(5) = -.882560531772885
    R(6) = -.829565764524011
    R(7) = -.7677774313483522
    R(8) = -.6978504949608971
    R(9) = -.6205261829691513
    R(10) = -.536624148142427
```

R(11) = -.4470337695383449
R(12) = -.3527047255308344
R(13) = -.2546369261678911
R(14) = -.1538699136085835
R(15) = -.05147184255531768
R(16) = -R(15)
R(17) = -R(14)
R(18) = -R(13)
R(19) = -R(12)
R(20) = -R(11)
R(21) = -R(10)
R(22) = -R(9)
R(23) = -R(8)
R(24) = -R(7)
R(25) = -R(6)
R(26) = -R(5)
R(27) = -R(4)
R(28) = -R(3)
R(29) = -R(2)
R(30) = -R(1)
C(1) = .007968190983633772
C(2) = .01846646958397418
C(3) = .02878471292532192
C(4) = .03879917826810256
C(5) = .04840269416474252
C(6) = .05749313279911294
C(7) = .06597425155169129
C(8) = .07375595616647974
C(9) = .0807559108368005
C(10) = .0868997741656539
C(11) = .0921225328883375
C(12) = .0963687288905029
C(13) = .0995934264835904
C(14) = .1017623862319278
C(15) = .1028526540601282
C(16) = C(15)
C(17) = C(14)
C(18) = C(13)
C(19) = C(12)
C(20) = C(11)
C(21) = C(10)
C(22) = C(9)
C(23) = C(8)
C(24) = C(7)
C(25) = C(6)
C(26) = C(5)
C(27) = C(4)
C(28) = C(3)
C(29) = C(2)
C(30) = C(1)

```
C FOR THE FOLLOWING VALUES
C       DOSE            DICENTRICS/CELL
C       50              .4052
C       75              .6026
C       100             .8174
C       150             1.26667
C       200             1.6429
C       250             2.1186
C       300             2.6216
c defines N as the number of data points
        N = 7
```

c defines SXX as the sum of the squares $\sum_{i=1}^{N} X_i^2 / N$

```
        SXX = 33304.0
```

c defines SXY as the sum of the squares $(\sum_{i=1}^{N} X_i Y_i) / N$

```
        SXY = 283.0
```

c defines SYY as the sum of the square $\left(\sum_{i=1}^{N} Y_i^2\right) / N$

```
        SYY = 2.408


c allows user to input the limits to plot φ2
    WRITE (*,*) 'ENTER THE LOWER LIMIT OF THE RANGE TO PLOT(NOT = 0)'
    READ (*,*) ALPHA1
    WRITE (*,*) 'ENTER THE UPPER LIMIT OF THE RANGE TO PLOT'
    READ (*,*) BETA1
    WRITE (*,*) 'ENTER THE INCREMENT'
    READ (*,*) INC

    DO PHI2 = ALPHA1, BETA1, INC

    H1 = (T2-T1)/2
    H2 = (T1+T2)/2
    JJ = 0

      DO i = 1, 30
      JJX = 0
      TAU = H1*R(i) + H2
      K1 = (B-A)/2
      K2 = (B+A)/2
        DO j1 = 1, 30
        JJY = 0
        THETA = K1*R(j1) + K2
        L1 = (BETA-ALPHA)/2
        L2 = (BETA+ALPHA)/2
```

```
          DO kk1 = 1, 30
                                    PHI1 = L1*R(kk1) + L2
        A1 = SXX*(THETA**2*TAU+PHI2)-2*SXY*THETA*TAU+SYY*(TAU+PHI1)
            B1 = PHI1*PHI2 + TAU*PHI2+TAU*PHI1*THETA**2
c defines Q as the natural logarithm due to underflow
            Q = (-0.5*N*A1/B1)-LOG(PHI1*PHI2*B1**(0.5*N))
            JJY = JJY + C(kk1)*Q
            END DO
          JJX = JJX + C(j1)*L1*JJY
          END DO
        JJ = JJ + C(i)*K1*JJX
        END DO
      JJ = H1*JJ
c writes the data to the output file
      WRITE (2, *) PHI2, JJ
      END DO
      END
```

B4. CALIBRATIVE DENSITY USING 30-POINT GAUSSIAN QUADRATURE

```
C CALCULATES THE CALIBRATIVE DENSITY
REAL ThLO,ThHI,TLO,THI,P1LO,P1HI,P2LO,P2HI
    DOUBLE PRECISION J

c defines the limits of θ
    ThLO = 0.0
    ThHI = 1.0
c defines the limits of τ
    TLO = 0.0
    THI = 1000.0
c defines the limits of φ1
    P1LO = 0.0001
    P1HI = 1000.0
c defines the limits of φ2
    P2LO = 0.0001
    P2HI = 20.0

c calls the subroutine to perform numerical integration over θ, τ, φ1 and φ2 using 30-point gaussian
quadrature
    CALL QUAD(ThLO,ThHI,TLO,THI,P1LO,P1HI,P2LO,P2HI,J)
    WRITE (*,*) 'THE APPROXIMATION IS =', J
    END



c subroutine performs numerical integration over θ, τ, φ1 and φ2 , assigns a value to Yf, and plots Xf vs. J
    SUBROUTINE QUAD(ThLO,ThHI,TLO,THI,P1LO,P1HI,P2LO,P2HI,J)
    REAL ThLO,ThHI,TLO,THI,P1LO,P1HI,P2LO,P2HI,THETA,TAU,PHI1,PHI2
    REAL H1,H2,HK1,HK2,HL1,HL2,HM1,HM2,PI, inc
    REAL A,B,C1,D,E,F,G,Z,Z1,PX,PX1,XFLO,XFHI,YF,NUM,SXX,SXY,SYY
    DOUBLE PRECISION Q,J,J1,K1,L1,M1
        INTEGER i,i1,i2,i3
        DIMENSION R(30), C(30)

c opens output file
    OPEN(2, FILE='cd2yf=.0225.DAT', STATUS = 'new')

C ASSIGNS THE GAUSSIAN QUADRATURE TO CONSIST OF 30 POINTS
C ROOTS ARE R(i), COEFFICIENTS ARE C(i)
        R(1) = -.996893
        R(2) = -.983668
        R(3) = -.960022
        R(4) = -.9262
        R(5) = -.882561
```

R(6) = -.829566
R(7) = -.767777
R(8) = -.69785
R(9) = -.620526
R(10) = -.536624
R(11) = -.447034
R(12) = -.352705
R(13) = -.254637
R(14) = -.15387
R(15) = -.0541718
R(16) = .0541718
R(17) = .15387
R(18) = .254637
R(19) = .352705
R(20) = .447034
R(21) = .536624
R(22) = .620526
R(23) = .69785
R(24) = .767777
R(25) = .829566
R(26) = .882561
R(27) = .9262
R(28) = .960022
R(29) = .983668
R(30) = .996893

C(1) =.00796819
C(2) =.0184665
C(3) =.0287847
C(4) =.0387992
C(5) =.0484027
C(6) = .0574931
C(7) =.0659743
C(8) =.073756
C(9) = .0807559
C(10) = .0868998
C(11) = .0921225
C(12) = .0963687
C(13) = .0995934
C(14) = .101762
C(15) = .102853
C(16) = .102853
C(17) = .101762
C(18) = .0995934
C(19) = .0963687
C(20) = .0921225
C(21) = .0868998
C(22) = .0807559
C(23) = .073756
C(24) = .0659743
C(25) = .0574931
C(26) = .0484027

```
      C(27) = .0387992
      C(28) = .0287847
      C(29) = .0184665
      C(30) = .00796819

c allows user to input the range to plot Xf
            WRITE (*,*) 'ENTER THE LOWER LIMIT TO PLOT XF'
            READ (*,*) XFLO
            WRITE (*,*) 'ENTER THE UPPER LIMIT TO PLOT XF'
            READ (*,*) XFHI
            WRITE (*,*) 'ENTER THE INCREMENT'
            READ (*,*) INC
c assigns a value to Yf
            WRITE (*,*) 'ENTER THE VALUE FOR YF'
            READ (*,*) YF

C  FOR THE DATA SET BELOW:
C          DOSE              DICENTRICS/CELL
C          50                      .4052
C          75                      .6026
C          100                     .8174
C          150                     1.26667
C          200                     1.6429
C          250                     2.1186
C          300                     2.6216
C   THE FOLLOWING VALUES WERE FOUND TO BE

c num is the number of data points
            NUM = 7
c defines SXX as the sum of the squares  SUM_{i=1}^{N} X_i^2 / N
            SXX = 33304.0
c defines SXY as the sum of the squares  ( SUM_{i=1}^{N} X_i Y_i ) / N
            SXY = 283.0
c defines SYY as the sum of the square  ( SUM_{i=1}^{N} Y_i^2 ) / N
            SYY = 2.408

            DO XF = XFLO, XFHI, INC

      H1 = (ThHI-ThLO)/2
            H2 = (ThHI+ThLO)/2
      J1 = 0

      DO i = 0,30
        THETA = H1*R(i)+ H2
        HK1 = (THI-TLO)/2
                  HK2 = (THI+TLO)/2
        K1 = 0
```

```
      DO i1 = 0, 30
      TAU = HK1*R(i1)+HK2
                  HL1 = (P1HI-P1LO)/2
                  HL2 = (P1HI+P1LO)/2
                  L1 = 0
                        DO i2 = 0, 30
                        PHI1 = HL1*R(i2)+HL2
                        HM1 = (P2HI-P2LO)/2
                        HM2 = (P2HI+P2LO)/2
                        M1 = 0
                              DO i3 = 0, 30
                              PHI2 = HM1*R(i3)+HM2
            A = PHI1*PHI2+TAU*PHI2+TAU*PHI1*THETA**2
            B = (THETA**2*TAU+PHI2)*(NUM*SXX+XF**2)
            C1 = 2*THETA*TAU*(NUM*SXY+XF*YF)
            D = (TAU+PHI1)*(NUM*SYY+YF**2)
            E = EXP(-0.5*(B-C1+D)/A)
            F = XF*PHI2+THETA*YF*PHI1
            G = TAU/(2*A**((NUM+3)/2))
            Z  = -F*SQRT(TAU/(2*PHI1*PHI2*A))
            Z1 = -Z
            PI = 3.14159265359
            PX = 2*(Z-Z**3/3+Z**5/10-Z**7/42)/SQRT(PI)
            PX1=2*(Z1-Z1**3/3+Z1**5/10-Z1**7/42)/SQRT(PI)
            Q = G*E*(2-PX-PX1)
            M1 = M1 + C(i3)*Q
            END DO
            L1 = L1 + C(i2)*HM1*M1
          END DO
          K1 = K1 + C(i1)*HL1*L1
        END DO
        J1 = J1 + C(i)*HK1*K1
    END DO
    J = H1*J1
c writes data to output file
      WRITE (2,*) XF, J
      END DO
  END
```

B5. POSTERIOR DENSITY OF τ USING THE MIDPOINT RULE METHOD

```
REAL ThLO,ThHI,TLO,THI,P1LO,P1HI,P2LO,P2HI
      REAL J

c allows user to input limits of integration
    WRITE (*,*) 'ENTER THE LOWER LIMIT FOR THETA'
    READ (*,*) ThLO
    WRITE (*,*) 'ENTER THE UPPER LIMIT FOR THETA'
    READ (*,*) ThHI
    WRITE (*,*) 'ENTER THE LOWER LIMIT FOR PHI1'
    READ (*,*) P1LO
    WRITE (*,*) 'ENTER THE UPPER LIMIT FOR PHI1'
    READ (*,*) P1HI
    WRITE (*,*) 'ENTER THE LOWER LIMIT FOR PHI2'
    READ (*,*) P2LO
    WRITE (*,*) 'ENTER THE UPPER LIMIT FOR PHI2'
    READ (*,*) P2HI

c calls the subroutine to perform numerical integration
    CALL QUAD(ThLO,ThHI,P1LO,P1HI,P2LO,P2HI,J)
    WRITE (*,*) 'THE APPROXIMATION IS =', J
    END

c subroutine performs numerical integration over θ, φ1, φ2 and plots τ vs. J
    SUBROUTINE QUAD(ThLO,ThHI,P1LO,P1HI,P2LO,P2HI,J)
    REAL ThLO,ThHI,P1LO,P1HI,P2LO,P2HI,THETA,TAU,PHI1,PHI2
    REAL H,HX,HZ,J1,L1,M1,J,L,M,N, INC
        REAL A,B,C,D,NUM,SXX,SXY,SYY,T1LO,T1HI
    INTEGER i,i2,i3

c opens the output file
        OPEN(2, FILE='TAUMIDPT2.DAT', STATUS = 'old')

c allows user to input the range to plot
        WRITE (*,*) 'ENTER THE LOWER LIMIT TO PLOT TAU'
        READ (*,*) T1LO
        WRITE (*,*) 'ENTER THE UPPER LIMIT TO PLOT TAU'
        READ (*,*) T1HI
        WRITE (*,*) 'ENTER THE INCREMENT'
        READ (*,*) INC

C  FOR THE DATA SET BELOW:
C       DOSE            DICENTRICS/CELL
C       50                      .4052
C       75                      .6026
C       100                     .8174
C       150                     1.26667
```

```
C       200                     1.6429
C       250                     2.1186
C       300                     2.6216
C  THE FOLLOWING VALUES WERE FOUND TO BE
c num is the number of data points
        NUM = 7
```

c defines SXX as the sum of the squares $\sum_{i=1}^{N} X_i^2 / N$

```
        SXX = 33304.0
```

c defines SXY as the sum of the squares $(\sum_{i=1}^{N} X_i Y_i) / N$

```
        SXY = 283.0
```

c defines SYY as the sum of the square $\left(\sum_{i=1}^{N} Y_i^2\right) / N$

```
        SYY = 2.408

C N IS THE NUMBER OF SUBINTERVALS;  N MUST BE EVEN.
        N = 50

        DO TAU = T1LO,T1HI,INC

c H is the subinterval length
    H = (ThHI-ThLO)/(2*(N+2))
    J1 = 0
    DO i = 0,N
      THETA = ThLO + H*(2*i+1)
      HX = (P1HI-P1LO)/(2*(N+2))
      K1 = 0
              DO i2 = 0, N
                      PHI1 = P1LO + (2*i2+1)*HX
                      HZ = (P2HI-P2LO)/(2*(N+2))
                      M1 = 0
                              DO i3 = 0, N
                              PHI2 = P2LO + (2*i3+1)*HZ
                              A = PHI1*PHI2+TAU*PHI2+TAU*PHI1*THETA**2
                              B = (THETA**2*TAU+PHI2)*NUM*SXX
                              C = 2*THETA*TAU*NUM*SXY
                              D = (TAU+PHI1)*NUM*SYY
c defines Q to be the natural logarithm of the equation due to underflow
                              Q = (-0.5*(B-C+D)/A)-LOG(PHI1*PHI2*A**(0.5*NUM))
                              M1 = M1 + Q
                              END DO
                              M = 2*HZ*M1
                              L1 = L1 + M
                      END DO
              L = 2*HX*L1
              J1 = J1 + L
      END DO
              J = 2*H*J1
c writes the data to the output file
```

```
    WRITE (2,*) TAU, J
    END DO
END
```

B6. POSTERIOR DENSITY OF ϕ_1 USING THE MIDPOINT RULE METHOD

```
c calculates the posterior density of φ1
REAL ThLO,ThHI,TLO,THI,P1LO,P1HI,P2LO,P2HI
        REAL J

c defines the limits of θ
    THLO = 0.
        THHI = 1.
C defines the limits of τ
        TLO = 0.
        THI = 1000.
C defines the limits of φ2
        P2LO = 0.
        P2HI = 20.

C calls the subroutine to perform numerical integration over θ, τ, φ2
    CALL QUAD(ThLO,ThHI,TLO,THI,P1LO,P1HI,P2LO,P2HI,J)
    WRITE (*,*) 'THE APPROXIMATION IS =', J
    END


c this subroutine performs numerical integration over θ, τ, φ2, and plots φ1 vs. J
   SUBROUTINE QUAD(ThLO,ThHI,TLO,THI,P1LO,P1HI,P2LO,P2HI,J)
    REAL ThLO,ThHI,P1LO,P1HI,P2LO,P2HI,THETA,TAU,PHI1,PHI2
    REAL H,HX,HZ,J1,L1,M1,J,L,M,N, INC
        REAL A,B,C,D,NUM,SXX,SXY,SYY
    INTEGER i,i2,i3

c opens the output file
        OPEN(2, FILE='phi1MIDPT2.DAT', STATUS = 'new')

c allows user to enter the range to plot φ1
        WRITE (*,*) 'ENTER THE LOWER LIMIT TO PLOT phi1'
        READ (*,*) p1LO
        WRITE (*,*) 'ENTER THE UPPER LIMIT TO PLOT phi1'
        READ (*,*) p1HI
        WRITE (*,*) 'ENTER THE INCREMENT'
        READ (*,*) INC

C  FOR THE DATA SET BELOW:
C       DOSE            DICENTRICS/CELL
C       50                      .4052
C       75                      .6026
C       100                     .8174
C       150                     1.26667
C       200                     1.6429
C       250                     2.1186
C       300                     2.6216
```

```
C  THE FOLLOWING VALUES WERE FOUND TO BE
c num is the number of data points
      NUM = 7
```

c defines SXX as the sum of the squares $\sum_{i=1}^{N} X_i^2 / N$

```
      SXX = 33304.0
```

c defines SXY as the sum of the squares $(\sum_{i=1}^{N} X_i Y_i) / N$

```
      SXY = 283.0
```

c defines SYY as the sum of the square $\left(\sum_{i=1}^{N} Y_i^2\right) / N$

```
      SYY = 2.408


C DEFINES N AS THE NUMBER OF SUBINTERVALS (POINTS):  N MUST BE EVEN.
      N = 50

      DO PHI1 = P1LO,P1HI,INC

C H IS THE SUBINTERVAL LENGTH
   H = (ThHI-ThLO)/(2*(N+2))
   J1 = 0

   DO i = 0,N
     THETA = ThLO + H*(2*i+1)
     HX = (THI-TLO)/(2*(N+2))
     K1 = 0
            DO i2 = 0, N
                    TAU = TLO + (2*i2+1)*HX
                    HZ = (P2HI-P2LO)/(2*(N+2))
                    M1 = 0
                          DO i3 = 0, N
                          PHI2 = P2LO + (2*i3+1)*HZ
                          A = PHI1*PHI2+TAU*PHI2+TAU*PHI1*THETA**2
                          B = (THETA**2*TAU+PHI2)*NUM*SXX
                          C = 2*THETA*TAU*NUM*SXY
                          D = (TAU+PHI1)*NUM*SYY
c defines Q to be the natural logarithm of the equation due to underflow
                          Q = (-0.5*(B-C+D)/A)-LOG(PHI1*PHI2*A**(0.5*NUM))
                          M1 = M1 + Q
                          END DO
                          M = 2*HZ*M1
                          L1 = L1 + M
                    END DO
               L = 2*HX*L1
               J1 = J1 + L
             END DO
         J = 2*H*J1
c writes the data to the output file
      WRITE (2,*) PHI1, J
```

```
        END DO
END
```

B7. POSTERIOR DENSITY OF ϕ_2 USING MIDPOINT RULE METHOD

```
C  USES MIDPOINT RULE TO APPROXIMATE THE POSTERIOR DENSITY OF phi2

      REAL ThLO,ThHI,TLO,THI,P1LO,P1HI,P2LO,P2HI
           REAL J

c defines the limits of theta
           THLO = 0.
           THHI = 1.
C defines the limits of tau
           TLO = 0.
           THI = 1000.
C defines the limits of phi1
           P1LO = 0.
           P1HI = 1000.

C calls the subroutine to perform numerical integration over theta, tau, phi1
      CALL QUAD(ThLO,ThHI,TLO,THI,P1LO,P1HI,P2LO,P2HI,J)
      END

c subroutine performs numerical integration over theta, tau, phi1 and plot phi2 vs. J
      SUBROUTINE QUAD(ThLO,ThHI,TLO,THI,P1LO,P1HI,P2LO,P2HI,J)
      REAL ThLO,ThHI,P1LO,P1HI,P2LO,P2HI,THETA,TAU,PHI1,PHI2
      REAL H,HX,HZ,J1,L1,M1,J,L,M,N, INC
           REAL A,B,C,D,NUM,SXX,SXY,SYY
      INTEGER i,i2,i3

c opens the output file
           OPEN(2, FILE='phi2MIDPT1.DAT', STATUS = 'new')

c allows user to enter the range to plot phi2
           WRITE (*,*) 'ENTER THE LOWER LIMIT TO PLOT phi2'
           READ (*,*) p2LO
           WRITE (*,*) 'ENTER THE UPPER LIMIT TO PLOT phi2'
           READ (*,*) p2HI
           WRITE (*,*) 'ENTER THE INCREMENT'
           READ (*,*) INC

C  FOR THE DATA SET BELOW:
C          DOSE              DICENTRICS/CELL
C          50                      .4052
C          75                      .6026
C          100                     .8174
C          150                     1.26667
C          200                     1.6429
C          250                     2.1186
C          300                     2.6216
C   THE FOLLOWING VALUES WERE FOUND TO BE
```

```
c NUM is the number of data points
      NUM = 7
c defines SXX as the sum of the squares  sum_{i=1}^{N} X_i^2 / N
      SXX = 33304.0
c defines SXY as the sum of the squares  (sum_{i=1}^{N} X_i Y_i) / N
      SXY = 283.0
c defines SYY as the sum of the square  ( sum_{i=1}^{N} Y_i^2 ) / N
      SYY = 2.408

C N IS THE NUMBER OF SUBINTERVALS;  N MUST BE EVEN.
      N = 50

      DO PHI2 = P2LO,P2HI,INC

   H = (ThHI-ThLO)/(2*(N+2))
   J1 = 0

   DO i = 0,N
     THETA = ThLO + H*(2*i+1)
     HX = (THI-TLO)/(2*(N+2))
     K1 = 0
       DO i2 = 0, N
                              TAU = TLO + (2*i2+1)*HX
                              HZ = (P1HI-P1LO)/(2*(N+2))
                              M1 = 0
                                    DO i3 = 0, N
                                    PHI1 = P1LO + (2*i3+1)*HZ
                                    A = PHI1*PHI2+TAU*PHI2+TAU*PHI1*THETA**2
                                    B = (THETA**2*TAU+PHI2)*NUM*SXX
                                    C = 2*THETA*TAU*NUM*SXY
                                    D = (TAU+PHI1)*NUM*SYY
c defines Q to be the natural logarithm of the equation due to underflow
                                    Q = (-0.5*(B-C+D)/A)-LOG(PHI1*PHI2*A**(0.5*NUM))
                                    M1 = M1 + Q
                                    END DO
                                    M = 2*HZ*M1
                                    L1 = L1 + M
                               END DO
                        L = 2*HX*L1
                        J1 = J1 + L
     END DO
               J = 2*H*J1
c writes data to the output file
       WRITE (2,*) PHI2, J
       END DO
   END
```

B8. CALIBRATIVE DENSITY USING THE MIDPOINT RULE METHOD

```
C APPROXIMATES THE CALIBRATIVE DENSITY
REAL ThLO,ThHI,TLO,THI,P1LO,P1HI,P2LO,P2HI
        REAL J

c allows user to enter the limits of integration
    WRITE (*,*) 'ENTER THE LOWER LIMIT FOR THETA'
    READ (*,*) ThLO
    WRITE (*,*) 'ENTER THE UPPER LIMIT FOR THETA'
    READ (*,*) ThHI
    WRITE (*,*) 'ENTER THE LOWER LIMIT FOR TAU'
    READ (*,*) TLO
    WRITE (*,*) 'ENTER THE UPPER LIMIT FOR TAU'
    READ (*,*) THI
   WRITE (*,*) 'ENTER THE LOWER LIMIT FOR PHI1'
    READ (*,*) P1LO
    WRITE (*,*) 'ENTER THE UPPER LIMIT FOR PHI1'
    READ (*,*) P1HI
    WRITE (*,*) 'ENTER THE LOWER LIMIT FOR PHI2'
    READ (*,*) P2LO
    WRITE (*,*) 'ENTER THE UPPER LIMIT FOR PHI2'
    READ (*,*) P2HI

c calls subroutine to perform numerical integration and plot Xf vs. J
    CALL QUAD(ThLO,ThHI,TLO,THI,P1LO,P1HI,P2LO,P2HI,J)
    END

c subroutine performs numerical integration over θ, τ, φ1, φ2 , assigns a value to Yf and plots Xf vs. J
    SUBROUTINE QUAD(ThLO,ThHI,TLO,THI,P1LO,P1HI,P2LO,P2HI,J)
    REAL ThLO,ThHI,TLO,THI,P1LO,P1HI,P2LO,P2HI,THETA,TAU,PHI1,PHI2
    REAL H,HX,HY,HZ,J1,K1,L1,M1,J,L,LL,M,Q,N,PI
    REAL A,B,C,D,E,F,G,Z,Z1,PX,PX1,XFLO,XFHI,YF,NUM,SXX,SXY,SYY
    INTEGER i,i1,i2,i3

c opens the output file
        OPEN(2, FILE='M1yf=.5.DAT', STATUS = 'new')

c allows user to input range to plot
        WRITE (*,*) 'ENTER THE LOWER LIMIT TO PLOT XF'
        READ (*,*) XFLO
        WRITE (*,*) 'ENTER THE UPPER LIMIT TO PLOT XF'
        READ (*,*) XFHI
        WRITE (*,*) 'ENTER THE INCREMENT'
        READ (*,*) INC
c allows user to input # dicentrics/cell
        WRITE (*,*) 'ENTER THE VALUE FOR YF'
        READ (*,*) YF
```

```
C  FOR THE DATA SET BELOW:
C        DOSE            DICENTRICS/CELL
C        50                      .4052
C        75                      .6026
C        100                     .8174
C        150                     1.26667
C        200                     1.6429
C        250                     2.1186
C        300                     2.6216
C   THE FOLLOWING VALUES WERE FOUND TO BE
c NUM is the number of data points
         NUM = 7
```

c defines SXX as the sum of the squares $\sum_{i=1}^{N} X_i^2 / N$

```
         SXX = 33304.0
```

c defines SXY as the sum of the squares $(\sum_{i=1}^{N} X_i Y_i) / N$

```
         SXY = 283.0
```

c defines SYY as the sum of the square $\left(\sum_{i=1}^{N} Y_i^2\right) / N$

```
         SYY = 2.408

C N IS THE NUMBER OF SUBINTERVALS;  N MUST BE EVEN.
         N = 100

         DO XF = XFLO, XFHI, INC

    H = (ThHI-ThLO)/(2*(N+2))
    J1 = 0

    DO i = 0,N
      THETA = ThLO + H*(2*i+1)
      HX = (THI-TLO)/(2*(N+2))
      K1 = 0

        DO i1 = 0, N
        TAU = TLO + (2*i1+1)*HX
        HY = (P1HI-P1LO)/(2*(N+2))
                        L1 = 0
                                DO i2 = 0, N
                                PHI1 = P1LO + (2*i2+1)*HY
                                HZ = (P2HI-P2LO)/(2*(N+2))
                                M1 = 0
                                        DO i3 = 0, N
                                        PHI2 = P2LO + (2*i3+1)*HZ
                                        A = PHI1*PHI2+TAU*PHI2+TAU*PHI1*THETA**2
                                        B = (THETA**2*TAU+PHI2)*(NUM*SXX+XF**2)
                                        C = 2*THETA*TAU*(NUM*SXY+XF*YF)
```

```
                D = (TAU+PHI1)*(NUM*SYY+YF**2)
                E = EXP(-0.5*(B-C+D)/A)
                F = XF*PHI2+THETA*YF*PHI1
                G = TAU/(2*A**((NUM+3)/2))
                Z = -F*SQRT(TAU/(2*PHI1*PHI2*A))
                Z1 = F*SQRT(TAU/(2*PHI1*PHI2*A))
                PI = 3.14159265359
                PX = 2*(Z-Z**3/3+Z**5/10-Z**7/42)/SQRT(PI)
                PX1=2*(Z1-Z1**3/3+Z1**5/10-Z1**7/42)/SQRT(PI)
                Q = G*E*(2-PX-PX1)
                M1 = M1 + Q
                END DO
                M = 2*HZ*M1
                L1 = L1 + M
            END DO
            LL = 2*HY*L1
            K1 = K1 + LL
        END DO
        L = 2*HX*K1
        J1 = J1 + L
    END DO
        J = 2*H*J1
c writes data to the output file
    WRITE (2,*) XF, J
    END DO
END
```

VITA

Cynthia Maples was born in Knoxville, Tennessee on July 7, 1974. She attended schools in the public system of Knoxville, Tennessee, the Knox County Public School System, where she graduated from Carter High School in June 1992. She entered The University of Tennessee, Knoxville during August of 1992 where in August 1996 she received the Bachelor of Science in Nuclear Engineering with a concentration in Radiological Engineering. She then entered the Master's program in Nuclear Engineering at The University of Tennessee, Knoxville in August 1996, officially receiving the Master of Science in Nuclear Engineering in May of 1998.